UNIVERSITA' DEGLI STUDI DI MILANO

Department of Medical Biotechnology and Translational Medicine

PhD programme in Biochemical Sciences XXXI cycle

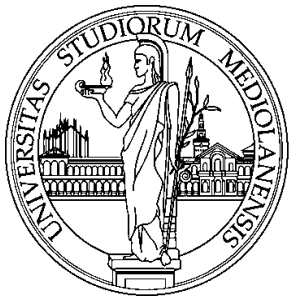

Ganglioside GM1 as adjuvant for Orkambi® therapy to restore plasma membrane stability and function of F508del-CFTR

Supervisor: Prof. Sandro SONNINO
Tutor: Dr. Massimo AURELI
Coordinator of PhD programme: Prof. Sandro SONNINO

PhD Thesis of
Giulia MANCINI
Student ID: R11421

Academic year 2017-2018

A mia madre che è stata ed è tuttora fonte di ispirazione, indipendenza e coraggio,

a mio padre che mi ha insegnato diplomazia, rigore e tenacia,

a mio fratello con cui condivido il viaggio.

A tutte le donne della mia famiglia, esempi di modernità, forza e resilienza, grazie per avermi insegnato a lottare per quello che desidero e grazie per avermi insegnato a trovare grazia ed eleganza nella fatica.

Summary

Cystic fibrosis (CF) is the most common, fatal genetic disease in the Caucasian population caused by loss of function mutations in gene encoding for the cystic fibrosis transmembrane conductance regulator (CFTR). CFTR is expressed at the apical surface of epithelial cells of different organs, such as: lungs pancreas, gut, and testes. For this reason even if in CF the pulmonary manifestations are the most severe, CF is considered a multi-system disease, which affects several bodily districts.

The new challenge for the CF therapy is based on the development of small molecules able to rescue the function of the mutated CFTR. Many pharmacological agents have been designed to increase the surface level of mutated CFTR (correctors), as well as its plasma membrane (PM) activity (potentiators).

Recently, combined therapy that includes a corrector of the CFTR folding (lumacaftor or VX-809) and a potentiator of the channel activity (ivacaftor or VX-770) called Orkambi®, was approved for CF patients homozygous for the deletion of phenylalanine at position 508 (F508del), the most common CF-causing mutation. Unfortunately, clinical studies revealed that the effects of Orkambi® on lung function were modest, due to low stability of rescued F508del-CFTR at the PM level.

Indeed, many factors contribute to PM CFTR stability, including its compartmentalization in PM macromolecular complexes composed of phospholipids, sphingolipids, with particular regards for monosialoganglioside 1 (GM1), and scaffolding proteins such as ezrin and NHERF-1.

Interestingly, it has been proved that in bronchial epithelial cells the lack of CFTR in the cell PM, such as in the case of the patients carrying the mutation F508del, is associated with a decreased content of GM1. By performing photolabelling experiments, I demonstrated for the first time that GM1 and CFTR at PM level reside in the same microdomain, suggesting a direct interaction between them. Then I investigated on the potential effect of the exogenous administration of ganglioside GM1 on the PM stabilization and function of F508del-CFTR rescued by Orkambi® treatment. In particular, I proved that in CF bronchial epithelial cells GM1 antagonizes the negative effect of VX-770, increasing F508del-CFTR maturation and its channel activity by the recruitment of the scaffolding proteins NHERF-1 and ezrin.

Taken together the results obtained during my PhD project pointed out the role of GM1 as possible adjuvant to Orkambi® therapy to restore the function of F508del-CFTR.

Introduction

Cystic Fibrosis

Cystic fibrosis (CF) is the most common life-limiting autosomal recessive disease among Caucasians, affecting approximately 1 every 2500-4000 newborns; this pathology is caused by mutations of a gene which encodes for a chloride-conducting transmembrane channel called Cystic Fibrosis Transmembrane Conductance regulator (CFTR). CFTR regulates anion transport and mucociliary clearance in the airways, and its functional damage results in mucus retention and chronic infection which causes local airway inflammation. CFTR is expressed at the apical surface of epithelial cells of different organs, such as: lungs, pancreas, gut, and testes. For this reason, even if in CF the pulmonary manifestations are the most severe, it is considered a multi-system disease which affects several bodily districts [1].

During the past six decades, the average age of survival has increased progressively, and thanks to the current CF therapies is now 40 years in developed countries [2].

CFTR genetics: gene and tissue expression

The gene responsible for the CF disorder called CFTR, was identified in 1989 and belongs to the long arm of chromosome 7 (7q31). The gene spans 190 Kb of genomic DNA and is composed of 27 exons, which encode for a 1480 aa protein.

The number of identified sequence variants in the CFTR gene has now exceeded 2000, although fewer than 200 have been definitively proved to be disease-causing.

The full-length CFTR mRNA contains 6128 nucleotides and all the CFTR transcription mechanisms start from the same site but there are also some mechanisms of alternative splicing. The promoter region is characterized by consensus binding sites for different transcriptions factors as AP-1, SP1, GRE, CRE, C/EBP. In addition, CFTR expression is regulated by hormone in both males and females [3].

The expression of CFTR was deeply analysed in both rodents and humans [4]. CFTR mRNA is constitutively expressed in sweat gland and in gastrointestinal tract starting from early development, [5] and it is maintained for the all-adult life.

Besides, the lung expression, CFTR was shown to be expressed at high levels in the pancreatic duct epithelium, and at lower levels detected in the larger intra- and interlobular ducts. High levels of CFTR expression were also seen in the crypts of the small intestinal epithelium.

CFTR is also expressed in mucin secretory cells, in gallbladder epithelia and in the Brunner glands. Measurable levels of CFTR were also detected in female and male reproductive tissue and organs, such as cervix, endometrium, fallopian tubes, and ovary as well as in epididymis head. Low and intermediate levels of CFTR transcripts can also be found in kidney, thyroid and salivary gland [6].

The expression patterns of CFTR in the fetus are maintained postnatally, with the exception of the respiratory system. Although high levels of CFTR expression are found in the epithelium of the airways in the fetal lung, this is in marked contrast to the relative lack of expression detected in the adult lung [7]. On the other hand, the expression in submucosal gland is detected only after birth, and it is not measurable in fetus, indeed in adult respiratory tissue the main site of expression of CFTR is the serous submucosal gland [3, 7, 8].

The mechanisms controlling the complex expression pattern of CFTR are not yet totally understood. The CFTR promoter has a housekeeping-type promoter, it is rich in CpG, without TATA box, and contains a number of putative Sp1 (specificity protein 1) binding sites [9, 10].

While the promoter is important for CFTR basal expression, it doesn't explain the complex tissue specific regulation of its expression, indeed, there are distal cis or trans-acting regulatory elements which are critical regulators of this process.

In sexually immature females and ovariectomized mature females the estrogen treatment upregulates CFTR levels in the uterine epithelium and the oviductal mucosa by the binding with glucocorticoid response elements located in the CFTR promoter [7].

CFTR structure

CFTR is a membrane protein, belonging to an ABC subfamily [11], with the typical ABC transporter structure composed of two transmembrane domains (TMDs), four intracellular linkers, (ICL1-ICL4), and two nucleotide binding domains (NBDs) [12]. CFTR has also an additional regulatory (R) region, as well as long N- and C-terminal extensions of about 80 and 30 residues in length, respectively [13].

TMDs are composed of six membrane-spanning α-helices and they are predicted to form a pore for ions passage. NBD1 has an additional insertion of 35 residues and NBD2 has 80 residues extension at its end, if compared with other ABC proteins. These additional peptides may regulate CFTR channel interaction with other cellular molecules.

The regulatory region R is a random coil highly charged, of 200 residues in length and is characterized by several consensus sequences (12 serines and 8 threonines) for protein kinase A

(PKA) phosphorylation. The four intra-cellular loops are predicted to interact and transduce information between TMDs and NBDs [14]. CFTR forms a channel at epithelial apical cell membranes [15-17], regulating Cl^-/HCO_3^-exchange [19, 20].

CFTR in PM is present in 3 possible status: open, closed and open-ready. The open-ready conformation doesn't allow chloride flux but it is poised to a rapid transition into the open state upon specific stimuli. CFTR channel activity is also PKA dependent on the phosphorylation of the region R and on intracellular availability of ATP. Structurally, the model connects ATP binding with the formation of a NBD head-to-tail sandwich heterodimer and probably this is responsible for the induction of conformational changes in the TMDs via NBD-TMD coupling helices that open the channel gate. The channel gate closes after ATP hydrolysis and comes back to inward-facing conformation [21].

More recently, evidence has proved that R region steric block can be alleviated via other mechanisms: calcium-loaded calmodulin was found to bind to the non-phosphorylated R region α-helices leading to channel activation [22].

Calmodulin binding inhibits phosphorylation by Protein Kinase A (PKA) and PKA phosphorylation inhibits calmodulin binding. This results in a complex interconnection in which PKA phosphorylation can synergize with the activating effects of calcium on CFTR or decouple CFTR from calcium activation [23]. Recently, it has been demonstrated that other binding partners of the R region include the C terminus of CFTR, which contains a PDZ-binding motif, the SLC26A3 transporter, which can co-regulate CFTR [24, 25].

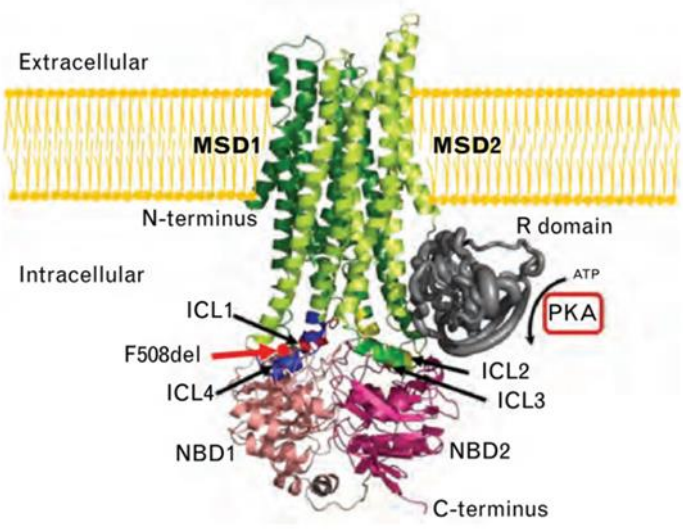

Figure 1: ***Theoretical domain organization of CFTR at the apical membrane based on analysis of crystal structures and structural homology models [26]***

CFTR biosynthesis

CFTR biosynthesis begins in the endoplasmic reticulum (ER) with the folding of the cytosolic domains, towards the acquisition of a fully folded native structure. CFTR folding starts early during its translation, which takes place in multiple cellular compartments along the secretory pathway (Figure 2). This process is assessed by the ER quality control system that allows the exit of folded proteins and targets unfolded/misfolded CFTR to the degradation.

The first step of folding control occurs in the ER, by chaperons protein such as Calnexin, Aha, and HSP40/70/90. Both inter and intra-domain folding are required for ER exit. If allowed to leave the ER, CFTR is modified at the Golgi and joins the post-Golgi compartments to be delivered to the PM [27].

After proper folding, CFTR moves from the ER to the Golgi apparatus, where the glycan moieties are processed, and finally, mature CFTR is carried in vesicles from the trans-Golgi network (TGN) to the PM. At the PM, CFTR levels result from a balance between membrane delivery (anterograde trafficking), endocytosis, and recycling. The PM provides the final stages of CFTR maturation, indeed, at the PM level CFTR takes part in an interactome, which includes members of Rab and Rho families, GTPase and cytoskeleton proteins, such as the PDZ-interacting NHERF protein [21]. Two glycosylations at 4^{th} extracellular loop, on the residue 894 and 900, characterize the correct and mature form of CFTR, even if this modification is not essential for the channel activity and for its PM localization. In fact, there are other different post-translational modifications such as methylation, palmitoylation, and phosphorylation which are important for the correct folding, the biological activity and finally, the stability of the protein [21].

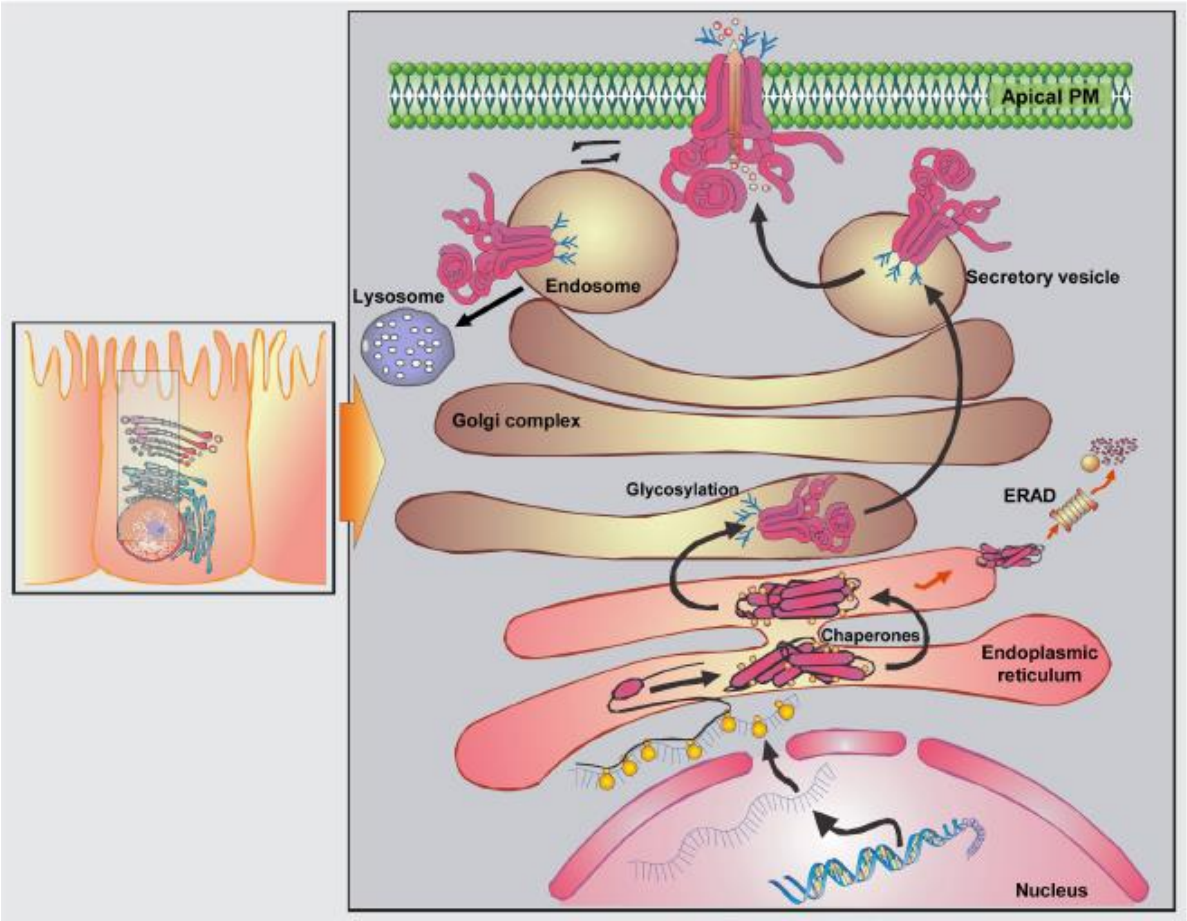

Figure 2: ***Successive steps of CFTR synthesis, trafficking and degradation***. *Figure adapted from [27]*

CFTR interactors and microenvironment

Once at the cell surface, CFTR stability is regulated by multiple protein interactors which regulate not only anterograde traffic to the PM, but also its endocytosis and recycling to reach a tight modulation of CFTR membrane levels [28-30].

Interactions at both the N-terminus and C-terminus of CFTR have been reported to regulate channel activity, including PDZ proteins such as NHERF-1 and CAL or other membrane proteins that interact with CFTR through large macromolecular complexes.

Recent works have demonstrated that the second messenger cAMP has a role in regulating CFTR PM stability. Intracellular cAMP effects are mediated by cAMP-dependent PKA, which directly phosphorylates CFTR's R domain, but interestingly, a family of guanine nucleotide-exchange factors, called EPACs, have been also discovered to respond to cAMP levels but they do not lead to PKA activation [31, 32]; moreover, EPACs regulate cell-to-cell and cell-to-matrix adhesion, cytoskeletal rearrangements, and cell polarization.

In addition, the interaction with membrane lipids also seems to have a crucial role in CFTR stability and function, in particular, recent works have described interactions with cholesterol, that regulate the distribution and dynamics of CFTR in PM [33, 34]. Moreover, they have suggested a role of sphingomyelin for the regulation of CFTR activity, by sphingomyelin-mediated signalling pathways.

Interestingly, it has been proved that in bronchial epithelial cells the lack of CFTR in the cell PM, such as in the case of the patients carrying the mutation F508del (the mutation with highest frequency), is associated with a decreased content of GM1 [35], suggesting a relationship between the channel and this ganglioside.

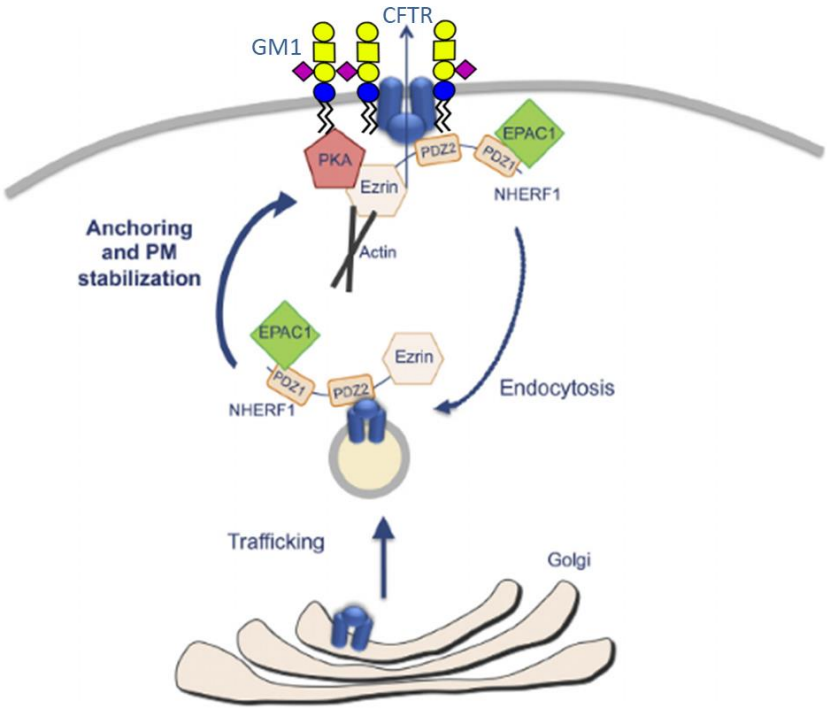

Figure 3: ***CFTR regulation and interactions****. Image modified from Farinha et al 2017* [36]

Cystic Fibrosis Epidemiology

Nowadays, the worldwide distribution of CFTR mutations that leads to CF, is still incomplete, for example in Eastern Asia the disease named panbronchiolitis is often associated with CFTR mutations, but its phenotype is completely different with respect to CF, in fact there isn't the involvement of pancreas and sweat glands. Although, CF is most prevalent in Caucasians (1 in 2,500), it is a panethnic disease in North America, found in all ethnicity, including African-American (1 in 15,000), Hispanic-American (1 in 13,500), and Asian-American (1 in 35,000).

The great phenotypic variability of CF has been shown to implicate not only the type of CFTR mutations, but also other genetic factors such as modifier genes, and environmental factors including the lifestyle [37, 38].

Most of CF patients suffer from classic CF, characterized by a multisystemic organs impairment and a sweat chloride concentration of >60 mmol/L.

They may have exocrine pancreatic insufficiency or pancreatic sufficiency. CF can have a severe course with fast progression of symptoms or a milder course with less lung deterioration. Classic CF patient mortality is mainly due to progressive respiratory disease [39].

Non-classic CF includes individuals with at least one CF phenotypic characteristic and a normal (<30 mmol/L)or borderline (30–60 mmol/L) sweat chloride level. These patients have both multi- and/or single-organ involvement. Most of them have exocrine pancreatic sufficiency and milder lung disease.

CFTR mutations

Over 2000 mutations have been identified in the CFTR gene [7], including missense, frameshift, splicing and nonsense mutations, inframe deletion, and insertions. On the basis of the effect on CFTR function, the mutations are classified into six major classes: class I, II and III mutations are associated with no residual CFTR function and the patient with these kind of mutations show a severe phenotype. While patients with mutations belonging to class IV, V and VI, show some residual CFTR function, and have a mild lung disease and pancreatic sufficiency [40].

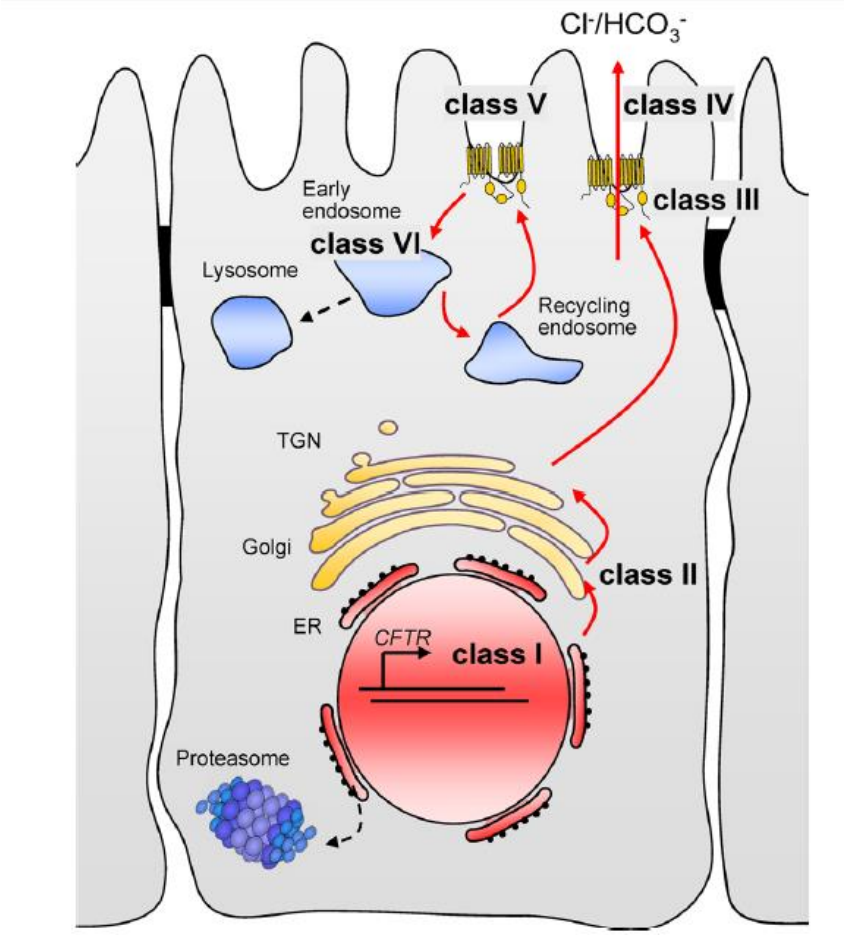

Figure 4: ***Classification of CFTR mutations*** *[41]*

Class I: mutations preventing the production of a full-length CFTR protein

Class I mutations result in the total or partial lack of production of a functional CFTR protein. Such mutations may be due to a nucleotide substitution which introduces an in-frame premature termination codon (W1282X, G542X and R1162X), a frame-shifting insertions or deletions, mutations at the invariant dinucleotide splice junctions of a PTC, resulting in complete skipping of an out of frame exon, and a complete or partial deletion of the CFTR gene or a rearrangement in the gene which can alter the exon sequence [42]. G542X is the most frequent mutation of this class and leads to a reduced steady state level of mRNA, caused by the presence of a premature stop codon in its sequences.

Class II: mutations altering the cellular processing of the protein

Class II mutations are associated with a defective processing due to misfolding of the protein and may be found within any domain of the CFTR. Even if it is translated into full-length polypeptide, the misfolded protein is retained into the ER, targeted to degradation by the

ubiquitin/proteasome pathway, rather than trafficked to the PM. The most frequent CF mutation of this class is the F508del. It has been shown that F508del leads to energetic and kinetic instability of the NBD1 domain due to improper local folding. This mutation causes the most severe phenotype in the patients.

Class III: mutations disturbing the regulation of the Cl^-channel

These mutations are frequently located in the ATP binding domains (NBD1 and NBD2) and are referred to as gating mutations; this group of mutations is mainly composed of missense mutations. The produced CFTR can reach the PM but has decreased channel opening time and decreased chloride flux, caused by resistance to activation by protein kinase A. The most described mutation of class III is p.Gly551Asp [16].

Class IV: mutations altering the conduction of the Cl^-channel

These mutations influence mainly the membrane spanning domains implicated in the constitution of the channel pore. The missense mutations located in these regions produce a protein which is inserted in the membrane, but with a reduced channel conductance. The p.Arg117His mutation is the best-characterized class IV mutation. Recently, the subclass IVb has been identified in relation to mutations regarding only defect in CFTR bicarbonate conductance.

Class V: mutations reducing the amount of functional CFTR protein

Most of these class V mutations reduce the total amount of CFTR protein by affecting pre-mRNA splicing. These splice site mutations can induce complete or partial exclusion of an exon. As result, CFTR is fully functional in the PM but with lower content. The most frequent and well-studied is the skipping of exon 10 [39].

Class VI mutations destabilize the channel in post-ER compartments and/or at the PM

This class is the most recent and includes those mutations which can destabilize CFTR in the post-ER compartments or at the PM, by reducing its conformational stability [43] and/or generating additional internalization signals [44]. These mutations can accelerate PM turnover and reduce apical PM expression [42,43]. Class VI mutation has recently been combined with class V as mutations leading to a reduced amount of functional CFTR protein [21], [39], [28].

Clinical feature of Cystic Fibrosis

The faulty secretion of chloride, sodium and water followed by the formation of viscous mucus at the respiratory level, and digestive and reproductive systems, represents the central problem in patients with CF, while the insufficiency in the reabsorption of these ions at the level of sweat glands is of lower significance.

Respiratory diseases are present in more than 90% of CF patients. CF usually shows signs of manifestations already in the first months after birth featuring pertussis-like cough, several bronchiolitis or obstructive bronchitis. These symptoms are due to difficulties with elimination of hyperviscous secretions and pulmonary hypoventilation [45].

Cystic fibrosis lung disease and inflammation

Lung disease is the major cause of mortality in CF patients, despite CF lung disease is primarily an infectious disorder, the consequent and associated inflammation is both intense and ineffective in eliminating pathogens. Persistent high-intensity inflammation leads to structural damage of the airways and impaired lung function that may result in respiratory failure and death. Several defective inflammatory responses have been linked to CFTR deficiency including innate and acquired immunity dysregulation, cell membrane lipid abnormalities, various transcription factor signalling defects, as well as altered kinase and toll-like receptor responses [46]. The most common pathologic findings are bronchiectasis, airways obstruction and chronic infection driven by different bacteria, in particular by *Pseudomonas aeruginosa* [47, 48]. The other persistent bronchopulmonary infections are driven by *Staphylococcus aureus, Burkholderia cepacia* and several other pathogens, leading to chronic airway and systemic inflammation, tissue destruction, and respiratory insufficiency [46].

Several studies demonstrate the large number of defects of the CF lung disease and inflammation, directly or indirectly correlated to CFTR, such as airway surface liquid and mucociliary clearance, the lower pH of airway surface liquid and sphingolipids abnormalities [49-51].

The airway mucus is a dynamic, complex and viscous colloid which can continuously modify in response to different signals. The mucus contains different molecules as antibacterial defensins, immunoglobulins, inorganic salts and the proteins mucins. Thanks to these components, the airway mucus is able to cover several functions, such as to create a protective barrier against toxic products and to clear pathogens. The mucus must be sufficiently fluid to allow the elimination of

particles and pathogens. The presence of CFTR influences the characteristics of the airway surface liquid and mucus layer [52, 53].

The water content of airway surface liquid is regulated by CFTR, by its capacity to secrete chloride ions and control sodium adsorption. The impaired regulation of sodium and chloride content in CF, leads to a defective osmotic pressure, an increased absorption of water and consequently to a dehydration of the airway surface liquid [50, 51, 54, 55]. As a consequence, there is the formation of a very viscous mucus unable to eliminate bacteria, leading to a chronic retention of pathogens and a strong inflammatory response [46, 56].

Another important parameter in CF is pH: the pH of CF airway surface liquid is eight-fold more acidic than that of individuals without CF [57]. CFTR is essential for normal bicarbonate secretion from cultured bronchial epithelial cells and from native small airways [58-60]. The low pH at the airway surface results in the inactivation of antimicrobial peptides thus creating a host defense defect [61]. Furthermore, recent evidence suggests that CFTR-dependent bicarbonate is important in defining the expansion and solubilization of mucin granules as well as the density of airway mucus. Moreover, local pH is essential to the correct function of several proteins, in particular, the proteins named mucins and principally MUC5A, MUC5B, and MUC2, which are able to attract water in the mucus [62]. These proteins can be transmembrane, on the apical surface of epithelial cells, or can float as a gel, but both these kinds of mucins are localized in the periciliary space forming a protective barrier. The absence of bicarbonate causes the formation of dense layer of mucins, tightly adherent to the epithelium surface. [46, 54, 63].

In addition, the low pH at the airway surface, results in the inactivation of proteins with antimicrobial properties [64].

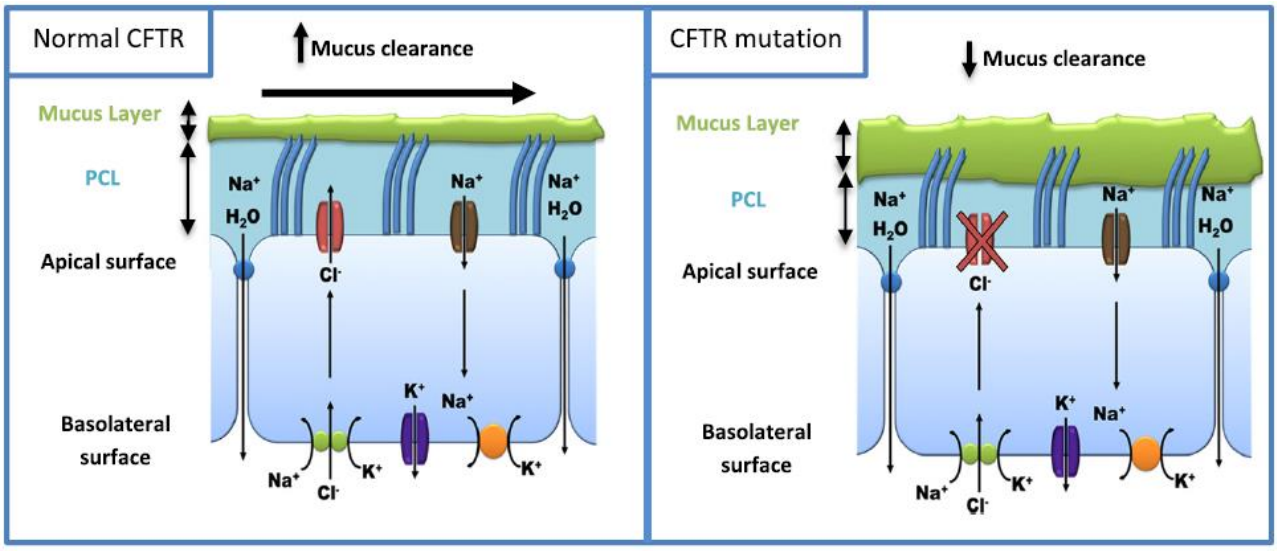

Figure 5: ***Mutation in the CFTR gene prevents Cl^- from being secreted and there is unrestrained Na^+ absorption, leading to defective mucus clearance*** *[65]*

Current therapy

Lung disease treatment

The treatment of lung disease in CF is central: oral antibiotics are used prophylactically in some countries to prevent *S. aureus* infection, despite the concerns of increasing risk of *P. aeruginosa* infection. In children, repeated infections are treated with oral antibiotics aimed at eliminating *S. aureus* and *H. influenza* colonization. People with CF have recurrent exacerbations of disease. Pulmonary exacerbations are episodes in which there is an increase in symptoms of chronic lung infection, they are associated with increased breathlessness, reduced exercise tolerance and systemic symptoms associated with an acute phase inflammatory response. Episodes of pulmonary exacerbation usually continue for several days and are treated with antibiotics and increased airway clearance. For *S. aureus* and *H. influenzae* infection, oral antibiotics are usually administered [66-68]. In patients chronically infected with *P. aeruginosa* or other Gram negative bacteria, these episodes usually need treatment with intravenous antibiotics. In addition to antibiotic therapy, patients with CF have to take also anti-inflammatory drugs, both non-steroidal anti-inflammatory drugs (NSAIDs) and steroidal anti-inflammatory drugs such as corticosteroids. As pulmonary damage in CF may occur as a consequence of inflammation, it has been hypothesized that prolonged use of NSAIDs may prevent progressive pulmonary deterioration and respiratory morbidity [69]. Furthermore, inhaled corticosteroids are often used to treat children

and adults with CF, in fact they have the potential to reduce lung damage arising from inflammation, as well as their effect on symptomatic wheezing [70, 71].

To ameliorate the breathing conditions, physiotherapy plays an important role in the management of CF [72].

Pancreatic and biliary disease

Epithelial cells in the pancreatic and biliary ducts are also involved in the CFTR dysfunction leading to pancreatic insufficiency, which associated to biliary cirrhosis though occurring in less than 10% of patients, and it can be treated with pancreatic enzyme replacement therapy [73, 74]. More commonly, people with CF have variably abnormal liver function, but just a small group of these patients develop cirrhosis or portal hypertension, whose unique treatment is the liver transplant [75, 76].

Innovative therapies

The new therapeutic strategies are aimed to develop drugs that correct the basic defect in CFTR function.

Gene and molecular therapies

Since the cloning of the CFTR gene, several studies have shown that CFTR function can be restored in the nose of CF patients by the transfection of the wild-type (WT) protein. The first major study of lung delivery has recently been reported and has shown some effects on important clinical parameters of FEV1, but this study suggests also that substantially more efficient vectors and delivery systems are required to achieve sufficient expression of CFTR [75].

CFTR chaperons

This strategy is based on the development of small molecules targeting CFTR as chaperons which are able to facilitate the folding of mutated CFTR and restoring its function.

The first proposed molecule was N-(2,4-di-tert-butyl-5-hydroxyphenyl)-4-oxo-1,4-dihydroquinoline-3-carboxamide (VX-770, ivacaftor); this drug was identified through highthroughput screening and subsequently modified to optimize its therapeutic effect [77]. Preclinical studies have shown that ivacaftor corrects CFTR-mediated chloride transport in most

class III mutations, class IV mutations in human bronchial epithelial cell cultures [78, 79], [80], [81], and may be administered to patients starting from 6 year of age [82].

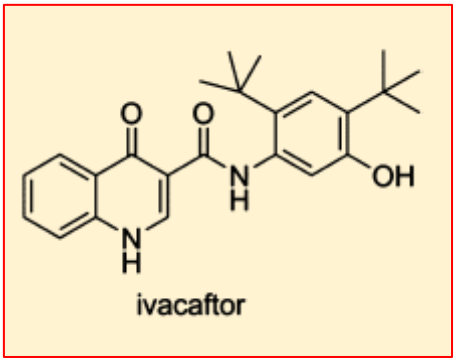

Figure 6: *Ivacaftor structure*

Ivacaftor is on clinical use for the patients carrying mutations G551D, with the commercial name of Kalydeco®.

The second chaperon strategy has been developed to target patients who are homozygous for the Phe508del mutation. Indeed, these two chaperons allow to restore trafficking of CFTR and to make it functional. F508del CFTR mutation impairs CFTR processing in the ER by preventing the properly protein folding [83], [84]. Misfolded F508del-CFTR is retained by the ER and degraded, reducing F508del-CFTR delivery to the cell surface. In this frame, the most promising molecule was the corrector VX-809.

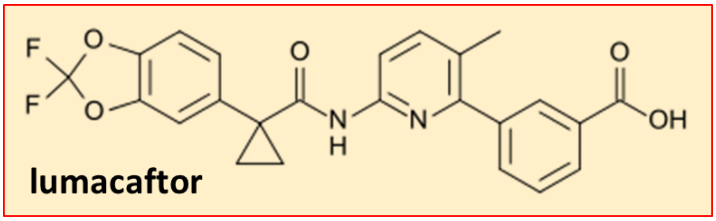

Figure 7: *Lumacaftor structure*

VX-809 acts early in CFTR biosynthesis to modulate the conformation of MSD1 and thereby suppresses folding defects in F508-CFTR and related MSD1 mutants. The combined therapy with the potentiator VX-770 is on clinical use in children older than 12 years, and has the commercial name of Orkambi®.

However, clinical studies revealed that the effect of Orkambi® on lung function is modest and it was proposed that this modest effect relates to a negative impact of VX-770 on the stability of F508del-CFTR in PM. Recent study shows also that there is a potential non-specific effects of VX-770 on the lipid bilayer and suggests that this may account for its destabilizing effect on VX-809-rescued F508del-CFTR [85].

Sphingolipids

PM is composed of an extremely complex lipid pattern including glycerophospholipids, cholesterol and sphingolipids [86]. Despite the fact that glycerophospholipids and cholesterol are the main lipids which compose eukaryotic cell membranes [87], nowadays emerging evidences support the important role of Sphingolipids (SLs) [88].

SLs are amphipathic molecules, mainly associated with the external leaflet of the cell PM, characterized by a hydrophobic group inserted in the lipid bilayer and a hydrophilic head of different complexity which protrudes toward the extracellular environment [89].

They have a common structure which comprises a backbone called “long-chain” or “sphingoid” base, which is formed by a 2-amino-1,3-dihydroxy-octadec-4-ene, an amino alcohol called sphingosine. Sphingosine has four different chemical configuration, but only the 2S, 3R is found in nature. It is the most abundant “sphingoid” base detected in mammals and is typically present linked with a long or very long fatty acid-chain, through an amide-bound. The fatty acid chains are predominantly composed of 14 to 36 carbon atoms in length and are usually saturated [90].

The N-acylated form of sphingosine is called Ceramide (Cer), and is the hydrophobic lipid moiety of sphingolipids. Cer is the starting point for the biosynthesis of the more complex sphingolipids and glycosphingolipids (GSLs) [89].

The hydrophilic head group R of sphingolipids is composed of phosphocoline in the case of sphingomyelin or of an oligosaccharide chain in the case of glycosphingolipids. The Gangliosides are a particular class of glycosphingolipids which have the oligosaccharide that contains a sialic acid residue [89].

Sphingolipids are a class of lipids essential for cell membranes architecture, but in the last two decades many studies have proved that SLs are not only structural components of biological membranes, but they also play other important roles in several cellular processes [91].

Indeed, a large variety of specific SLs have been shown to modulate the cellular signaling pathway [92].

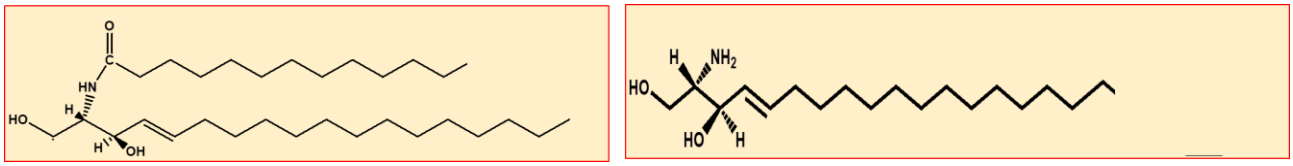

Ceramide **Sphingosine**

***Figure 8**: Chemical structure of ceramide and sphingosine*

Biosynthesis

Sphingomyelin and glycosphingolipid biosynthesis in mammals requires the intracellular formation of the membrane anchor, the ceramide [93] and the subsequent addition of single component of the hydrophilic head [94]. Both events are coupled to intracellular movement of metabolic intermediates and final products to the PM [95]. The variety of naturally occurring complex sphingolipids can be largely attributed to the combination of enzymes with transferase activities, which are expressed in specific cell types, and the brain is the organ where functional aspects of glycolipids are most evident.

Ceramide

The production of Cer in mammalian cells occurs through three different metabolic ways: de novo biosynthesis, complex sphingolipids catabolism and sphingosine recycling.

De novo biosynthesis of Cer, starts with the condensation of the amino acid L-serine with a fatty acyl coenzyme A, usually palmitoyl coenzyme A, to 3-ketosphinganine and it is catalysed by the enzyme serine palmitoyl transferase [96], [97], [98]. In the following NADPH-dependent reaction, 3-ketosphinganine is reduced to d-erythro-sphinganine by 3-ketosphinganine reductase [99]. Sphinganine is subsequently acylated to dihydroceramide by a N-acyltransferase (ceramide synthase) [100], [101]. The major part of the dihydroceramide pool is desaturated to Cer in the dihydroceramide desaturase reaction [102].

Cer is also generated during the catabolism of all complex sphingolipids. The catabolism occurs in the lysosomes by the action of specific glycohydrolase which removes single saccharidic units from the not reducing extremity of the oligosaccharides. Sphingomyelin (SM) hydrolysis is catalyzed by the action of sphingomyelinases (SMases) [103]. Different forms of SMases are known, and are characterized by specific optimum pH, subcellular localization, cation dependence. Ceramide

synthase is able to use as substrate both sphingosine and sphinganine with similar efficiency, so Cer can be also formed by N-acylation of sphingosine produced by the catabolism of complex sphingolipids.

Sphingomyelin

SM biosynthesis occurs on the luminal part of Golgi membranes [104]. It is formed by the transfer of phosphorylcholine from the phospholipid phosphatidylcholine, onto the 1-hydroxyl group of Cer, with the liberation of diacylglycerol.

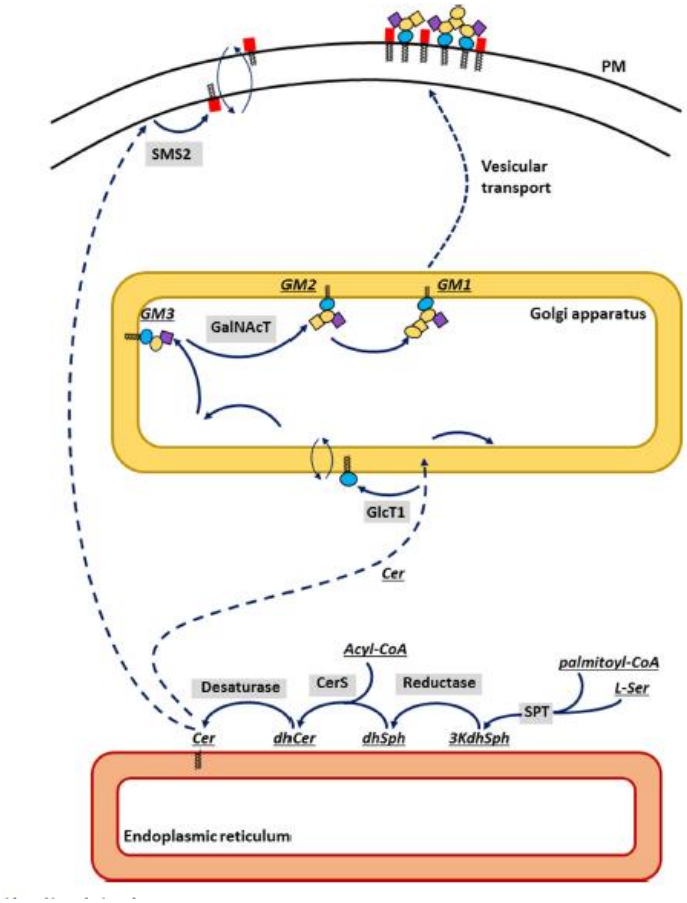

***Figure 9: Sphingolipid neo-biosynthetic pathway**, image from Aureli et al 2016* [105]

Complex GSLs

Glycosyltransferases catalyze the reaction of transfer of a specific carbohydrate, from the sugar nucleotide (UDP-Glucose, UDP-Galactose) to a specific type of acceptor, as ceramide or the non-reducing end of a carbohydrate chain attached to Cer [106].

The first step of glycosylation leads to the production of glucosylceramide (GlcCer), whose formation is catalyzed by a ceramide glucosyltransferase, called GlcCer synthase [107], in the cytosolic side of the early Golgi membrane [108]. The neo-synthetized GlcCer can follow two different ways: it reaches the PM or it can be translocated to the luminal side of the Golgi, where the GlcCer is further glycosylated by different glycosyltransferase to form more complex glycosphingolipids.

The addition of a galactose residue from UDP-Gal to GlcCer, driven by a galactosyltransferase, leads to the formation of Lactosylceramide (LacCer).

One of the major branch of metabolism of LacCer is the formation of ganglio series. The gangliosides are a class of GSLs characterized by the presence of sialic acid on their oligosaccharide chain. This class is particularly abundant in the cell of the central nervous system.

The biosynthesis of the complex ganglioside occurs in the lumen of the Golgi apparatus by different glycosyltransferase. The GM3 synthase or sialyl-transferase is responsible for the sialylation of LacCer to form GM3. The other downstream metabolites in this pathway are formed by analogous reactions; GM3 is converted to GM2 by GM2 synthase or β-galactosamynil transferase, which transfers an N-acetylgacatosamine to GM3, and GM2 is converted to GM1 by GM1b synthase.

Neo-synthetized glycosphingolipids reach the PM through the exocytotic vesicular traffic.

In addition, the neo-synthesized Cer, in Golgi apparatus, can be used for Sphingomyelin biosynthesis [109].

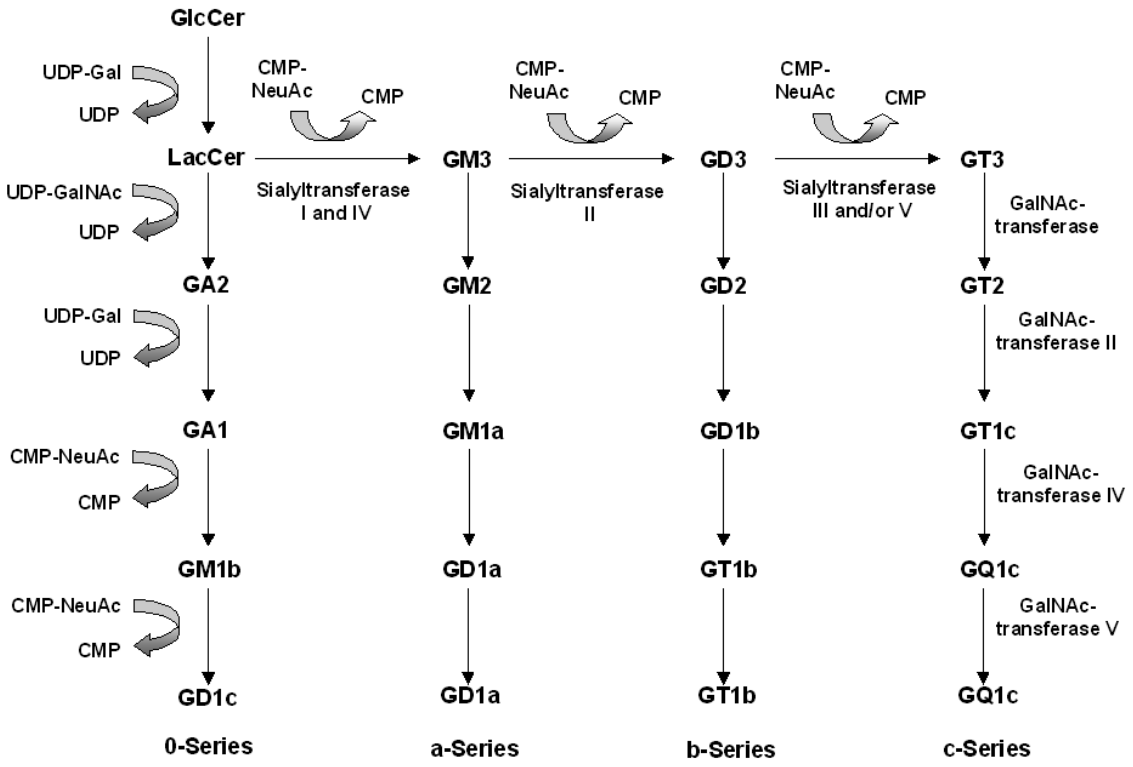

***Figure 10: Ganglioside biosynthesis**: All enzymatic steps (possibly except formation of LacCer) take place at the luminal surfaces of the Golgi membranes.*

Catabolism

Lysosomal Glycolipid Degradation

Constitutive glycolipid degradation occurs in the acidic compartments of the cells, the endosomes and the lysosomes. Within the digestion of cellular membranes, cellular glycolipids are also cleaved into their building blocks. To this purpose, parts of the PM are endocytosed and trafficked through the endosomal compartment to the lysosomes. Lysosomal glycosidases sequentially cleave off the sugar residues from the non-reducing end of their glycolipid substrates. The resulting monosaccharides, sialic acids, fatty acids and sphingoid bases can leave the lysosome and are used within salvage processes or are further degraded.

SLs metabolic homeostasis is obtained with the balancing of biosynthesis, degradation and recycling [110]. The central hub of SL anabolism is the vesicular transport of neo-biosynthesized SLs from the ER and Golgi apparatus to the PM.

Moreover, metabolic turnover and degradation of PM sphingolipids are processes occurring in the lysosomes, which are the acidic compartments of the cells, by the presence of specific acidic

hydrolases [111]. The degradation process consists in the remodeling of the hydrophilic head, driven by the lysosomal glycosidase from the non-reducing end of the glycolipid substrates. The molecules resulting from the catabolism can leave the lysosomes and can further be degraded or used again to form more complex structures [112].

For example, during the ganglioside catabolism, GM1 is cleaved to GM2 by β-galactosidase. The resulting GM2 is then degraded to GM3 and N-acetyl-galactosamine through the action of β-hexosaminidase A (HexA). The β-hexosaminidases are dimeric enzymes composed of two different subunits α and β. The different possible dimerization of their subunits leads to three different isoforms of the enzymes: Hex A, Hex B and Hex S [113].

GM3 is a substrate of sialidase Neu1 and Neu3, which leads to the formation of LacCer and sialic acid. Sialidases are glycohydrolases that catalyze the removal of α-glycosidically linked sialic acid. Four different isoforms have been isolated from four different genes: Neu1, Neu2, Neu3 and Neu4 [114]. Neu1, Neu2, Neu3 are predominantly localized in the lysosomes, cytosol and PM respectively. Neu4 is present in mitochondria and ER.

The degradation of LacCer is driven by β-galactocerebrosidase, which removes galactose obtaining GlcCer [115].

The GlcCer obtained by the reaction of β-galactocerebrosidase is further degraded to ceramide by the action of β-Glucocerebrosidase (GCase), a lysosomal-associated enzyme that hydrolyze the glycosidic linkage of GlcCer producing ceramide and glucose, and is irreversibly inhibited by conduritol B Epoxide (CBE). Besides SM is converted to Cer by sphingomyelinase (SMase).

In the eukaryotic cells there are acid sphingomyelinase (aSMase) and neutral sphingomyelinase. The acid one is principally located in lysosomes [116].

Plasma membrane sphingolipids metabolism

Several process are responsible for the PM sphingolipids' pattern and content. The main are neo-biosynthesis in ER and Golgi apparatus, the membrane turnover with final lysosomal catabolism and vesicles shedding.

Moreover, some recent data reported that enzymes involved in the sphingolipids metabolism are able to modify the sphingolipids head group directly at the PM level [117].

Indeed, some of the same enzymes of the sphingolipids biosynthesis and catabolism are found to be associated with the cell surface. It has been observed that these enzymes are often available as a series of couple that catalyze the same reaction in the opposite direction, contributing to the in

situ modifications of SL composition. These phenomena lead to very important biological consequences, considering that they could be instrumental to modulate cell function, with no involvement of the complex intracellular metabolic machinery.

For instance, it has been demonstrated also the presence of β-hexosaminidase A at the PM level, in combination with the β-hexosaminyl transferase.

A particular case is represented by a PM-associate sphingomyelin synthase (SMS2) because it is genetically distinct from the Golgi's one. SMS2 is present in combination with SMases. Three different SMases are available in eukaryotic cells: secreted SMase, acid SMase and neutral SMase. Only a particular isoform of neutral SMase, the nSMase2, works at the PM level.

In addition, the β-galactosidase and the β-glucosidase act at the cell surface. In particular, two different β-glucosidase have been detected; GCase which works in the lysosome and a non-lysosomal β-glucosylceramidase (NLGase).

NLGase, like GCase, is involved in the degradation of GlcCer to glucose and ceramide. It is considered a central enzyme in the glycosphingolipids homeostasis. NLGase is not localized in the lysosome but it is strongly associated with the PM, with five possible transmembrane domains. The most powerful inhibitor of GBA2 is N-5-adamantane-1-yl-methoxypentyl) deoxynojirimicin (AMP-DNM), followed by miglustat [118].

NLGase is ubiquitously distributed in several tissue and cell lines, in particular it is expressed in brain, heart, skeletal muscle, kidney and placenta. In minor part it is detectable in spleen, liver, small intestine and lung [119-121], [122].

Of particular interest in the context of CF are the enzymes involved in the catabolism of sphingolipids, leading to the formation of ceramide and in the regulation of its content at the PM level, considering the particular role of glycosphingolipids in the formation of specific PM portions called "lipid rafts" which allow to organize the correct microenvironment of several PM proteins including CFTR.

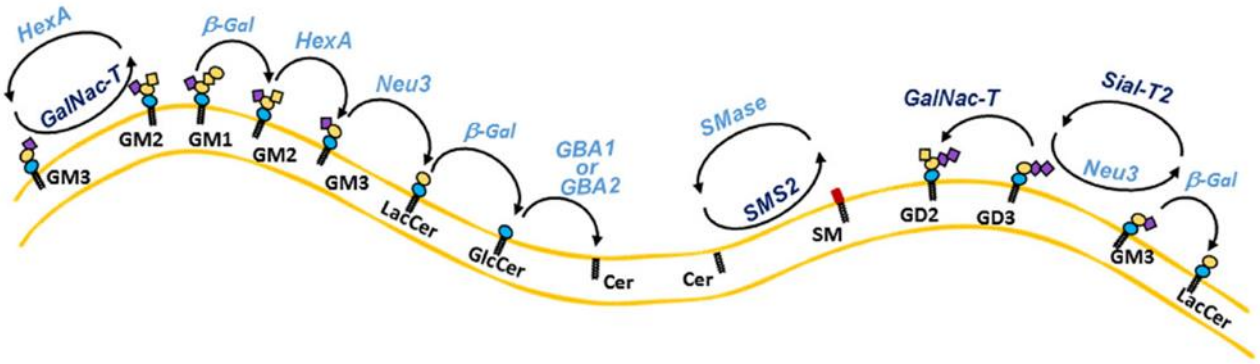

Figure 11: Representation of sphingolipid metabolism occurring at the cell surface *[105].*

Biochemical role of sphingolipids

Several evidences in literature suggest that lipids are not merely a structural component of cell membrane but they are also fundamental players of cell signaling and regulatory pathways [123], [124, 125].

Ceramide, ceramide-1-phosphate, sphingosine, and sphingosine-1-phosphate (S1P) have been shown to be involved in the regulation of a number of cellular events such as proliferation, differentiation, motility, growth, senescence, and apoptosis [126]. Ceramide and S1P have been proposed to have opposite roles in these processes. The balance between ceramide and S1P, which are metabolically interconnected, determines the entrance into one or more of these pathways.

Complex GSLs are also involved in cell physiology by acting as antigens, mediators of cell adhesion, binding agents for microbial toxins and growth factors, and modulators of signal transduction [127, 128]. In particular, as said before, SLs together with cholesterol, saturated phospholipids and a specific pool of proteins organize macromolecular complex at the cell PM called lipids rafts. The lipids rafts theory was postulated on the basis of the spontaneous lateral segregation of sphingolipids. This definition was subsequently modified to introduce the notion that lipid rafts correspond to membrane areas stabilized by the presence of cholesterol within a liquid-ordered phase [129].

Nowadays, different studies describe membrane rafts as a dynamic nanoscale domain enriched in sphingolipids, cholesterol and gangliosides, which have several roles in cell signal transduction [130].

The complex processes that control the formation and dynamics of lipid rafts are not completely understood yet, but one of the most important point is that the saturated hydrocarbon chains in cell SLs allows cholesterol to be tightly interacted [86].

Lipids rafts are mainly studied taking advantage of their resistance to solubilization by non-ionic detergent, such as Triton X-100 and Brij-96. Detergent-resistant membrane (DRM) complexes float to low density during sucrose gradient centrifugation and are enriched in rafts proteins and lipids, providing a simple means of identifying possible rafts component [86].

Probably, in lipid rafts, SLs modulate the functional features of several membrane proteins by lateral interactions between SLs and PM proteins, and by short-range alterations of the physico-chemical properties of the protein membrane microenvironment. Indeed, one of the most important property of lipid rafts is that they can include or exclude proteins to variable extents [95].

Proteins with rafts affinity include glycosylphosphatidylinositol (GPI)-anchored proteins, doubly acylated proteins, such as Src-family kinases or the α-subunits of heterotrimeric G proteins, cholesterol-linked and palmitoylated protein and transmembrane proteins.

The reasons why some transmembrane proteins are included in lipid rafts is not clear, but some evidences suggest that the amino acids in the transmembrane domains near the exoplasmic leaflet are critical as well as specific post-translational modification like palmitoylations or myristoylations. In addition, a monomeric transmembrane protein may have a short residence time in rafts, but when the same protein is crosslinked or oligomerized, its affinity for rafts increases.

The distribution of lipid rafts over the cell surface depends on the cell type. Generally, they are more abundant at the PM level, but they are also present in the biosynthetic and endocytic pathway, as Golgi apparatus and ER. For example, in polarized epithelial cells, as epithelial bronchial cells, lipid rafts accumulate in the apical PM.

Generally, raft binding recruit proteins to a new-environment, where the phosphorylation state can be modified by local kinases and phosphatases, resulting in downstream signaling. Nervous system provides many examples of lipid rafts associated signaling. One example is represented by GDNF signaling. The glial-cell-derived neurotrophic factor (GDNF) family of ligands is important for the development and maintenance of the nervous system. GDNF binds to a multicomponent receptor complex that is composed of GPI-linked GDNF receptors-α (GFR-α) and the trans-membrane tyrosine kinase, RET. The receptor subunit GFRα and RET are not associated with each

other in the absence of ligand. However, after extracellular GDNF stimulation, RET moves into rafts, where it associates with GFRα in lipid rafts.

CFTR has been detected in a detergent-resistant membrane fraction prepared from airway epithelial cells, suggesting that it may partition into cholesterol-rich membrane microdomains (lipid rafts), its compartmentalization has not been demonstrated in intact cells and the influence of microdomains on CFTR lateral mobility is unknown [34].

Gangliosides, including GM1, contribute to cluster β1-integrin in the membrane [35]. This study, in particular, shows that CFTR-silenced cells had a 60% decrease in the glycosphingolipid GM1, reduced β1-integrin activation, and decreased phosphorylation of FAK and CAS. The addition of GM1 to CFTR-silenced cells was able to restore β1-integrin activation and phosphorylation of FAK and CAS to control levels. GM1 supplementation enhanced also the migration of CFTR-silenced cells, although it did not fully restore the migration rate to the levels observed in controls. These findings suggest that a reduction in GM1 in CFTR-silenced cells contributes to delayed wound repair in these cells via inhibition of β1-integrin activation and signaling.

Sphingolipids in Cystic Fibrosis

Lung Sphingolipids

A complex pattern of SLs characterizes human lung tissue. Globosides, including globotetraosylCer and globotriaosylCer, are the major class of neutral glycolipids, followed by LacCer, GlcCer and tetrahexosylCer. In addition, among sialylated GLSs, in the lung fourteen different types of gangliosides are present. The most abundant is GM3 followed by GM1, disialo GD3, and trisialosyllactosylCer GT3 [131, 132].

The regulation of ceramide levels is important for lung homeostasis maintenance. Different studies reported the involvement of Cer in pulmonary infection, driven by a wide range of pathogens including *Neisseria gonorrhoeae, Neisseria meningitidis*, *Staphylococcus aureus*, *Pseudomonas aeruginosa*, *Listeria monocytogenes*, *Salmonella typhimurium*, *Escherichia coli*, *mycobacteria*, *measles virus*, *rhinovirus*, and *sindbis virus* [133].

Cer is suitable to manage bacterial and viral infection thanks to its biophysical properties. Cer is characterized by high hydrophobicity, low amphiphilicity and is able to create small Cer-enriched

membrane domain thanks to hydrophobic interaction. Indeed, it is reported that, different stimuli, including bacterial infections, are responsible for the creation of Cer-enriched platforms [134].

Sphingolipids involvement in Cystic Fibrosis lung disease and infection

Large amount of pro-inflammatory mediators, such as interleukin-8 (IL-8), IL-6 and tumor necrosis factor (TNF)-α characterize the airways of CF patients. This condition causes the recruitment of neutrophils, unable to eliminate bacteria, leading to an amplification of inflammation and perpetual infection.

Bacterial components bind different receptors, expressed on epithelial cell surface, such as Toll like receptors 2, 4 and 5. This binding activates a series of kinases leading to the nuclear translocation of transcription factor and expression of pro-inflammatory genes.

As regards the involvement of SLs in CF lung infection, some studies reported that GSLs belonging to the cell surface of epithelial cells could operate as receptor for microorganism. In particular, for *P. aeruginosa*. Indeed, it has been shown that some clinically strains of this bacterium are able to bind asialo-GM1 and asialo-GM2.

Conversely, the role of Cer in CF inflammation and infection is under debate. For instance, Guilbault and colleagues demonstrated that plasma of CF patients displays significantly low levels of several Cer species. In particular, they found in C57BL/6-CFTR mice an overall reduction of Cer level in lung, plasma, ileum and pancreas compared with WT mice [135]. Vilela and co-workers tried to explain the possible molecular mechanism involved in the reduction of ceramide in CF. CF tracheal epithelial cells are characterized by a high level of glutathione that could decrease the intracellular Cer content through the inhibition of neutral sphingomyelinase. The increased activation of the pro-inflammatory transcription factor (NF)-kB, which is responsible for the abnormally high inflammatory response in CF, seems to be due to Cer deficiency. In fact, increased Cer levels, obtained by treatment of CFTR-deficient tracheal epithelial cells with fenretinide, results in an improved ability to control *Pseudomonas aeruginosa* infection [136] [137, 138].

As CFTR-dependent binding of P. aeruginosa and subsequent nuclear signaling appear to be part of the normal host response to this pathogen, the mechanisms and pathways need to be better elucidated. Lipid rafts have been shown to be involved in numerous signaling pathways, as well as in internalization of various microorganisms [139] [140-142].

As previously explained, rafts are dependent on the presence of cholesterol [143] and sphingolipids such as ganglioside GM1 in the cell membrane [144]. Rafts formation leading to the

start of signaling either by the concentration of a low number of appropriate proteins into a high local concentration or by exclusion of certain proteins from the microenvironment [145, 146]. Therefore, the localization of a protein to lipid rafts is often an indicator that the protein is essential for some signaling process. It is hypothesized that CFTR relocates to lipid rafts upon infection with *P. aeruginosa*. In addition, CFTR and GM1 colocalize at the site of *P. aeruginosa* internalization into epithelial cells as demonstrated in the study of Kowalski and colleagues in 2004 [147].

CFTR and sphingolipids

As explained before, literature describes CFTR as a transmembrane protein associated with lipid rats. Taking into account this characteristic, it is reasonable to speculate that the stabilization of the protein or the modulation of its function is driven by SLs interaction.

For instance, Hamai et al reported a relationship between CFTR expression and SL synthesis. Mutated CFTR or decreased expression leads to an increased SL synthesis and as consequence, an increased content of SM, sphingosine and sphinganine at the PM level. In addition, it was observed that the lack of CFTR causes an alteration of PM ceramide composition, with an increased content of long-chain Cer species. The increased Cer production can be interpreted as a cellular response to the PM destabilization. In this context, even the SL synthesis could be a compensatory mechanism directed to increase membrane stability [148].

Another example is represented by the study of Itokazu and colleagues, which described a direct correlation between PM levels of ganglioside GM1 and CFTR expression. CFTR-silenced human airway cells show a decreased content of GM1 and a lower β1-integrin signalling, resulting in a reduction of cell motility. They demonstrated that the addition of GM1 to this type of cells, partially restores cell migration. In addition, they demonstrated that the recovery of CFTR in CFTR-silenced cells significantly increases GM1 levels. On the other hand, the pharmacological inhibition of CFTR in normal cells, decreases GM1 content [35]. These data have implications for the CF pathology, where altered SL levels in CF airway epithelial cells is probably involved in a diminished process of wound repair.

Ramu and colleagues published data related to the regulation of CFTR function by the PM micro-environment. They described that the inhibition of CFTR current is caused by the formation of ceramide from SM hydrolysis. The clusterization of CFTR in membrane areas rich in ceramide makes more difficult the channel activation by phosphorylation of regulatory domain [149].

This set-up gets worse with the presence of some pathogens, such as *Pseudomonas aeruginosa*, which has a SMase activity that hydrolyses SM in situ, leading to the formation of Cer. The reduced CFTR activity caused by *P. aerugionosa*, is accompanied also by an impaired mucociliary clearance and, as consequence, a decreased ability to clear bacteria [150].

Ceramide produced by bacterial SMase has an effect on CFTR stabilization even influencing the regulation of a scaffolding protein ERM (ezrin/radixin/moesin). The ERM complex regulates cytoskeletal PM interaction.

In particular, Ezrin is important for the CFTR activation because it acts as a PKA-anchoring protein, recruiting a PKA to the proximity of CFTR, leading to its activation. Some data reported that ceramide promotes ERM dephosphorylation and, as consequence its inactivation, through a protein phosphatases.

Although several findings clearly demonstrated that CF pulmonary disease is characterized by altered SL metabolism, unfortunately, the direct involvement of SLs in the pathogenesis of CF lung disease is still unclear.

Future progress in understanding the critical role of SLs in the pathophysiology of CF could open new perspectives for the development of alternative SL-based therapeutic strategies to increase the CFTR stability and function at the cell PM.

Aim of the study

The new challenge for the CF therapy is based on the development of small molecules able to rescue the function of the mutated CFTR. Many pharmacological agents have been designed to increase the surface level of mutated CFTR (correctors), as well as its PM activity (potentiators).

Deletion of phenylalanine at position 508 (F508del) in CFTR is the most common CF-causing mutation. Recently, Orkambi®, a combination therapy that includes a corrector of the folding defect of F508del-CFTR (lumacaftor or VX-809) and a potentiator of channel activity (ivacaftor or VX-770), was approved for CF patients homozygous for this mutation. However, clinical studies revealed that the effect of Orkambi® on lung function is slight and very variable [151], [152], [153]. Some *in vitro* findings suggest that the moderate *in vivo* effect may be due to an adverse effect of VX-770 on the stability of the VX-809-corrected protein at PM level [151], [152], [153].

Indeed, many factors contribute to PM CFTR stability, including its compartmentalization in PM macromolecular complex composed by phospholipids, sphingolipids, with particular regards to monosialoganglioside 1 (GM1), and scaffolding proteins such as ezrin and NHERF-1 [154].

Interestingly, it has been proved that in bronchial epithelial cells the lack of CFTR in the PM, such as in the case of the patients carrying the mutation F508del, is associated with a decreased content of GM1 [35]. GM1 is an important bioactive sphingolipid that studies have been reported to play an important role in the control of several PM proteins and its correlation with CFTR lets speculate on its possible role in the CFTR interactome.

In addition, a recent work from Chin and colleagues suggests that VX-770 and its derivatives, due to their high lipophilicity, interact with the lipid bilayer determining changes in the fluidity that are responsible for the destabilization of the VX-809-rescued F508del-CFTR.

On the basis of these evidence, clearly emerges the necessity to develop new strategies that allow to stabilize F508del-CFTR rescued by Orkambi® therapy. On this frame, the main objective of my PhD project was to investigate if interventions aimed at modifying the lipid PM composition of CF bronchial epithelial cells may allow to stabilize F508del-CFTR rescued upon Orkambi® treatment.

In particular, due to the peculiar properties of the ganglioside GM1 and of its lack on CF bronchial epithelial cells, my studies were mainly focused to investigate on the role of this ganglioside in CF, with particular regards to its relationship with CFTR.

Considering all these aspects, the specific aims of my PhD project were:

1. To investigate in bronchial epithelial cells line if gangliosides GM1 and CFTR residing in the same PM microenvironment.

2. To analyse the potential effect of the exogenous administration of ganglioside GM1 on the PM stabilization and function of F508del-CFTR rescued by Orkambi® treatment.
3. Evaluate the potential cytotoxicity of the exogenously administered GM1.

Materials & Methods

Materials

All the commercial products show the highest degree of purity. Water for solution preparation was prepared by using the purification system Milli-Q (Millipore). Trypsin, EDTA Trypan Blue, Trizma base, Glycin, Aprotinin, Albumin, Tween-20, sodium dodecyl sulfate (SDS), NaCl, KCl, Na_2HPO_4, KH_2PO_4, CH_3OH, CH_3CH_2OH, $CHCl_3$, KOH, HCl, $CaCl_2$, citric acid, acetic acid, D-Glucose, BSA, polyisobuthylmethacrylate, O-phenylenediamine, H_2O_2 were purchased from SIGMA-ALDRICH®. Eagle's Minimum Essential Medium (EMEM), fetal bovin serum and sodium pyruvate were bought from Euroclone®; Conduritol-β-epoxide (CBE) from Calbiochem® AMP-DNM [adamantane-pentyl-dNM; N-(5-adamantane-1-yl-methoxy-pentyl) deoxynojirimycin] was a generous gift by *Prof Aerts of Leiden University;* DC Protein Assay by Bio-Rad®. The fluorigenic substrates 4-methylumbelliferyl-β-D-glucopyranoside (MUB-β-Glc), 4-methylumbelliferyl-β-D-galactopyranoside (MUB-β-Gal), 4-methylumbelliferyl n-acetyl-β-d-glucosaminide (MUG), were purchased from Glycosinth™, 6-Hexadecanoylamino-4-methylumbelliferyl phosphorylcholine (HMUB-PC) Moscerdam. Disposable flasks for cell culture of 25 cm^2 and 75 cm^2, 96 multi-well and Petri plates (Ø 100, 60, 35 mm), penicillin/streptomycin, and glutamine were bought from Euroclone®; the 96 microplate with black bottom from PerkinElmer®; PVDF membranes from GE Healthcare Life Sciences; the HPTLC plates and Triton X-100 from Merck Millipore™.

^{3}H-GM1-N_3, [^{3}H]-GM1, Ceramide (Cer), GlucosylCeramide (GlcCer), LactosylCeramide (LacCer), Globotryaosylceramide (Gb3), Sphingomyelin (SM), Phosphatidylethanolamine (PE), Phosphatidylcoline (PC), GM3, GD3 are materials produced directly in the laboratory where I carried out my PhD project.

Methods

Cell models

WT-CFBE, F508del-CFBE: these cell lines are a generous gift *from Gaslini medical Hospital of Genova belonging to "Cell line and DNA Biobank from patient affected by Genetic Disease"*.

CFBE41o$^-$, are CF human bronchial epithelial cells characterized by the loss of CFTR expression; WT-CFBE, F508del-CFBE were stably transfected with the same lentiviral vector, expressing respectively WT-CFTR and F508del/F508del-CFTR. The two cell lines grow up into normal plastic flasks using Eagle's-minimum essential-medium E-MEM, supplemented with 10% of FBS, glutamine (2mM), Penicillin/Streptomycin (100 u/ml and 100 µg/ml respectively), and puromicyn 2 µg/mL for F508del-CFBE while for WT-CFBE I used the concentration of 0,5 µg/mL. The cells were cultured as monolayer in a humidified atmosphere at 37°C and 5% CO_2.

F508del-CFBE-YFP: these cells were a generous gift from the *Lab of Dr. Nicoletta Pedemonte, from Gaslini Hospital, Genova*. The cells were obtained by transfection of F508del-CFBE with the halide-sensitive yellow fluorescent protein (HS-YFP) YFPH148Q/I152L, as previously reported [155]. F508del-CFBE-YFP cells were cultured in the same conditions of F508del-CFBE as reported above for the exception of the fibronectin-collagen coating of the growth area of the support. The coating solution was composed by:

- 1 mg of Human Fibronectin resuspended in 10 mL of LHC-Basal medium,
- 1 ml of bovine collagen type I (30 mg),
- 100 µL of BSA (1 mg/ml),
- and LHC-Basal Medium for reaching 100 ml. Finally the above coating solution was filtered with filter membrane of 0.2 µm.

Cell treatment with CFTR-modulators

Ivacaftor (VX-770) and Lumacaftor (VX-809) purchased from Selleckchem, were solubilized in DMSO (from Sigma) and were administered directly into the cell's medium at the final concentration of 5 µM; as control, I treated the cells only with the same volume of Dimethylsulfoxide (DMSO).

Cell feeding with exogenous ganglioside GM1

GM1 was purified in my laboratory and solubilized in the complete cell culture medium at the final concentration of 10, 50 and 100 µM. In particular, appropriate amount of GM1 powder was solubilized in methanol in a glass tube, dried under gentle N_2 flux, after the total evaporation of the solvent, complete cell medium was added and 5 cycles of shaking and sonication were performed allowing the complete solubilisation of the ganglioside.

MTT assay

Cells were plated at the density of 13500 cells/ cm^2 in 96-wells microplate, and subjected to the different treatment for 6, 12, 24 and 48 hours. After each time-point, the medium was removed and the cells were washed with PBS, after the wash I added 71 µL of MTT solution to each well, prepared by dissolving thiazolyl blue tetrazolium bromide in PBS at the concentration of 4 mg/ml, subsequently they were dissolved in cell culture medium with the ratio of 1:4. The cells were incubated for 4 hours in a humidified atmosphere at 37°C and 5% CO_2. After that, MTT solution was removed and 57 µL of lysis buffer were added (95% isopropanol, 5% formic acid). After ten minutes of shaking, the concentration of the formation of formazan salts, was evaluated using a microplate reader Victor (Perkin-Elmer), at the wave-length of 570 nm.

Determination of protein content through DC protein assay

Samples protein content was determined using DC Protein Assay (Bio-Rad), which is based on Lowry's method. The assay was performed in a 96-well microplate using 5 µl of H_20 for the background, 5 µl containing growing amounts of bovine serum albumin (BSA) for the standards, and 5 µl of cell lysates. After sequential addition of 25 µl of reagent A (alkaline solution of copper tartrate) and 200 µl of reagent B (dilution of Folin reagent), the microplate was incubated in mild agitation for 15 minutes followed by spectrophotometric reading at 750 nm wavelength by a microplate reader (Victor, Perkin-Elmer). Protein content was calculated by interpolation of the average absorbance value of the sample within the calibration curve built using BSA standards. The assay was considered linear in a 0.2-2 mg/ml range.

SDS-PAGE and Western Blotting

The samples were analysed using electrophoresis on a polyacrylamide gel in denaturing conditions. The samples were resuspended in Laemmli buffer (62.5 mM Tris-HCl pH 6.8, 2% SDS, 5% 2-mercaptoethanol, 0.01% Bromophenol blue, 10% glycerol) and boiled for 10 minutes at 100°C before being analysed. Otherwise, the sample dedicated to the analyses of CFTR were resuspended in Laemmli buffer and treated at 40°C for 10 minutes. The electrophoresis run was performed using a Miniprotean II unit, produced by Bio-Rad. Proteins from cell homogenates sample were separated using a precasted gel with the gradient of 4-20% of poly-acrylamide (Bio-Rad).

After electrophoresis separation, proteins were transferred into polyvinylidene difluoride (PVDF) membranes, at 200 mA for 3 hours at 4°C with a wet blotting (Mini Transblot Biorad). The transfer buffer used is Blotting buffer (25 mM Tris-HCl, 192 mM glycine, 15 % methanol, pH 8.0-8.5) Briefly, after the transfer the PVDF membrane were incubated in 5% skim milk in TBS-T 0,01% buffer (1 mM Tris-HCl pH 8, 150 mM NaCl, 0.01% Tween) to block the aspecific binding sites of the membrane. Then the PVDF was then washed three times with TBS-T 0.01% and incubated for 1 hour at room temperature (RT), membranes were incubated overnight at 4°C with the appropriate primary antibodies diluted in 5% skim milk in TBS-T 0,01% buffer or in 5% bovine serum albumin (BSA) in TBS-T 0,01%. CFTR antibody, purchased from the Cystic Fibrosis North American Foundation, was used at the final dilution of 1:2000; Caspase 3, Cyclin-d2 (Cell Signaling), were used at the final dilution of 1:1000; EBP50 (NHERF-1), ezrin and p-ezrin antibodies (BD sciences) were used at the final dilution of 1:500.

After washing with TBS-T 0,1%, the PVDF was incubated for 1 hour at RT with secondary antibodies resuspended in 5% skim milk in TBS-T 0,1 % or in 5% BSA in TBS-T 0,1%. The Calnexin antibody (BD sciences) was used at the final dilution of 1:1000. GAPDH antibody (Sigma) was used at the dilution of 1:7000 and β-actin antibody (Cell signalling) was used at the dilution of 1:1000.

The membrane was then washed again for three times and the peroxidase activity was assessed through incubation with a non-radioactive light emitting substrate for the detection of immobilized specific antigens conjugated with horseradish peroxidase-linked antibodies (Westar Cyanagen) for 1,5 minutes. The signals were revealed using a Mini HD9 (UviTec, Cambridge) and analyzed by Nine Alliance mini HD9 software.

Cell feeding with [1-^{3}H]-GM1

The [1-^{3}Hsph]-GM1 was administered to the cells plated in petri plate at the concentration of 90 nM (corresponding to 0,09 µCi for each plate). Briefly, [1-^{3}Hsph]-GM1 dissolved in methanol was transferred into a sterile glass tube and dried under a nitrogen stream, and [1-^{3}H]-GM1 was solubilized in an appropriate volume of pre-warmed (37° C) medium (E-MEM).

The correct solubilisation was verified by measuring the radioactivity associated with an aliquot of medium by using beta-scintillator.

After different time-points, (12, 24 and 48 hours), cells were collected and were used to perform the analysis of radioactive lipids. Briefly, cells were lyophilized and subjected to lipid extraction.

Total lipids from lyophilized cells were extracted with $CHCl_3$:CH_3OH:H_2O 20:10:1 by vol, followed by a second extraction with $CHCl_3$:CH_3OH 2:1 by vol. The radioactivity associated with the total lipid extract, was evaluated by liquid scintillations using beta-counter system.

[^{3}H]SLs of total extracts were separated by high performance thin layer chromatography (HPTLC) using the solvent system $CHCl_3$:CH_3OH: aqueous solution of 0.2% $CaCl_2$ 50:42:11 by vol. [^{3}H]-SLs were identified by digital autoradiography using ^{T}Racer system (Biospace Lab) and quantified by M3vision software. The lipids identification was performed using purified radioactive standards [156].

Evaluation of the lipids pattern

Lipids from the lyophilized samples were extracted with chloroform:methanol:water 20:10:1 (v:v:v) and subjected to a two-phase Folch's partitioning to obtain the aqueous (AP) and the organic phases (OP) [157]. Briefly, 1550 µL of the solvent system were added to the lyophilized samples. The samples were then mixed at RT for 15 minutes and centrifuged at 16.000 x g, for 10 minutes at RT. The supernatant was collected as total lipid extract (TLE) and the extraction was repeated again by adding the solvent system to the pellets. The pellets were air dried and resuspended in 1 N NaOH and incubated overnight at RT and then NaOH was diluted to 0.05 N for the determination of the protein content with DC assay.

Aliquots of the TLE were then subjected to phase partitioning adding 20% of water by volume. The samples were then mixed at RT for 15 minutes and centrifuged at 16.000 x g, for 15 minutes at RT. The AP was recovered, and an equivalent volume of CH_3OH:H_2O 1:1 (v:v) was added to the organic

phase and processed as described before in order to recover all cell gangliosides in AP fraction. The aqueous phases were dried under N_2 flux, and resuspended in water before undergoing dialysis and lyophilization. The organic phases were dried under N_2 flux and resuspended in a known volume of chloroform:methanol 2:1. Aliquots of the organic phases were then subjected to alkaline treatment to remove glycerophospholipids. Alkaline treatment allows to remove glycerophospholipids from the organic phases, breaking their ester bonds, and maintaining the amide linkage of sphingolipids unaltered. Aliquots of organic phases were dried under nitrogen flow and the residue was resuspended with 100 µl of 0,6 M NaOH in methanol and incubated at 37°C for three hours and overnight at RT. The reaction was blocked by adding 120 µl 0,5 M HCl in methanol. Finally, after phase separation (by adding 1.050 µl of chloroform:methanol:water 70:18:17 by vol), the new organic phases were used for TLC analysis. [157]

Thin layer chromatography

To determine endogenous lipid content, the various samples were analysed by monodimensional silica gel HPTLC using different solvent systems. The lipids contained in OP and MetOP were separated using a solvent system composed by chloroform:methanol:H_2O 110:40:6 (v:v:v) and visualised with anisaldehyde reagent, whereas for AP chloroform:methanol:0.2% aqueous $CaCl_2$ 50:42:11 (v:v:v) were used and GM1 was revealed by immunostaining with cholera toxin. Glycerophospholipid pattern was determined on OP using the solvent system: chloroform:methanol:acetic acid:water 30:20:2:1 (v:v:v:v) and it was visualised with phosphorous reagent. Cholesterol content was evaluated on MetOP using exane:ethyl acetate 3:2 as solvent system and it was visualised with anisaldehyde reagent. The lipids were identified by the comigration on the same HPTLC of authentic standards.

TLC immunostaining with cholera toxin

Cholera toxin binding to GM1 was assessed by TLC immunostaining following standard protocols [158]. Briefly, after chromatographic separation (as described above) the TLC plates were coated with a polyisobuthylmethacrylate solution [157], three times, and air dried for 1 hour before being immersed in blocking solution (3% BSA in PBS) for 1 hour. The plates were then incubated with cholera toxin at 10 µg/mL in 1% BSA in PBS for 1 hours at RT. After the incubation, two washes

with PBS were performed and the immunoreactive bands were revealed using o-phenylenediamine (OPD)/H_2O_2 in 0.05 M citrate-phosphate buffer pH 5.0.

Photolabelling experiment

[1-^{3}H]-GM1-N_3 is a radioactive and photoactivable GM1 derivative. In particular, ^{3}H-GM1-N_3 is radioactive on sphingosine and carries a photoactivable group at the terminal portion of the fatty acid. As photoactivable group, I used the azide linked to nitrophenyl which is very sensitive to light and it must be handled with care in dark conditions (i.e. under red safelight).

[1-^{3}H]-GM1-N_3 was administered at the concentration of 1.25 µM in presence of the same amount of normal GM1. Briefly, under dark conditions, the appropriate amount of [1-^{3}H]-GM1-N_3 dissolved in 2-propanol was transferred into a sterile glass tube and dried under a nitrogen stream. After that, [1-^{3}H]-GM1-N_3 was solubilized in an appropriate volume of pre-warmed (37° C) medium (E-MEM) and administered to the cells previously plated in petri plate and subjected to different treatments. After six hours in dark conditions, the medium was collected and its radioactivity was evaluated. The cells were washed with medium containing FBS, for 30 minutes and then with PBS containing Na_3VO_4. Finally, the cells were illuminated with UV lamp for 40 minutes. After this, the cells were collected in PBS containing Na_3VO_4, and lysed to performed the SDS-PAGE analysis.

Enzymatic activity associated with cell lysate

The enzymatic activities of β-Glucocerebrosidase (GCase), non lysosomal β-glucosylceramidase (NLGase), β-Galactosidase (β-Gal), β-Hexosaminidase (β-Hex), and sphingomyelinase (SMase) in the total cell lysates were determined using fluorigenic substrates as described by Aureli and colleagues, with few modifications [159, 160]

Briefly, cells were washed twice with PBS and were harvested and suspended in water in the presence of a protease inhibitor cocktail (Sigma-Aldrich). Total cell protein content was evaluated by DC protein assay (Biorad) according to manufacturer instructions.

Equal amount of cell proteins were transferred into a 96-well microplate and the assay was performed three-fold in replicate. MUB-Glc was solubilized in McIlvaine buffer (pH 6) at the

concentration of 24 mM. MUB-Gal, MUG and H-MUB-PC were solubilized in McIlvaine buffer (pH 5.2) at the concentration of 250 µM, 2 mM and 100 µM respectively.

For GCase and NLGase assays, cells were pre-incubated for 30 minutes at RT with 5 nM AMP-dNM [adamantane-pentyl-dNM; N-(5-adamantane-1-yl-methoxy-pentyl) deoxynojirimycin] and 1 mM Conduritol B Epoxide (CBE) respectively.

The reaction mixtures were incubated at 37°C under gentle shaking. After transferring 10 µl of the reaction mixtures to a 96 black well microplate and adding 190 µl of glycine (0.25M, pH 10.7), the obtained fluorescence was detected at different time points by a Victor microplate reader (Perkin Elmer), (MUB: λ_{ex}: 355 nm /λ_{em}: 460nm; H-MUB: λ_{ex}: 405 nm /λ_{em}: 460nm) after adding 190 µl of 0.25 M glycine (containing 0,3% Triton X-100 for SMase assay), pH 10.7.

Standards free MUB and H-MUB were used to set the calibration curves in order to quantify the substrates hydrolysis.

The enzymatic activity was expressed as pmol of product on mg protein per hour.

Enzymatic activity associated with cell plasma membrane

The assay, used during my experiments, allows the detection of the PM associated enzymatic activity directly on living cells, using fluorigenic substrates. This method is based on the observation that the fluorigenic substrates commonly used for the in vitro assay of glycohydrolase activities are not taken up by living cells [161].

Indeed, under the appropriate experimental conditions, it is not possible to observe any fluorescence associated with cells. Moreover, the artificial substrates did not undergo to spontaneous hydrolysis or to hydrolysis driven by secreted enzymes. Thus, their hydrolysis under these experimental conditions is due exclusively to the PM-associated enzymatic activities [162].

PM associated activities of β-Galactosidase (β-Gal), β-Glucocerebrosidase (GCase), non lysosomal β-glucosylceramidase (NLGase), β-Hexosaminidase (β-Hex) and sphingomyelinase (SMase) activities were determined on living cells, plated in 96-well microplate at density of 20000 cells/well, by a high throughput assay.

For GCase and NLGase assays, cells were pre-incubated for 30 minutes at RT in DMEM-F12 with 5 nM AMP-dNM [adamantane-pentyl-dNM; N-(5-adamantane-1-yl-methoxy-pentyl)

deoxynojirimycin] and 1 mM CBE respectively [163] and then incubated with MUB-Glc solubilized in DMEM-F2 pH 6.2 at the final concentration of 6 mM. β-Gal, and β-Hex activities were assayed using the artificial substrates MUB-Gal and solubilized in DMEM-F12 without phenol red at pH 6, at the final concentrations of 250 µM and 2 mM respectively. SMase activity was assayed using the artificial substrates 6-hexadecanoylamino-4-methylumbelliferyl-phosphoryl-choline (H-MUB-PC) solubilized in the same DMEM-F12 at the final concentration of 100 µM. At different time points aliquots of medium (10 µl) were analyzed by fluorimeter in a microplate reader (Victor, Perkin Elmer) (MUB: λ_{ex}: 355 nm /λ_{em}: 460nm; H-MUB: λ_{ex}: 405 nm /λ_{em}: 460nm) after adding 190 µl of 0.25 M glycine (containing 0,3% Triton X-100 for SMase assay), pH 10.7.

Standards free MUB and H-MUB were used to set the calibration curves in order to quantify the substrates hydrolysis.

The enzymatic activity was expressed as pmol of products on 10^6cells, per hour.

Study of CFTR function using video-live image microscopy

The following experiments were carried out in collaboration with Dr. Anna Tamanini from the Department of Pathology of Verona University Hospital.

F508del-CFBE-YFP cells were plated on sterile glass coverslips in complete medium (diameter 24 mm, thickness 0.13-0.17 from VWR International, West Chester, Pennsylvania, USA) previously coated with Fibronectin-Collagen as described above. In particular, $30x10^6$ cells were plated for each coverslip in order to reach the 80% of confluence after 48 hours at the time of the incubation.

The day after seeding, the F508del-CFBE-YFP cells were treated with CFTR-modulators and ganglioside GM1 as previously described.

After 48 hours treatment, the culture medium was removed and the cells were washed two times with Dulbecco's PBS (137 mM NaCl, 2,7 mM KCl, 8,1 mM Na_2HPO_4, 1,5 mM KH_2PO_4, 1 mM $CaCl_2$, 0.5 mM $MgCl_2$) and after this, they were incubated with stimulation cocktail (Forskolin + VX-770 in Dulbecco's PBS) or inhibition cocktail (CFTR Inhibitor-172 in Dulbecco's PBS) for 30 minutes. After that, cells were washed with Dulbecco's PBS and the coverslips were transferred into a thermostatically controlled perfusion chamber of the microscope, to maintain the cells alive and in their physiological conditions.

The microscope used was Nikon TMD inverted microscope with a Nikon Fluor 40 objective. The signal was acquired with a Hamamatsu C2400–97 charge-coupled intensified video camera at a rate of 1 frame/3 s. Fluorescence coming from each single cell was analyzed by customized software (Spin, Vicenza, Italy). Results are presented as transformed data to obtain the percentage signal variation (Fx) relative to the time of addition of the stimulus, according to the equation: Fx ([Ft- Fo]/Fo) 100, where Ft and Fo are the fluorescence values at the time t and at the time of addition of iodide, 20 respectively.

Statistical analysis

All the experiments were performed in triplicate and statistical significance was determined by Student-Neumann-Keuls post hoc test (comparison between two groups) and for more than two groups by one-way or two-way ANOVA (followed by Turkey or Dunnett Neueman-Keuls on Bonferroni post test), with $p < 0.05$ as significant.

Results

Overexpression of F508del-CFTR induces alteration of the lipid composition in cystic fibrosis bronchial epithelial cells CFBE

CF, the most common genetic disease, caused by mutations in the CFTR gene, affects several organs, with major complications observed in the lung. Indeed, the major cause of morbidity and mortality in CF patients is respiratory failure secondary to pulmonary infections and inflammation.
In the lung of CF patients, the lack of CFTR is responsible for secondary alteration especially in the physiology of the bronchial epithelial cells that contributes to aggravates the phenotypical manifestation of the disease.
Recent data from literature show that the reduced content of CFTR at PM in CFTR-silenced cells is followed by a decreased content of ganglioside GM1 [35]. GM1 is an important bioactive lipid involved in the organization of macromolecular complex belonging to PM, called lipid rafts.
Interestingly, it has been demonstrated that CFTR is associated with this particular membrane structure and that only a precise coordination between the lipids and CFTR-scaffolding proteins allow CFTR to exert its main function. In particular, just the loss of only one among the components, could compromise the formation of the entire complex and could be at the basis of the incapability of the current CF therapy to stably restore the function of F508del-CFTR.
Based on these considerations, the main aim of my PhD project was to investigate the possible role of the ganglioside GM1 on the CFTR PM stabilization and function. To this purpose, I first need to select the suitable cellular model which can mimic physiological feature of CF and non-CF bronchial epithelial cells.
One of the more used *in vitro* model of CF bronchial epithelial cells, is represented by the CFBE41o$^-$ cell line: these cells have lost CFTR protein expression and so they represent the appropriate cellular model on which induce the stable expression of:
I) the WT form of CFTR to have a control cell line (WT-CFBE) and
II) the F508del-CFTR to have the pathological counterpart with the same genetic background (F508del-CFBE).
To do this, CFBE41o$^-$ cells were transfected with a lentiviral vector for the expression of WT-CFTR or F508del-CFTR; these cell lines are cultured with the same medium, E-MEM added up with the selecting antibiotic puromycin.
Using these cell lines, I firstly performed lipid analysis by thin layer chromatography. The cells were collected at the 80% of confluence, lysed and lyophilized. Lipids from the lyophilized samples

were extracted with a solvent system composed of chloroform:methanol:water 20:10:1 (v:v:v) and subjected to a two-phase Folch's partitioning to obtain the aqueous (AP) and the organic phases (OP). Aliquots of the organic phase were then subjected to alkaline treatment to remove glycerophospholipids (MetOP) [157]. Aliquots of AP, OP and MetOP corresponding to the same amount of cellular proteins of each cell lines, were loaded on a plate for thin layer chromatography and the lipids were then separated by using different solvent systems and visualized by specific reagents.

As shown in figure 12, F508del-CFBE cells revealed differences in gangliosides composition; in particular, GM1 seems to be slightly decreased while ganglioside GM3 was significantly higher with respect to WT-CFBE cells. From the analysis of neutral lipids, the most significant difference was represented by lactosylceramide, which was abundant in WT-CFBE cells and scantly detectable in the pathological counterpart. I also analysed cholesterol content and as shown in panel C, F508del-CFBE cells are characterized by a reduced content of cholesterol with respect to WT-CFBE cells.

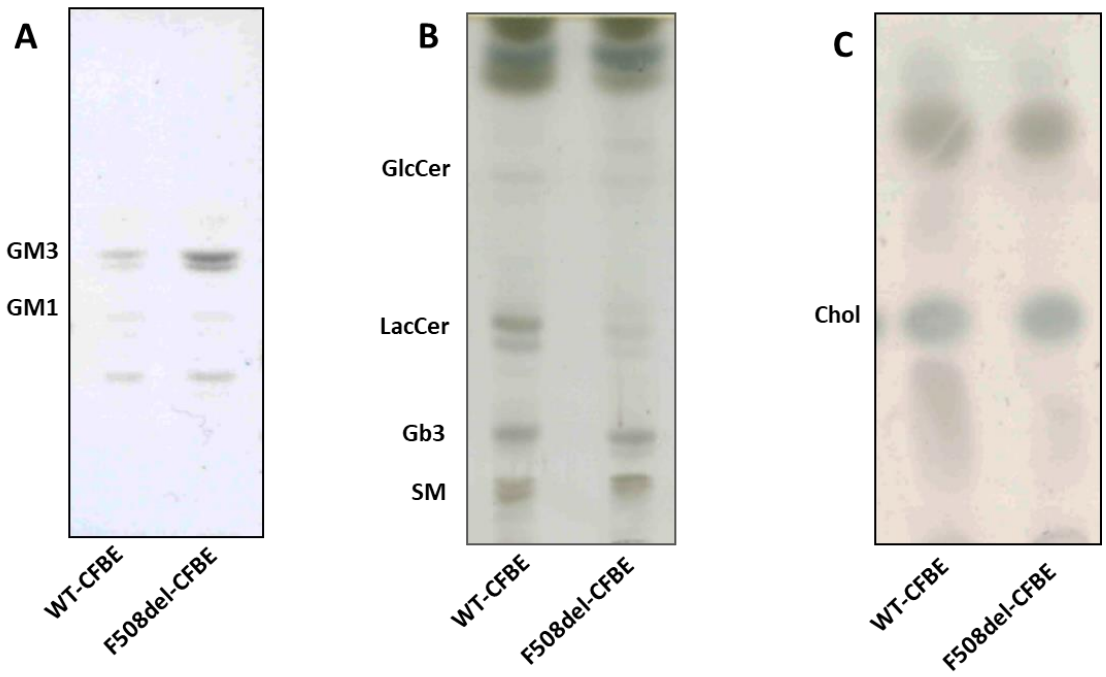

Figure 12: Lipid composition of WT and F508del-CFBE cells
Cells lysates from CFBE overexpressing WT or F508del-CFTR were subjected to lipid extraction with $CHCl_3$:CH_3OH:H_2O 20:10:1 (v:v:v). Total lipid extracts were further subjected to a two-phase partitioning resulting in the separation of an aqueous phase (AP) containing gangliosides and in an organic phase (OP) containing all other lipids. Aliquots of the organic phases were then subjected to alkaline treatment to remove glycerophospholipids (MetOP).
***(A)**: ganglioside pattern were evaluated loading TLC with a volume of AP equivalent to 700 µg of cell lysate. Lipids were separated using the solvent system $CHCl_3$:CH_3OH:0,2% aqueous solution of $CaCl_2$ 50:42:11 (v:v:v) and visualized by Earlich reactive.*
***(B):** neutral lipids were evaluated loading TLC with a volume of MetOP equivalent to 500 µg of cell lysate. Lipids were separated using the solvent system $CHCl_3$:CH_3OH: H_2O 110:40:6 (v:v:v) and visualized by anisaldehyde reagent.*
***(C)**: cholesterol was evaluated loading TLC with a volume of MetOP equivalent to 300 µg of cell lysate. Lipids were separated using the solvent system Hexane: Ethyl Acetate 3:2 (v:v) and visualized by anisaldehyde reagent.*
GlcCer: glucosylceramide; LacCer: Lactosylceramide; SM: sphingomyelin; GM1: ganglioside, Gb3: Globoatriosylceramide; chol: Cholesterol

To further confirm the modifications in the cellular content of GM1, I performed an immunostaining analysis with cholera toxin because of the high affinity of its subunit β for the above said ganglioside. After separation with thin layer chromatography, which was performed in the same conditions used before for the gangliosides analyses, the plate was incubated with the β-subunit of cholera toxin HRP-conjugated and then the signal was revealed using o-phenylenediamine.

As shown in figure 13, the immunostaining with cholera toxin revealed a decreased content of GM1 in F508del-CFBE cells of about ~ 40% with respect to WT-CFBE cell line.

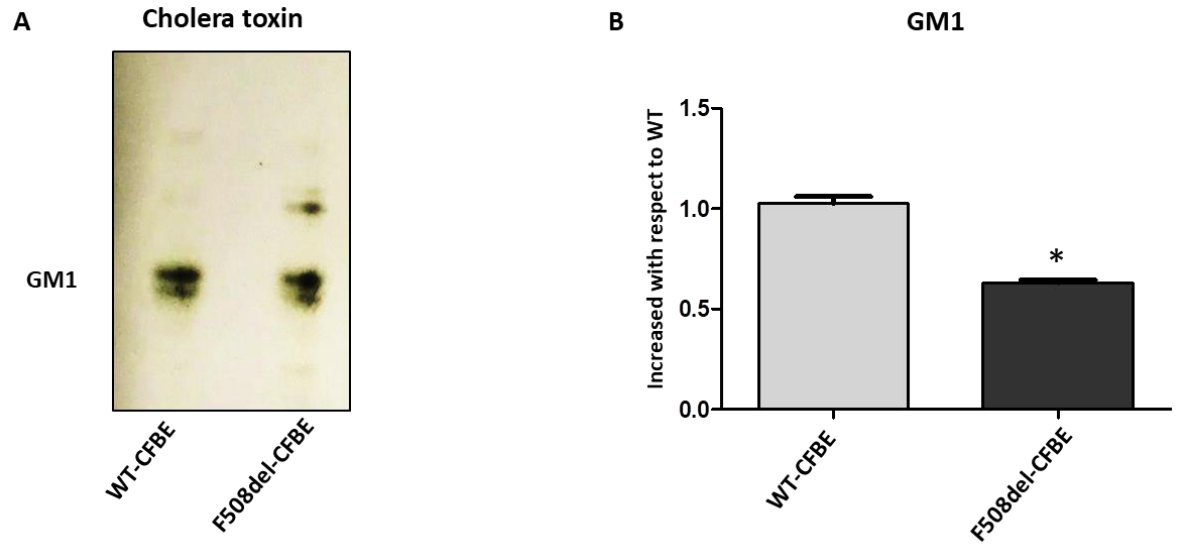

Figure 13: GM1 levels in CFBE cells over-expressing wild type and F508del-CFTR
(A): *TLC immunostaining with cholera toxin: briefly, TLC was loaded with aqueous volume equivalent to the same amount of total cell protein (150 µg each). After chromatographic separation with solvent system: $CHCl_3$:CH_3OH:0,2% aqueous solution of $CaCl_2$ 50:42:11 by vol., TLC plates were fixed with a polyisobuthylmethacrylate solution, air dried and incubated with 3% BSA in PBS for 1 hour. Plates were then incubated with cholera toxin at the concentration of 10 µg/mL in 1% BSA in PBS for 1 hour at room temperature (RT). After washes with PBS the immunoreactive bands were revealed using o-phenylenediamine (OPD)/H_2O_2 in 0.05 M citrate-phosphate buffer pH 5.0.*
(B)*: Semi quantitative graph of GM1 content in WT and F508del-CFBE cell lines obtained by densitometric quantification of GM1 positive bands using ImageJ software; the content of GM1 was represented as fold increase with respect to WT-CFBE.*
**p<0.05 vs WT-CFBE*

Taken together these results suggest that in bronchial epithelial cells the expression of F508del-CFTR induces modifications in sphingolipid composition.

Evidences in literature proved that mutations in CFTR affects also the endo-lysosomal compartment which is one of the main cellular districts involved in the SLs catabolism. I evaluated the effect of the overexpression of F508del-CFTR on the main hydrolases involved in the sphingolipid catabolism. In particular, I evaluated the enzymatic activities of β-glucocerebrosidase (GCase), non lysosomal β-glucosylceramidase (NLGase), β-galactosidase (β-gal), β-hexosaminidase (β-hex), and sphingomyelinase (SMase) by an *in vitro* assay based on the use of fluorigenic substrates as described by Aureli and colleagues, with few modifications [159], [160].

Interestingly, this analysis revealed some differences in the hydrolases activity (figure 14). In particular the activity of GCase, NLGase, β-gal, SMase were increased respectively of 3, 1.5, 2, and 2.5 fold in F508del-CFBE with respect to WT-CFBE cells. No differences were detected for β-hex.

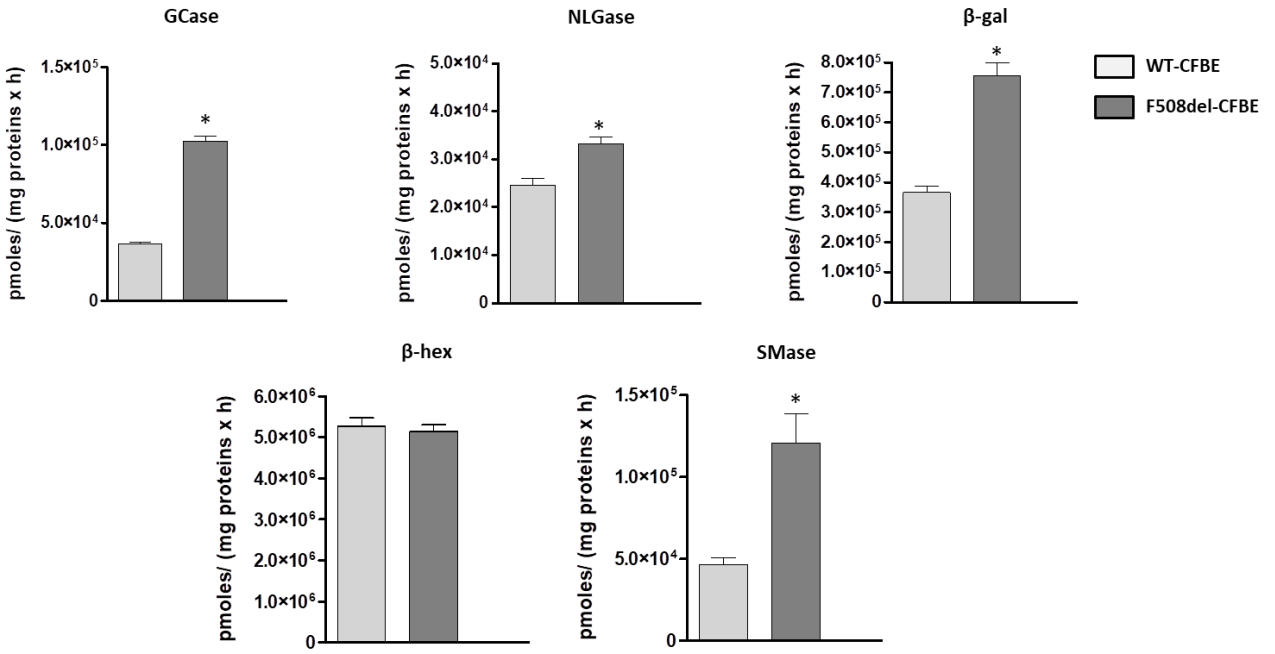

Figure 14: Hydrolases activity associated with total cell lysate of WT and F508del-CFBE cell lines
The measurement of the hydrolases activity was conducted on cell lysates using an in vitro assay based on artificial fluorigenic substrates. The enzymatic activity was expressed as pmoles of product on mg of proteins per hour.
GCase: β-Glucocerebrosidase; NLGase: Non lysosomal β-Glucosylceramidase; β-gal: β-galactosidase; β-hex: β-hexosaminidase; SMase: Sphingomyelinase
**p<0.05 vs WT-CFBE*

It is nowadays demonstrated the existence of a crosstalk among the lysosomal enzymes and the counterpart associated with the PM. For this reason, I subsequently measured the enzymatic activities of the same hydrolases but using an assay that allow to detect the activity only of the enzymes associated with the cell surface.

As result, I found that F508del-CFTR cells were characterized by 1.5 fold increase in GCase and NLGase, whereas the activity of β-hex and SMase decreased of about 2 fold with respect to WT-CFBE cells. No changes were found in the activity of PM β-gal (figure 15).

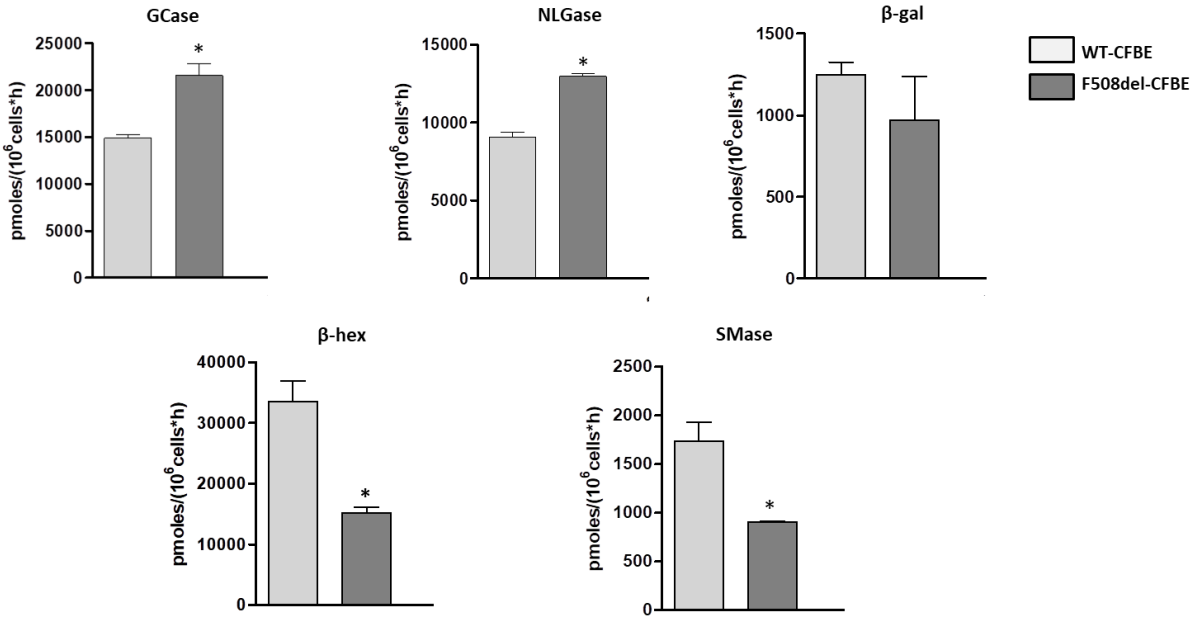

Figure 15: Hydrolases activity associated with the cell plasma membrane of WT and F508del-CFBE cell lines

The measurement of the plasma membrane hydrolases activities were conducted on living cells, using artificial fluorigenic substrates. The enzymatic activity was expressed as pmoles of product, on 10^6 cells per hour.

GCase: β-Glucocerebrosidase; NLGase: Non lysosomal β-Glucosylceramidase; β-gal: β-galactosidase; β-hex: β-hexosaminidase; SMase: Sphingomyelinase

**p<0.03 vs CFBE*

Taken together these results indicate that the expression of F508del-CFTR induces in bronchial epithelial cells changes in the sphingolipids composition and in their catabolism both intracellularly and at the PM level. In addition, This result confirm the validity of WT-CFBE and F508del-CFBE cell lines as experimental model to study the relationship between CFTR and PM sphingolipids.

The chronic treatment of F508del-CFBE cells with potentiator VX-770 reverts the effect of the corrector VX-809 in terms of F508del-CFTR maturation, CFTR scaffolding protein content and lipid composition

Nowadays the new therapeutic strategies for the treatment of CF are focused on restoring mutated-CFTR function. Indeed, small molecules that are able to restore mutated-CFTR function have recently been developed. The first small molecule enrolled in a clinical trial was the potentiator VX-770 Ivacaftor (Kalydeco®, Vertex Pharmaceuticals). The drug was able to increase chloride transport by potentiating the channel-open probability (or gating) of the G551D-CFTR protein. Ivacaftor has been approved by the US Food and Drug Administration (FDA) and European Commission for the treatment of CF in patients aged ≥ 6 years who have the G551D mutation in the CFTR gene [164]. Unfortunately, the mutation G551D includes only the 2% of CF patients, while the most common mutation is the F508del, which affects around the 75% of Caucasian population. F508del mutation affects not only the open state of the channel but also its folding in the ER, for this reason the use of the only VX-770 is not enough to restore its activity.

The challenge was the development of a molecule which could drive protein folding, to this aim it has been developed the corrector VX-809, Lumacaftor a drug able to correct mutated-CFTR increasing its targeting to the cell PM. The therapeutic strategy followed for CF patients carrying F508del was the combined treatment with Lumacaftor and Ivacaftor called with the commercial name of Orkambi®. Despite an improvement of F508del-CFTR activity upon an acute treatment, during the chronic treatment Orkambi® loose its beneficial function suggesting an instability of the channel at the cell surface.

Interestingly, *in vitro* studies suggested that VX-770 contributes to F508del-CFTR destabilization at the PM level by an interaction with the lipid environment of CFTR.

To further investigate this issue, I evaluated the effect of VX-770, VX-809 and of their combination on F508del-CFTR cells in terms of F508del-CFTR maturation, CFTR content, scaffolding proteins ezrin and NHERF-1, and on lipid composition.

F508del-CFBE cells were treated for 48 hours with 5μM of VX-770, and VX-809 alone or in combination. After the incubation, I analysed CFTR maturation by using SDS-PAGE and Western Blot technique with a specific antibody against CFTR.

As shown in figure 16, untreated F508del-CFBE cells are characterized by the presence of the only immature form of CFTR known as b-band. When the cells were treated with only potentiator VX-

770, I didn't observe any change in CFTR maturation. Indeed, when I treated the cells with corrector VX-809, it was possible to detect a remarkable maturation of the protein indicated as band c. Unfortunately, after treating the cells with both drugs, the positive effect of VX-809 on CFTR maturation was completely lost, suggesting a negative effect of VX-770.

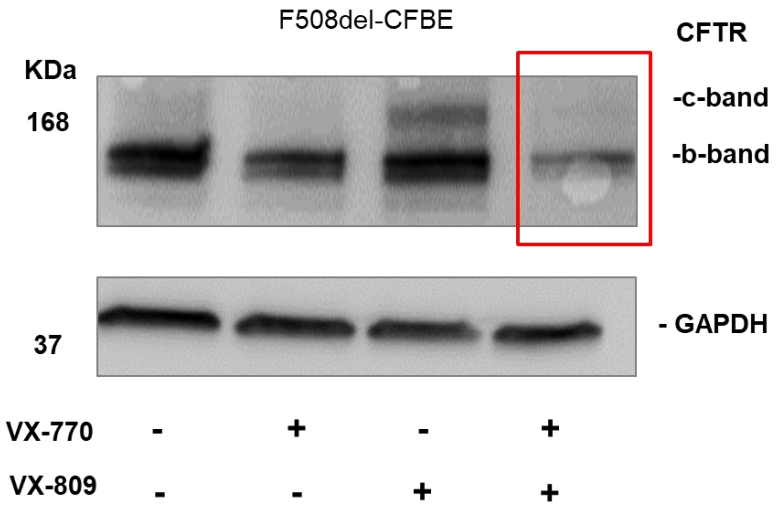

Figure 16: Effect of VX-770 and VX-809 on F508del-CFTR maturation
Cells overexpressing F508del-CFTR were treated or not for 48 hours with 5 µM VX-770 and/or VX-809. CFTR was evaluated by immunoblotting. GAPDH was evaluated as loading control.

After that, I evaluated the effect of the different treatments on the protein levels of CFTR-scaffolding proteins such as ezrin and NHERF-1.

As shown in the Western blot reported in figure 17, the treatment of the F508del-CFBE cells with corrector VX-809 induced an increase in the protein level of NHERF-1, ezrin and its bioactive form p-ezrin, with respect to untreated cells. Instead, when I treated the cells with the potentiator VX-770, I observed that all of them have significantly decreased, condition preserved also in presence of the combined treatment. These data highlight that once again the potentiator seems to have a negative effect on F508del-CFTR maturation and in the formation of the interactome that is involved in its PM stability and function.

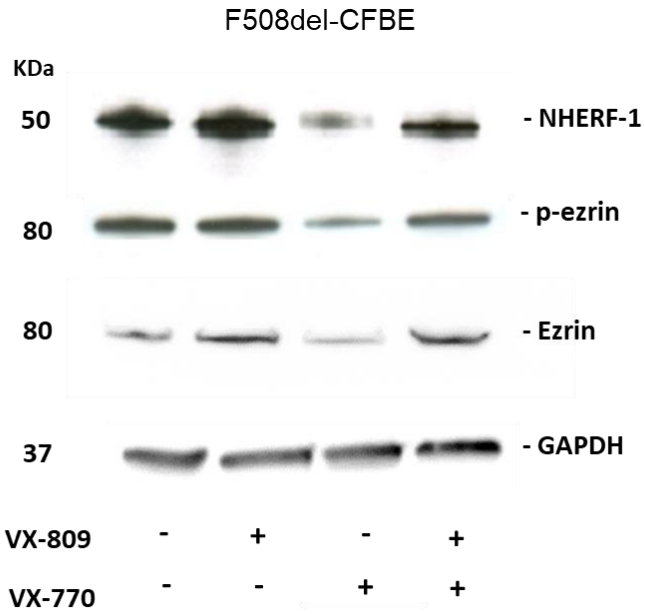

Figure 17: VX-770 induces a decrease on content of CFTR scaffolding proteins
Cells overexpressing F508del-CFTR were treated or not for 48 hours with 5 µM VX-770 and/or 5 µM VX-809. NHERF-1, ezrin and p-ezrin were evaluated by immunoblotting. GAPDH was evaluated as loading control.

As above said, CFTR at cell PM needs to have a specific microenvironment, featured by both specific lipids and proteins. Since VX-770 compromises the expression of the CFTR-scaffolding proteins I evaluated the effects of corrector and potentiator treatment on lipid composition.

Treated cells were collected, lysed and lyophilised; lipids from the lyophilised samples were extracted with chloroform:methanol:water 20:10:1 (v:v:v) and subjected to a two-phase Folch's partitioning to obtain the aqueous (AP) and the organic phases (OP). Aliquots of the organic phase were then subjected to alkaline treatment to remove glycerophospholipids (MetOP) as previously described. The lipids were then separated by TLC using different solvent systems.

The analysis of neutral lipids, as shown in figure 18 panel A, indicate that all the treatment induced a decrease in the content of globoatriosylceramide with respect to untreated cells. Whereas, the potentiator induced a decrease also in the cellular levels of lactosylceramide. I also analyzed the phospholipids pattern and as pointed out in figure 18 panel B, I couldn't observe relevant differences between control and treated cells. By the analyses of the cholesterol emerges that in presence of VX-770 its cellular content decreased (figure 18 panel C).

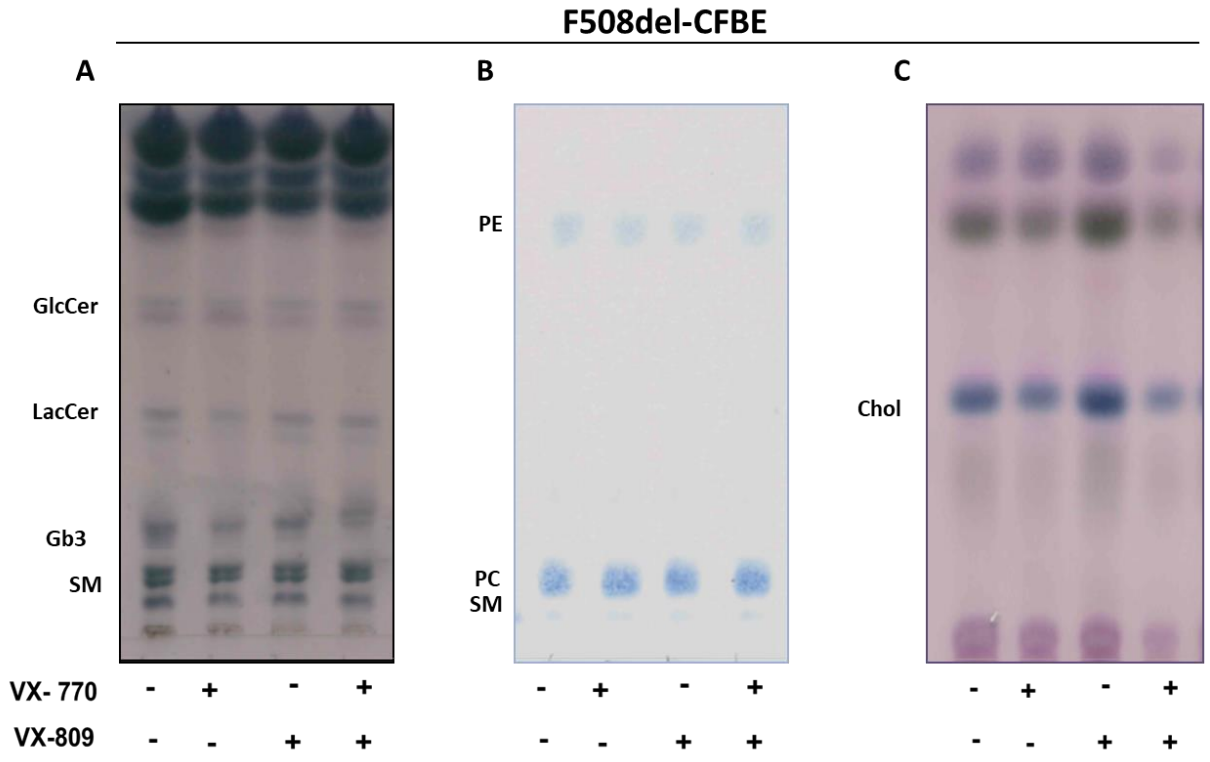

Figure 18: Effect of VX-770 and VX-809 on F508del-CFBE cells

Cells overexpressing F508del-CFTR were treated or not for 48 hours with 5 µM VX-770 and/or 5 µM VX-809. Cells lysates were then subjected to lipid extraction with $CHCl_3$:CH_3OH:H_2O 20:10:1 (v:v:v). Total lipid extracts were further subjected to a two-phase partitioning resulting in the separation of an aqueous phase (AP) containing gangliosides and in an organic phase (OP) containing all other lipids. Aliquots of the organic phases were then subjected to alkaline treatment to remove glycerophospholipids (MetOP).

***(A)**: neutral lipids were evaluated loading TLC with a volume of MetOP equivalent to 500 µg of cell lysate. Lipids were separated using the solvent system $CHCl_3$: CH_3OH: H_2O 110:40:6 (v:v:v) and visualized by anisaldehyde reagent.*

***(B):** phospholipids were evaluated loading TLC with a volume of OP equivalent to200 µg of cell lysate. Lipids were separated using the solvent system $CHCl_3$:CH_3OH:Acetic Acid: H_2O 30:20:2:1 (v:v:v), and visualized with phosphorus reactive.*

***(C)**: cholesterol was evaluated loading TLC with a volume of MetOP equivalent to 300 µg of cell lysate. Lipids were separated using the solvent system Hexane: Ethyl Acetate 3:2 (v:v) and visualized by anisaldehyde reagent.*

GlcCer: glucosylceramide; LacCer: Lactosylceramide; SM: sphingomyelin; Gb3: Globoatriosylceramide; PC: phosphatidylcholine, PE: phosphatidylethanolammine, chol: Cholesterol

Moreover, by immunostaining with cholera toxin I evaluated the effect of the drugs treatments on the cellular levels of GM1. As it is possible to observe in the image and the relative semiquantitative graph reported in figure 19, when the cells were subjected to treatment with corrector, potentiator individually or in combination, the GM1 content decreases significantly of about 25 -30%.

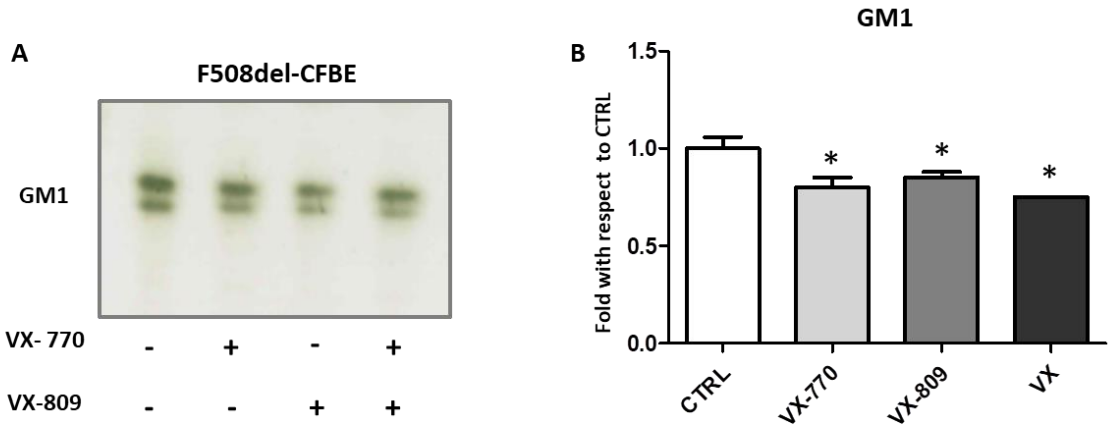

Figure 19: The pharmacological treatment of F508del-CFBE cells with VX-770 and VX-809 reduces the levels of ganglioside GM1

(A): *TLC immunostaining with cholera toxin: briefly, TLC was loaded with aqueous volume equivalent to the same amount of total cell protein (150 µg each). After chromatographic separation with solvent system: $CHCl_3$:CH_3OH:$CaCl_2$ 50:42:11 by vol., TLC plates were fixed with a polyisobuthylmethacrylate solution, air dried and incubated with 3% BSA in PBS for 1 hour. Plates were then incubated with cholera toxin at 10 µg/mL in 1% BSA in PBS for 1 hour at room temperature (RT). After washes with PBS, the immunoreactive bands were revealed using o-phenylenediamine (OPD)/H_2O_2 in 0.05 M citrate-phosphate buffer pH 5.0.*

(B)*: Semi quantitative graph of GM1 content in F508del-CFBE cells, obtained by densitometric quantification of GM1 positive bands using ImageJ software; the content of GM1 was represented as fold increase respect to CTRL.*

**p<0.008 vs CTRL*

In conclusion, this set of analysis revealed that potentiator VX-770 seems to be responsible for an alteration of CFTR protein and lipid interactome that could be responsible for the destabilization at PM of the F508del-CFTR restored by VX-809.

GM1 and WT-CFTR are closely associated at plasma membrane level

To further investigate the relationship between CFTR and GM1, with particular regard for their possible localization at the same PM domain, I performed photolabelling experiments using a GM1 derivative tritium labelled on the sphingosine moiety and carring a photoactivable group at the end of the fatty acid (figure 20 panel A). The photoactivable group is an azide linked to a nitrophenyl moiety. In this configuration the azide group is very sensitive to UV light with λ 360 nm. Indeed, after UV irradiation the azide is converted to a nitrene group that is very instable catalysing three main reactions: addition, insertion, and nucleophilic reactions (figure 20 panel B). In these view, the nitrene group can covalently bind the molecules close to the ganglioside, making it radioactive and consequently detectable. For this reason, if I detected by digital radiography radioactive proteins after the SDS-PAGE separation, I could conclude that these ones in their natural environment, were strictly closed to GM1.

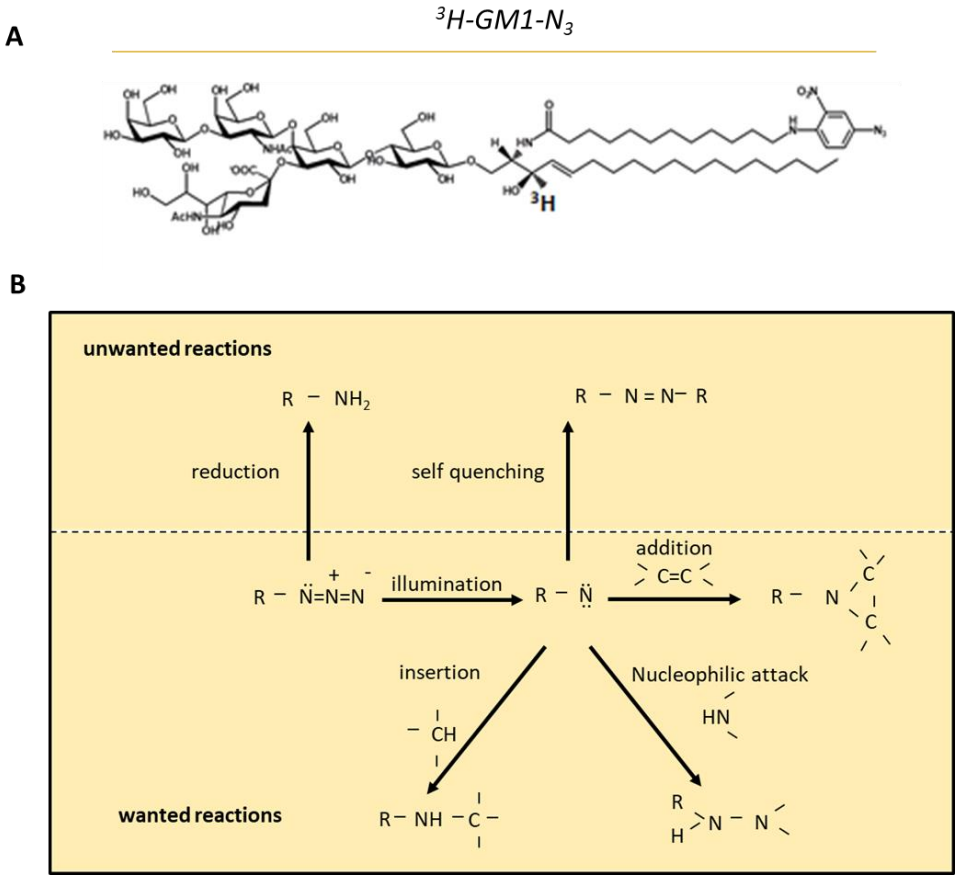

Figure 20:characteristic of the radioactive and photoactivable GM1 derivative
(A):*Structure of the radioactive and photoactivable GM1 derivative.*
(B)*:Schematic representation of the reaction catalysed by the nitrene group produced by the UV irradiation of the azide.*

To this purpose, I administered in dark condition (i.e. under red safe light), ^{3}H-GM1-N_3 to WT-CFBE and F508del-CFBE seeded in petri plates of Φ 100 mm. After 6 hours of incubations, the medium contained ^{3}H-GM1-N_3 was removed and the cells were washed three times with complete culture medium and irradiated in PBS under UV rays for 40 minutes. After that, the cells were harvested and proteins were separated by SDS-PAGE.

First, I analyzed the presence of CFTR by Western blotting analyses. As shown in figure 21, I detected in WT-CFBE cells both b-band and c-band of CFTR, whereas in F508del-CFBE cells I was able to detect only the immature form of CFTR (b-band). The same PVDF was subsequently analysed for the presence of radioactive proteins generated by the crosslink with the photoactivable and radioactive GM1. For this reason the PVDF were subjected to digital autoradiography using the ^{T}Racer instrumentation. The results obtained are reported in figure 21, where it is possible to observe in WT-CFBE cells, the presence of a radioactive band correspondent to the same molecular weight of the mature form of CFTR, which is the one associated with PM, whereas no radioactive signals were detected in F508del-CFBE cells.

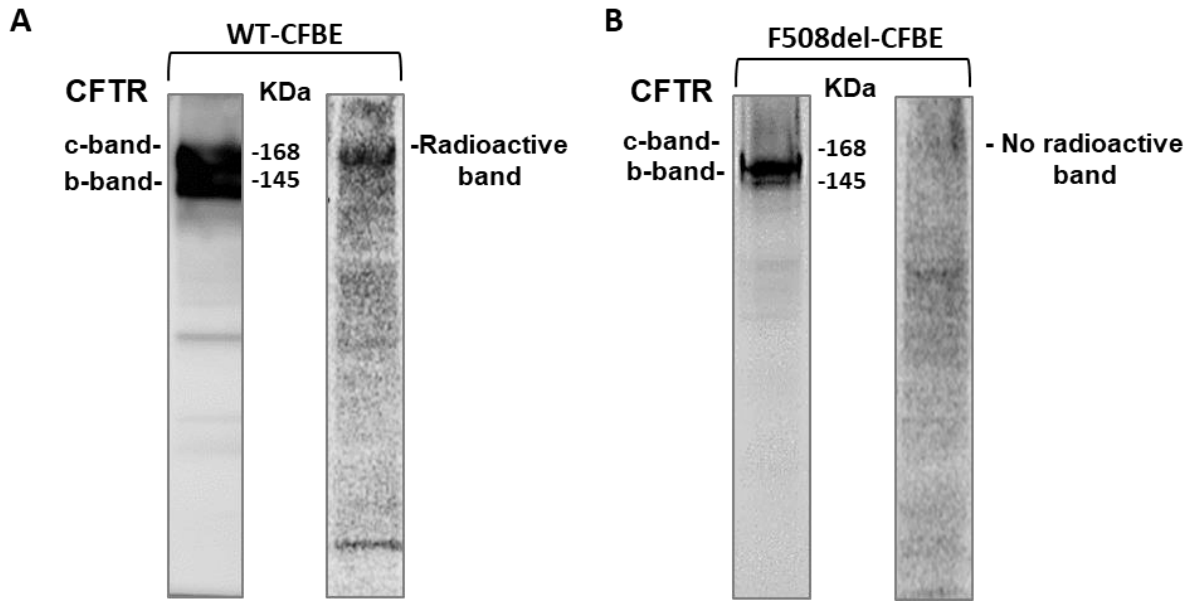

Figure 21: Ganglioside GM1 interacts with CFTR

CFBE overexpressing the WT and the F508del-CFTR were treated with tracer quantity of ^{3}H-GM1-N_3 in dark conditions and after 6 hours, cells were illuminated under UV light, harvested and subjected to SDS-PAGE and Western Blotting analyses for the detection of CFTR. Subsequently, the same PVDF was subjected to digital autoradiography to revealed the radioactivity due to the cross-link between GM1 and neighbouring proteins.

***(A)**: At left immunoblotting analysis of CFTR performed in WT-CFBE cells, at right digital autoradiography of the same PVDF.*

***(B)**: At left immunoblotting analysis of CFTR performed in F508del-CFBE cells, at right digital autoradiography of the same PVDF.*

The results of photolabelling experiments proved a remarkable proximity between GM1 and CFTR suggesting a direct interaction between them at the cell surface.

Ganglioside GM1 is adjuvant to Orkambi®therapy in stabilising F508del-CFTR at the plasma membrane

The results obtained so far, suggested a possible direct role of the ganglioside GM1 in the stabilization and functional regulation of CFTR at the PM of bronchial epithelial cells. Indeed, the expression of F508del-CFTR is paralleled to a decreased content of ganglioside GM1, and the same ganglioside seems to have a direct interaction with the WT-CFTR. To further support its active role in the CFTR interactome, I exogenously administered the ganglioside to F508del-CFBE cells, using a culture medium containing Orkambi®.

The cells were seeded and treated with 5 μM of both corrector VX-809 and potentiator VX-770, and with 10, 50 and 100 μM GM1 for 48 hours. At the end of the incubation, cells were collected, lysed, subjected to SDS-PAGE and Western blot analysis to investigate the effect of GM1 and Orkambi® on the maturation of F508del-CFTR.

The results shown in figure 22, indicate that the treatment with GM1 positively influences CFTR maturation. Indeed, for all the treatment I could observe an increase of c-band, the mature form, with respect to untreated cells. However, the 50 μM GM1 is the concentration that shown the highest recovery and for this reason was selected to be used for the subsequent experiments.

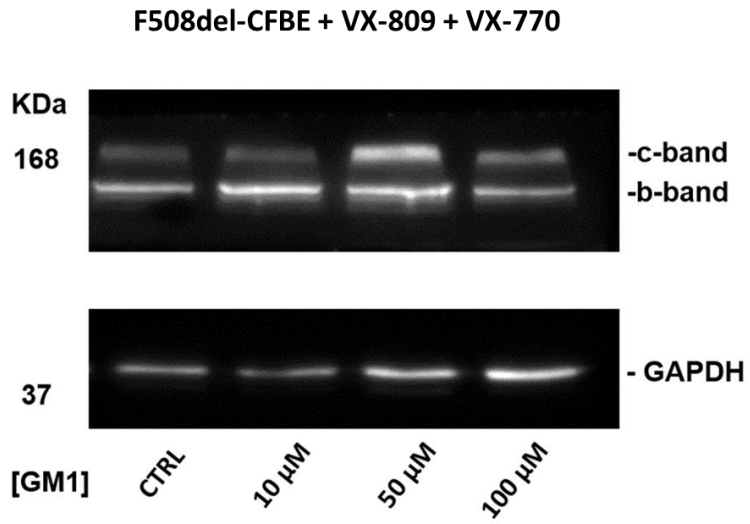

Figure 22: Effect of GM1 administration on F508del-CFTR maturation upon treatment with corrector VX-809 and potentiator VX-770

Representative Western-blot images of the content of CFTR performed on F508del-CFBE cells subjected to the treatment for 48 hours, with 5 µM corrector VX-809, 5 µM potentiator VX-770 and ganglioside GM1 at the concentration of 10, 50 and 100 µM. GAPDH was evaluated as loading control.

c band: mature and glycosylated form of protein CFTR, inserted in plasma membrane; b band: immature form of protein CFTR

After that, I performed immunostaining analyses with cholera toxin to confirm the association of GM1 with treated cells. F508del-CFBE cells were treated for 48 hours with 50 µM of GM1, then cells were washed many times with fresh medium containing 10% of FBS, to eliminate any trace of ganglioside not directly associated with PM, cells were collected, lysed and lyophilized. The content of GM1 was evaluated as previously described. The results are shown on figure 23, where clearly emerges that the exogenous GM1 was taken up by the F508del-CFBE cells. Indeed, as it is possible to observe from the TLC immunostaining (figure 23, panel A) and from the semi-quantitative graph (figure 23, panel B) the amount of GM1 in the F508del-CFBE cells has notably increased of about ~ 3,5 fold, with respect to control untreated cells.

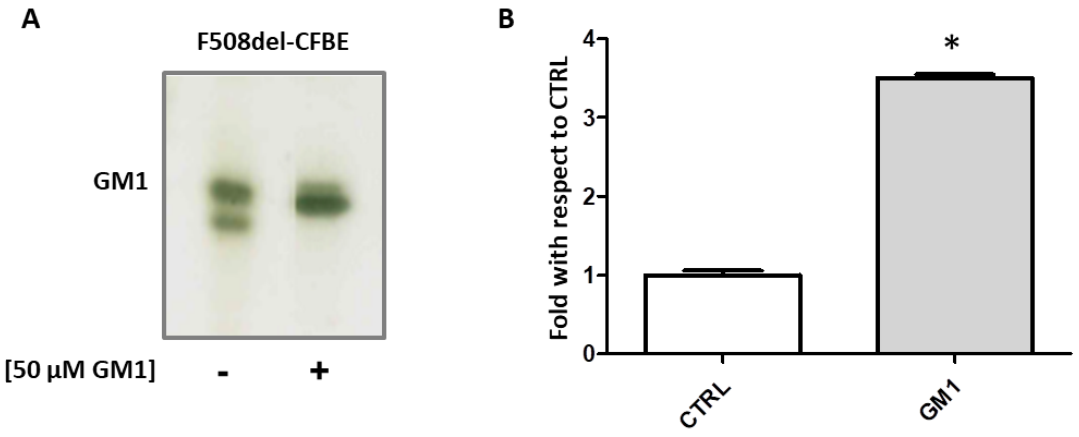

Figure 23: Evaluation of GM1 association with F508del-CFBE cells
F508del-CFBE cells were treated for 48 hours with 50 µM GM1, then were collected for lipid analysis.
(A): *TLC immunostaining with cholera toxin: briefly, TLC was loaded with aqueous volume equivalent to the same amount of total cell proteins (150 µg each). After chromatographic separation with solvent system: $CHCl_3$:CH_3OH:$CaCl_2$ 50:42:11 by vol., TLC plates were fixed with a polyisobuthylmethacrylate solution, air dried and incubated with 3% BSA in PBS for 1 hour. Plates were then incubated with cholera toxin at 10 µg/mL in 1% BSA in PBS for 1 hour at room temperature (RT). After washes with PBS the immunoreactive bands were revealed using o-phenylenediamine (OPD)/H_2O_2 in 0.05 M citrate-phosphate buffer pH 5.0.*
(B)*: Semi quantitative graph of GM1 content in F508del-CFBE cells treated or not with 50 µM GM1, obtained by densitometric quantification of GM1 positive bands using Imagej software; the content of GM1 was represented as fold increase respect to CTRL.*
**p<0.02 vs CTRL*

Furthermore, I investigated the metabolic fate of the exogenously administered GM1. To perform this study, I treated F508del-CFBE cells for different time points (up to 48 hours) with 5 µM of corrector VX-809, 5 µM of potentiator VX-770, and with 50 µM of the same GM1 used before, mixed with trace of GM1 derivative radioactive on the sphingosine moiety (^{3}H-GM1). By the analysis of the radioactive lipids, I can evaluate the metabolism of the only administered GM1, excluding the contribution of the endogenous counterpart.

After 12, 24 and 48 hours the cells were collected lysed and lyophilised. Radioactive lipids were separated with HPTLC and visualized by digital autoradiography. The results obtained are reported in figure 24 and I found that, for each considered time point, the only radioactive lipid detectable was the ganglioside GM1.

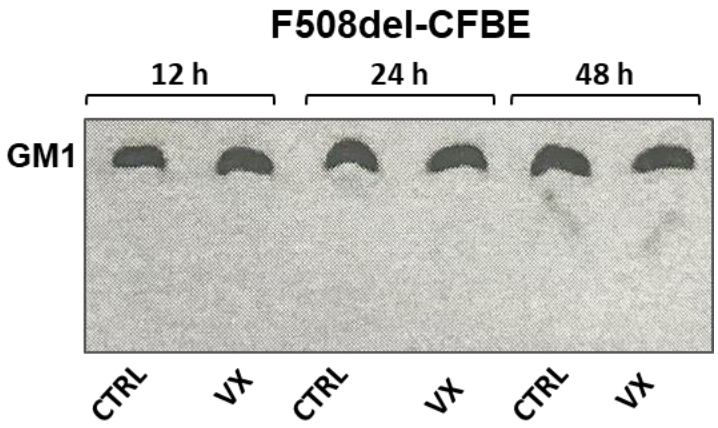

Figure 24: Metabolic fate of the exogenous administered GM1 in F508del-CFBE cells, in presence or not of 5 µM VX-809 and VX-770

F508del-CFBE were treated with 50 µM GM1 and *90 nM of ^{3}H-GM1 (corresponding to 0,09 µCi) and with 5 µM VX-809 and VX-770 (VX); CTRL cells were not treated with potentiator and corrector. After 12, 24 and 48 hours the cells were lysed and resuspended in ice-cold water and briefly subjected to sonication before being lyophilized. The samples were then subjected to lipid extraction with $CHCl_3$:CH_3OH:H_2O 20:10:1 (v:v:v). Each sample was loaded on HPTLC using the same amount of radioactivity. Lipids were separated, using the solvent system $CHCl_3$:CH_3OH:$CaCl_2$ 50:42:11 by vol and then revealed by digital autoradiography.*

With this experiment, I have demonstrated that the exogenously administered GM1 is not metabolized by the cells at least up to 48 hours.

After that, I verified if corrected F508del-CFTR localizes in the same PM microenvironment of GM1, as previously demonstrated for the WT-CFTR, also in this case by photolabelling experiments.

F508del-CFBE cells were seeded and treated for 48 hours as follows:

- Untreated cells as control
- 5 µM VX-809 and 5 µM VX-770
- 50 µM GM1
- 5 µM VX-809 and 5 µM VX-770 + 50 µM GM1

For the last 6 hours ^{3}H-GM1-N_3 was administered to the cells in dark conditions. After the incubations, the cells were washed and illuminated for 40 minutes with UV rays and processed as previously described. Consequently, I performed a SDS-PAGE and relative immunoblotting analysis to separate and identifiy the two bands of CFTR. After Western blotting, the same PVDF was subjected to autoradiography to reveal the presence of potential radioactive bands. The results obtained are shown in figure 25. In control cells, Western blot analyses revealed the presence of only the b-band of CFTR without the presence in the digital autoradiography of any radioactive band corresponding to the mature form of CFTR. The same result was observed for the conditions

of double treatment with the corrector and potentiator. Interestingly, in the case of treatment with exogenous GM1 by Western blot, I observed a remarkable staining of the mature form of CFTR and in the digital autoradiography I detected a radioactive band corresponding to the c-band of CFTR. These data suggest that the rescued mutated protein interacts directly with ganglioside GM1 and were located in the same PM microenvironment.

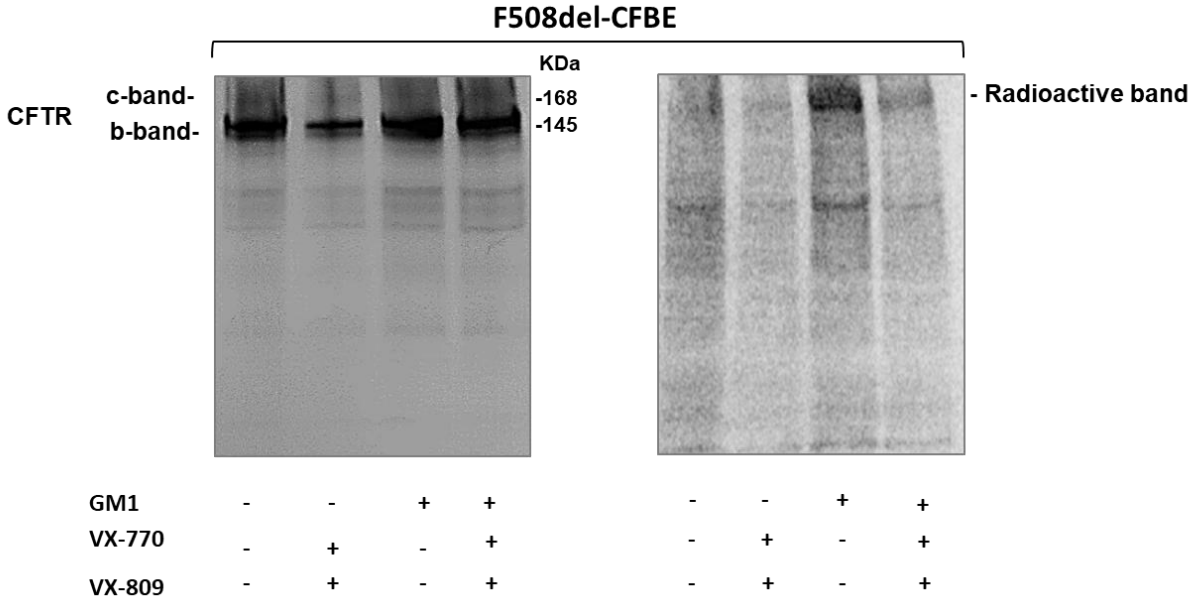

Figure 25: Study of CFTR-GM1 association in F508del-CFBE cells treated with corrector VX-809 and potentiator VX-770

F508del-CFBE were treated with corrector VX-809 and potentiator VX-770, in presence or not of 50 µM GM1 for 48 hours, then the cells were treated with tracer quantity of ^{3}H-GM1-N_3 in dark conditions and after 6 hours, were illuminated under UV light, harvested and subjected to SDS-PAGE and Western Blotting analyses. After this, the same PVDF was subjected to autoradiography to revealed the radioactivity
Left: Immunoblotting analysis for CFTR identification, Right: digital autoradiography of the same PVDF

I verified the impact of GM1 administration on the lipid composition of treated cells. I treated or not F508del-CFBE cells with 50 µM GM1 for 48 hours and after that the cells were collected, lysed and lyophilised; lipids from the lyophilised samples were extracted with chloroform:methanol:water 20:10:1 (v:v:v) and subjected to a two-phase Folch's partitioning to obtain the aqueous (AP) and the organic phases (OP). Aliquots of the organic phase were then subjected to alkaline treatment to remove glycerophospholipids (MetOP) as previously described. The lipids were then separated by HPTLC using different solvent systems and the results are shown in figure 26. As it is possible to see, I didn't detect any significant difference in neutral lipid composition upon GM1 treatment, for the exclusion of cholesterol that slightly increase.

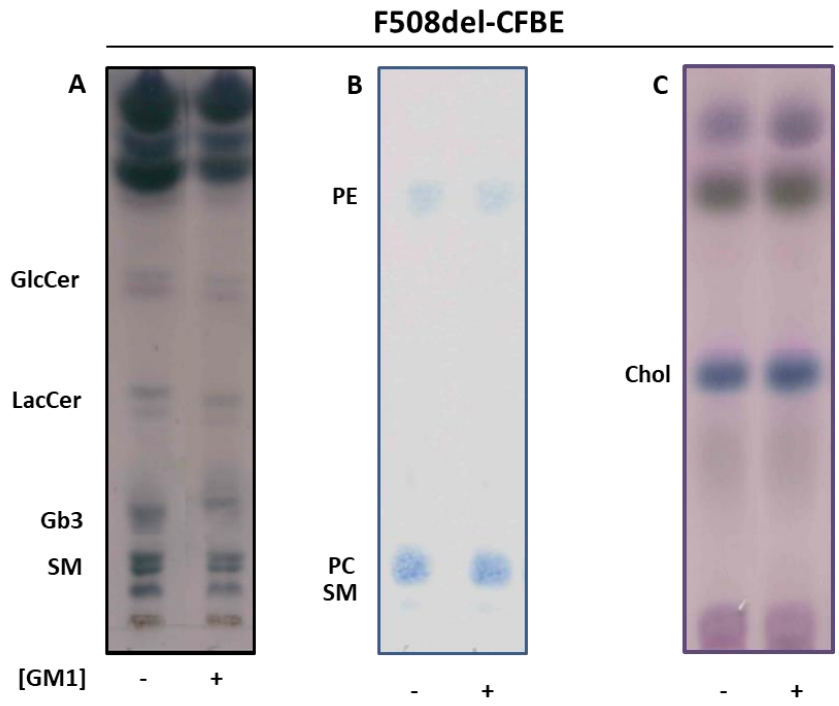

Figure 26: Evaluation of ganglioside GM1 administration on the F508del-CFBE cell lipids composition
F508del-CFBE cells were treated for 48 hours with 50 µM GM1 and then subjected to lipid analysis. Cells lysates were subjected to lipid extraction with $CHCl_3$:CH_3OH:H_2O 20:10:1 (v:v:v). Total lipid extracts were further subjected to a two-phase partitioning resulting in the separation of an aqueous phase (AP) containing gangliosides and in an organic phase (OP) containing all other lipids. Aliquots of the organic phases were then subjected to alkaline treatment to remove glycerophospholipids (MetOP).
***(A)**: neutral lipids were evaluated loading TLC with a volume of MetOP equivalent to 500 µg of cell lysate. Lipids were separated using the solvent system $CHCl_3$:CH_3OH:H_2O 110:40:6 (v:v:v) and visualized by anisaldehyde reagent.*
***(B):** phospholipids were evaluated loading TLC with a volume of OP equivalent to 200 µg of cell lysate. Lipids were separated using the solvent system $CHCl_3$:CH_3OH:Acetic Acid: H_2O 30:20:2:1 (v:v:v), and visualized with phosphorus reactive.*
***(C)**:cholesterol was evaluated loading TLC with a volume of MetOP equivalent to 300 µg of cell lysate. Lipids were separated using the solvent system Exane: Etil Acetate 3:2 (v:v) and visualized by anisaldehyde reagent.*
GlcCer: glucosylceramide; LacCer: Lactosylceramide; SM: sphingomyelin; Gb3: Globoatriosylceramide; PC: phosphatidylcholine, PE: phosphatidylethanolammine, chol: Cholesterol

As emerges from the literature the ganglioside GM1, hasn't only a structural role in membrane architecture, but it is also a bioactive signalling molecules with potential toxic effect.

I performed MTT assay to verify the possible cytotoxicity of the exogenously administered GM1. F508del-CFBE cells were seeded at the same density into 96-microplate and treated with 50 µM of exogenous GM1 and MTT assay was performed after 6, 12, 24 and 48 hours. As sown in figure 27 I observed only an apparent, but not statistically significant reduction in cell viability upon the treatment.

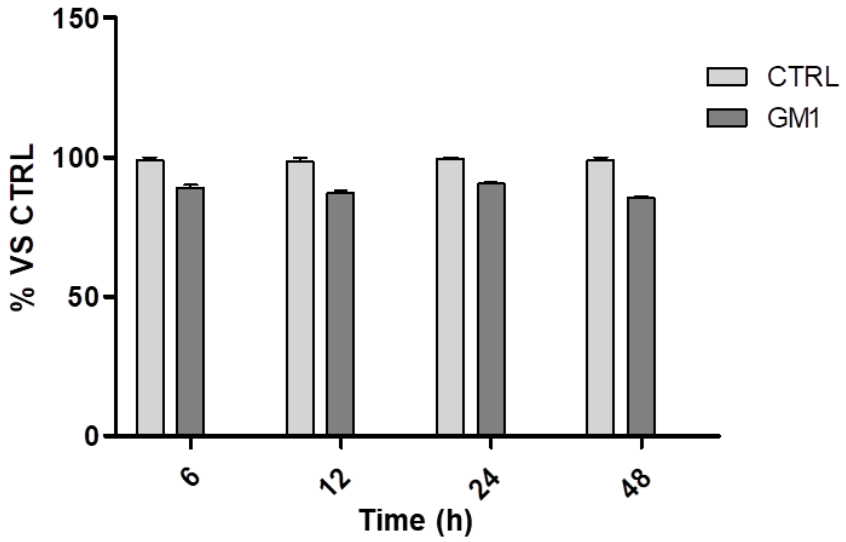

Figure 27: Cell viability of F508del-CFBE treated with 50 µM of ganglioside GM1
Cells were seeded at the density of 13500 cells/cm^2 into 96 multi-well, and at the end of every time-point, cell viability was evaluated by MTT assay. The data were expressed as % VS untreated cells.

Subsequently, I further investigated the possible cytotoxic effects of GM1 evaluating, by Western blot analyses, the markers of cellular damage such as caspase-3 and Cyclin D2.

F508del-CFBE cells were treated in the same conditions of the previous experiment, and after 6, 12, 24 and 48 hours the cells were collected, lysed and subjected to SDS-PAGE and immunoblotting analysis. The results of both Western blot are shown in figure 28, where it is possible to exclude in treated cells the activation of the apoptosis since I could not detect the presence of the cleaved form of caspase 3. In addition, also the level of Cyclin D2 is the same in control and treated cells, indicating that GM1 does not alter cell proliferation.

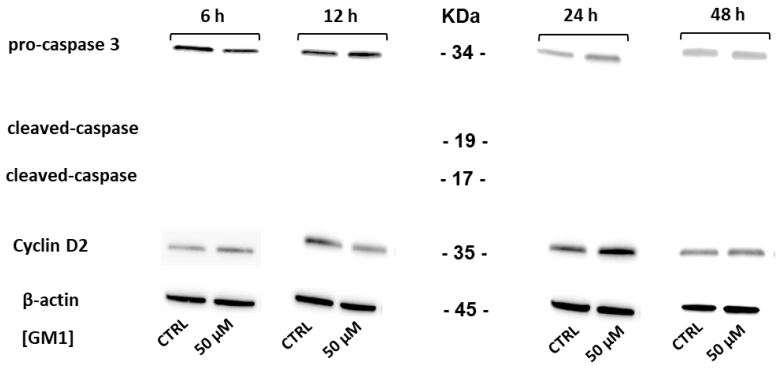

Figure 28: Evaluation by immunoblotting analyses of the effect of GM1 treatment on the cell damage biomarkers
Representative Western-blot images of pro-caspase 3, its cleaved form and of cyclin D2 protein expression in F508del-CFBE cells treated with 50 µM of GM1 for 6, 12, 24 and 48 hours. β-actin was evaluated as loading control.

The exogenous administration of GM1 antagonises the negative effect of potentiator VX-770 on F508del-CFTR plasma membrane stability

To deeply investigate the relationship between Orkambi® and GM1 in the PM stabilization of F508del-CFTR, I performed experiments on F508del-CFBE cells corrected for GM1 content and subjected to the single treatment with corrector and potentiator.

The experimental plan consisted in the treatment of F508 del-CFBE cells as follows:

- untreated cells
- 5 μM VX-809
- 5 μM VX-770
- 5 μM VX-809 + 5 μM VX-770

The above 4 conditions in presence or not of 50 μM GM1.

The cells were treated for 48 hours after which they were collected and finally lysed to perform an immunoblotting analysis to reveal the role of GM1 on F508del-CFTR maturation upon the different pharmacological treatments. As reported in the representative immunoblotting images in figure 29, the treatment with only GM1 does not increase the maturation of F508del-CFTR as occurs in the presence of corrector VX-809. These results confirm only those presented before regarding the positive effect of GM1 in case of the double treatment with corrector and potentiator. Moreover in presence of Orkambi® and GM1, the rescued mature F508del-CFTR, that was lost in the treatment without GM1, has been recovered.

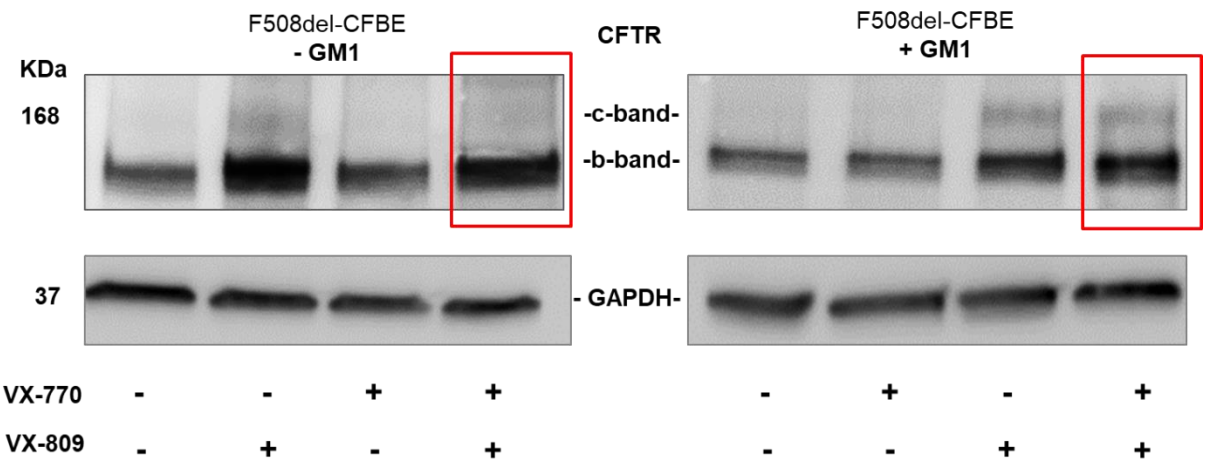

Figure 29: Exogenous administration of GM1 increased the plasma membrane stability of F508del-CFTR rescued by Orkambi®

Representative Western-blot analysis of the content of CFTR performed in F508del-CFBE cells subjected to the treatments with corrector VX-809, potentiator VX-770 individually or in combination and subjected or not to exogenous treatment with 50 µM GM1. GAPDH was evaluated as loading control.

C band: mature and glycosylated form of protein CFTR, inserted in plasma membrane

B band: immature form of protein CFTR

Subsequently, I analysed in the same samples, the cellular levels of the CFTR scaffolding protein NHERF-1, ezrin and its bioactive form p-ezrin. As sown in figure 30, once again, I observed an increase of NHERF-1, ezrin and p-ezrin after the treatment with VX-809, while in presence of potentiator VX-770 I observed their decrease as previously demonstrated. Surprisingly, when the cells were treated with also GM1, I observed an increase of protein level in all the conditions. This result suggests that GM1 plays an active role in the control of CFTR PM interactome.

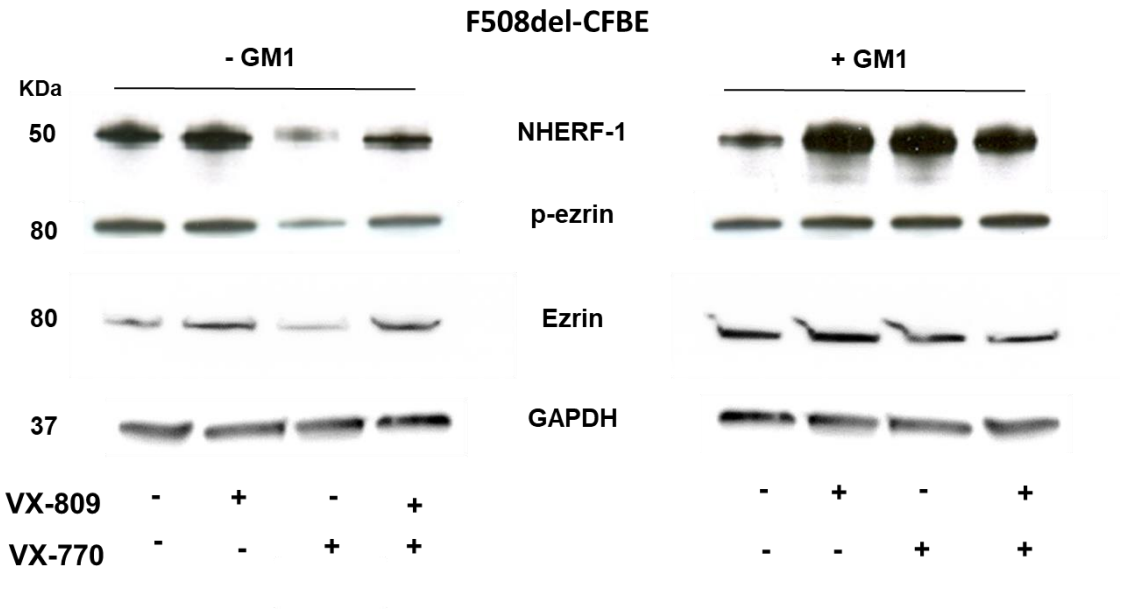

Figure 30: The treatment with GM1 abolishes the negative effect of VX-770 on CFTR scaffolding proteins
Immunoblotting analyses of CFTR-scaffolding protein NHERF-1, ezrin and its bioactive form p-ezrin were performed on F508del-CFBE cells subjected to the treatment with corrector VX-809, potentiator VX-770 individually or in combination and subjected or not to treatment with 50 µM GM1. GAPDH was evaluated as loading control.
Left: F508del-CFBE without GM1
Right:F508del-CFBE treated with GM1

I verified the effect of the different drugs treatments in terms of both GM1 association and lipid composition. I first performed an immunostaining with cholera toxin after treating the cells as previously described in latest experiment, and as shown in figure 31 the pharmacological treatments did not alter the GM1 cellular uptake, and compensate the induced lack of GM1 in treated cells.

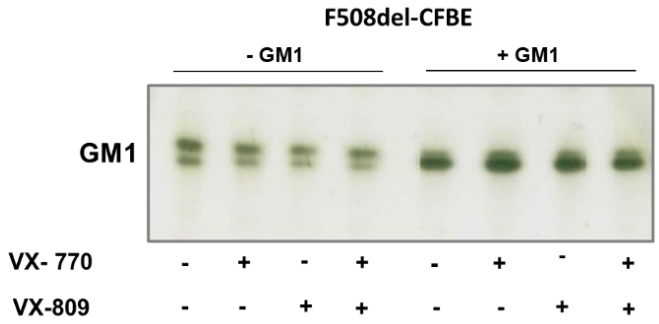

Figure 31: GM1 administration compensate the negative effect of the pharmacological treatment on GM1 levels in F508del-CFBE cells

F508del-CFBE cells were treated with 5 µM corrector VX-809, potentiator VX-770 individually or in combination and subjected or not to exogenous treatment with 50 µM GM1. In the image is shown the TLC immunostaining with cholera toxin: briefly, TLC was loaded with aqueous volume equivalent to the same amount of total cell protein (150 µg each). After chromatographic separation with solvent system: $CHCl_3$:CH_3OH:$CaCl_2$ 50:42:11 by vol., TLC plates were fixed with a polyisobuthylmethacrylate solution, air dried and incubated with 3% BSA in PBS for 1 hour. Plates were then incubated with cholera toxin at 10 µg/mL in 1% BSA in PBS for 1 hours at room temperature (RT). After washes with PBS the immunoreactive bands were revealed using o-phenylenediamine (OPD)/H_2O_2 in 0.05 M citrate-phosphate buffer pH 5.0.

In all the conditions tested I didn't observe any significant change between pharmacological treated cells in presence or not of GM1 in term of: glucosylceramide, lactosylceramide, globoatriosylceramide, sphingomyelin and glycerophospholipids composition (figure 32).

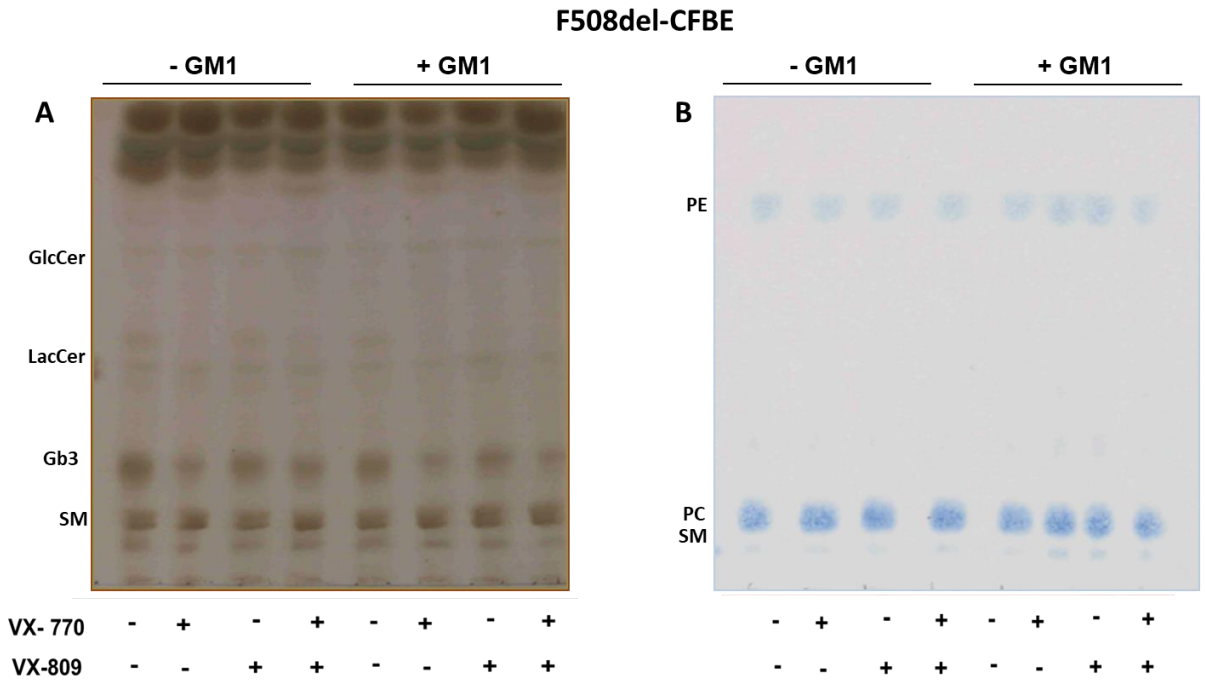

Figure 32: Evaluation of lipid composition in F508del-CFBE cells treated with corrector VX-809, potentiator VX-770 and subjected or not to 50 µM GM1

F508del-CFBE cells were treated with 5 µM corrector VX-809, potentiator VX-770 individually or in combination and subjected or not to exogenous treatment with 50 µM GM1 and then subjected to lipid analysis. Cells lysates were subjected to lipid extraction with $CHCl_3$:CH_3OH:H_2O 20:10:1 (v:v:v). Total lipid extract were further subjected to a two-phase partitioning resulting in the separation of an aqueous phase (AP) containing gangliosides and in an organic phase (OP) containing all other lipids. Aliquots of the organic phases were then subjected to alkaline treatment to remove glycerophospholipids (MetOP).

***(A)**: neutral lipids were evaluated loading TLC with a volume of MetOP equivalent to 500 µg of cell lysate. Lipids were separated using the solvent system $CHCl_3$:CH_3OH:H_2O 110:40:6 (v:v:v) and visualized by anisaldehyde.*

***(B):** phospholipids were evaluated loading TLC with a volume of OP equivalent to 200 µg of cell lysate. Lipids were separated using the solvent system $CHCl_3$:CH_3OH:Acetic Acid: H_2O 30:20:2:1 (v:v:v), and visualized with phosphorus reactive.*

GlcCer: glucosylceramide; LacCer: Lactosylceramide; SM: sphingomyelin; Gb3: Globoatriosylceramide; PC: phosphatidylcholine, PE: phosphatidylethanolammine

Finally, I analyzed cholesterol content and surprisingly I noticed that its content didn't vary after GM1 administration in fact is still decreased when the cells were treated with potentiator VX-770, as it is shown in figure 33.

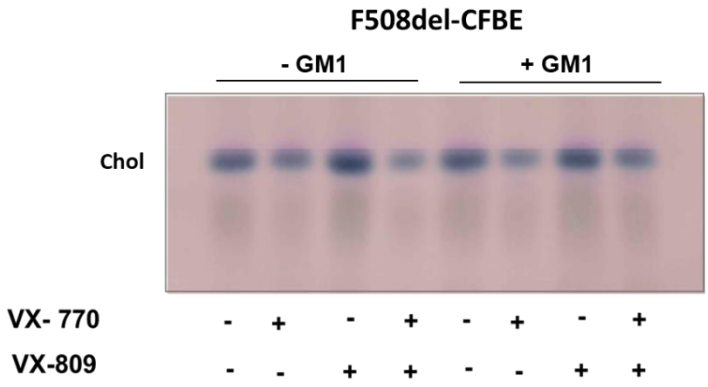

Figure 33: VX-770 reduces the cholesterol levels in F508del-CFBE cells, under treatment with corrector VX-809, potentiator VX-770 and subjected or not to 50 µM GM1

F508del-CFBE cells were treated with corrector VX-809, potentiator VX-770 individually or in combination and subjected or not to exogenous treatment with 50 µM GM1 and then subjected to lipid analysis. Cells lysates were subjected to lipid extraction with $CHCl_3$:CH_3OH:H_2O 20:10:1 (v:v:v). Total lipid extract were further subjected to a two-phase partitioning resulting in the separation of an aqueous phase (AP) containing gangliosides and in an organic phase (OP) containing all other lipids. Aliquots of the organic phases were then subjected to alkaline treatment to remove glycerophospholipids (MetOP).

Cholesterol was evaluated loading TLC with a volume of MetOP equivalent to 300 µg of cell lysate. Lipids were separated using the solvent system Exane: Etil Acetate 3:2 (v:v) and visualized by anisaldehyde.

Chol: cholesterol

Treatment with GM1 improves CFTR function

Until now, I demonstrated that the recovery of the cell content of GM1 causes important effects on the stability of F508del-CFTR rescued by the Orkambi® treatment. I demonstrated for the first time that in WT-CFBE cells, GM1 is closely associated to CFTR, and this association is maintained also by the rescued F508del-CFBE upon the treatment of the cells with exogenous GM1. In addition, I demonstrated also that ganglioside GM1 is an adjuvant for Orkambi® therapy on stabilizing F508del-CFTR at PM by the recruitment of the CFTR scaffolding proteins NHERF-1, ezrin and p-ezrin.

However, I didn't have information regarding the effect of GM1 on the recovery of F508del-CFTR channel activity. To this purpose, I performed, in collaboration with Dr. Anna Tamanini from the university Hospital of Verona, assays aimed to verify the activity of corrected-CFTR. To perform these assays I took advantage by the use of F508del-CFBE-YFP cells. These cells were stably transfected with the halide-sensitive yellow fluorescent protein (HS-YFP) YFPH148Q/I152L, allowing to rapidly test the effect of modulators by measuring Iodide influx [165], [166], [167]. In addition, since cells were maintained alive at 37°C, CFTR activity can be assessed in physiological conditions. In particular, the differences in CFTR activity were measured by detecting channel activity after the use of a stimulation cocktail and comparing it with the activity measured after treatment with CFTR inhibitor cocktail. In this way was possible to determine if the treatment with CFTR-modulators and GM1 might affect CFTR activity.

The cells were treated for 48 hours as follows:

- 5 μM VX-809
- 50 μM GM1
- 5 μM VX-809 + 50 μM GM1

At the end of the incubation, the activity of CFTR was measured. As it possible to notice from the graph (Figure 34), I detected an increase on F508del-CFTR activity, also after treatment with just GM1 with respect to control cells; the activity of the channel after treatment with corrector VX-809 had increased too, as expected. Surprisingly when F508del-CFBE cells have been treated with both GM1 and VX-809 the activity was the highest. These data suggest that GM1 may have a corrective effect on CFTR.

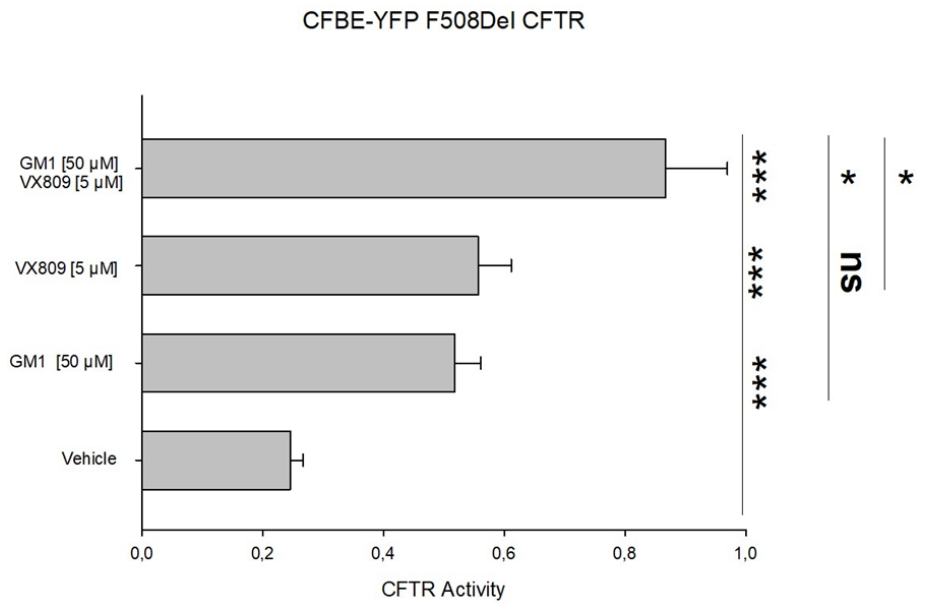

Figure 34: The exogenous administration of ganglioside GM1 potentiates the effect of corrector VX-809
CFBE-YFP F508del-CFTR cells were seeded on round glass coverslips and were preincubated for 48 hours with vehicle (DMSO), 5 µM VX-809 and 50 µM GM1 individually or in combination. At the end of 48 hours cells were incubated with stimulation cocktail (20 µM forskolin and 5µM VX-770, in presence or not of 10 µM of CFTR inhibitor (CFTRInh-172) for 30 minutes. CFTR dependent chloride efflux was assayed by single-cell fluorescence imaging analysis of YFP fluorescence quenching by iodide. Fluorescence coming from each single cell was recorded.
*Each bar corresponds to the mean ±SEM of at least three different experiments. Statistical comparison were made using an unpaired Mann-Whitney (*p<0,05, **p<0,01 and ***p<0,001).*

Then I verified if GM1 might have the same activity also in combination with potentiator VX-770. For this reason, the cells were treated for 48 hours as follows:

- 5 µM VX-770
- 50 µM GM1
- 5 µM VX-770 + 50 µM GM1

As emerge from the graph reported in figure 35, after treatment with VX-770 I could observe a little increase with respect to control cells, less marked than the increment detected with GM1 alone. Interestingly, when F508del-CFBE cells have been treated with GM1 and VX-770, the activity of CFTR has decreased with respect to the activity measured in the cells treated with just GM1, suggesting that as previously observed, the treatment with VX-770 had a negative effect, probably due to a destabilization of CFTR at PM.

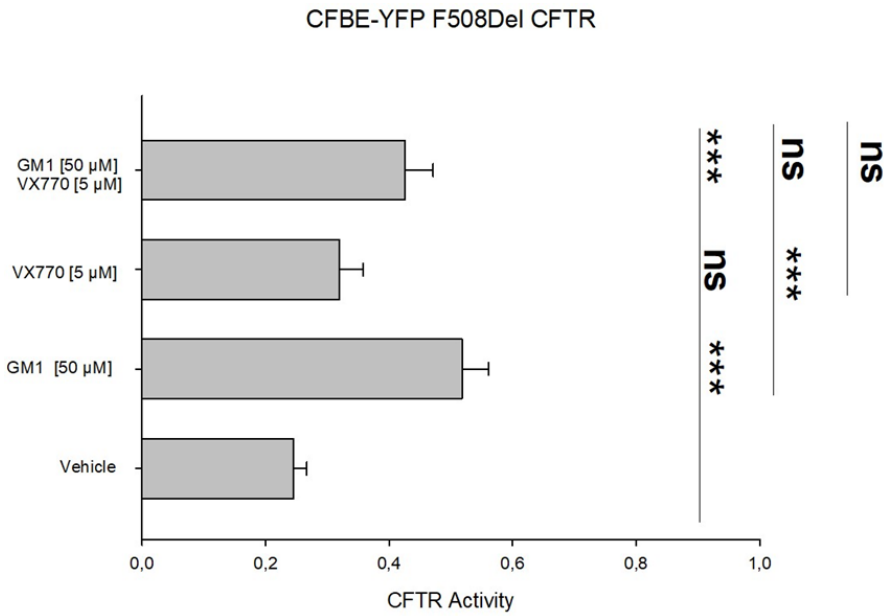

Figure 35: Ganglioside GM1 has itself a corrective effect and antagonize the negative effect of VX-770

CFBE-YFP F508del-CFTR cells were seeded on round glass coverslips and were preincubated for 48 hours with vehicle (DMSO), 5 µM VX-770 and 50 µM GM1 individually or in combination. At the end of 48 hours cells were incubated with stimulation cocktail (20 µM forskolin and 5µM VX-770, in presence or not of 10 µM of CFTR inhibitor (CFTRInh-172) for 30 minutes. CFTR dependent chloride efflux was assayed by single-cell fluorescence imaging analysis of YFP fluorescence quenching by iodide. Fluorescence coming from each single cell was recorded.

*Each bar corresponds to the mean ±SEM of at least three different experiments. Statistical comparison were made using an unpaired Mann-Whitney (*p<0,05, **p<0,01 and ***p<0,001).*

Finally, to complete the study, I analysed the effect of GM1 treatment in combination with Orkambi® therapy. F508del-CFBE cells were subjected for 48 hours to the following treatments:

- 5 µM VX-809
- 5 µM VX-809 +5 µM VX-770
- 5 µM VX-809 +5 µM VX-770 + 50 µM GM1

Then CFTR activity was revealed; the results are shown in the following figure 36.

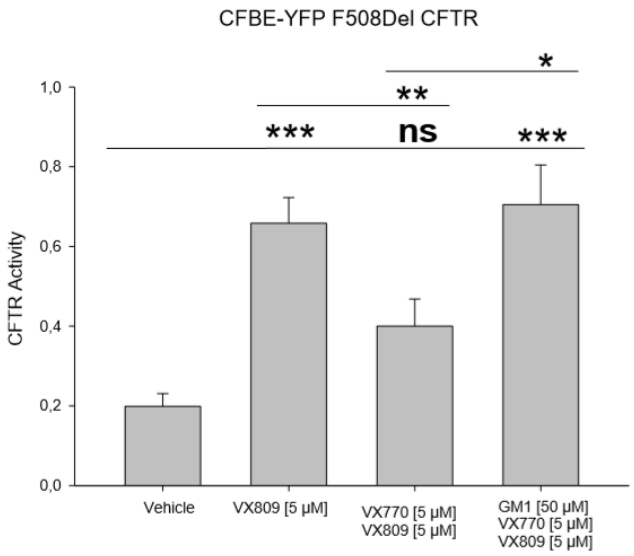

Figure 36: GM1 is an adjuvant for Orkambi® therapy

CFBE-YFP F508del-CFTR cells were seeded on round glass coverslips and were preincubated for 48 hours with vehicle (DMSO), with 5 µM VX-809, with 5 µM VX-809 +5 µM VX-770, and with 5 µM VX-809 +5 µM VX-770 + 50 µM GM1. At the end of 48 hours cells were incubated with stimulation cocktail (20 µM forskolin and 5µM VX-770, in presence or not of 10 µM of CFTR inhibitor (CFTRInh-172) for 30 minutes. CFTR dependent chloride efflux was assayed by single-cell fluorescence imaging analysis of YFP fluorescence quenching by iodide. Fluorescence coming from each single cell was recorded.

*Each bar corresponds to the mean ±SEM of at least three different experiments. Statistical comparison were made using an unpaired Mann-Whitney (*p<0,05, **p<0,01 and ***p<0,001).*

As previously observed, also in this case the treatment with VX-809 causes an increase in CFTR activity, while the treatment with the combination of potentiator and corrector, decreased this recovered function. Surprisingly, when the F508del-CFBE cells were subjected to Orkambi® therapy with 50 µM GM1, the activity was the highest observed, with respect to the other analysed conditions.

To conclude I can summarize that GM1 has also an important effect on CFTR activity, suggesting its use as adjuvant for Orkambi® therapy.

Discussion

Several studies reported in literature, support the active role of sphingolipids in CF. Indeed, sphingolipids alterations in CF bronchial epithelial cells seem to be involved in the establishment of the high pro-inflammatory state typical of CF patients as well as in the inflammatory response and susceptibility to bacterial infections.

A peculiar role during the bacterial infections, seems to be played by ceramide. Increased levels of PM ceramide in CF bronchi correlates with the pro-inflammatory status typical of CF lung disease [134, 168]. Furthermore, the GSLs asialo-GM1 and asialo-GM2 could operate as receptor for *P. aeruginosa* binding, even if a direct proof with the clinical relevant strains of this bacterium has not been available so far [169, 170].

Recent data have described for the first time a direct relationship between CFTR and sphingolipids in human bronchial epithelial cells. In 2014 Itokazu and colleagues demonstrated that CFTR-silenced cells are characterized by a 60% decrease in the glycosphingolipid GM1 content, which is responsible for a reduced β_1-integrin activation with a consequent decreased phosphorylation of FAK and CAS and block of cell motility. To note, the addition of GM1 to CFTR-silenced cells was able to revert the phenotype [35]. Ramu and colleagues described that the ceramide produced at the cell surface through the sphingomyelin (SM) hydrolysis promoted by bacterial infection induces the clusterization of CFTR making difficult the channel activation by the phosphorylation of regulatory domain [149]. Moreover, several studies reported that CFTR at the apical membrane of epithelial cells is associated with lipid rafts [34].

As it is well known, lipids rafts are specific portion of the PM enriched on saturated lipids, sphingolipids, and cholesterol that by the recruitment and stabilization of a selected number of proteins, organize macromolecular complexes involved in the control of cell signaling.

An impressive study performed by Pankow S. and colleagues, reveals that PM CFTR interactome is composed of a wide number of proteins involved in the control of the channel activity and in its stabilization at the PM level [169, 170]. Interestingly, they showed that in case of F508del-CFTR the macromolecular complex is completely different with respect to the one of WT-CFTR.

No information has been available so far on the lipid-based interactome involved in the control of CFTR properties. However, the existence of a direct correlation between the expression at the PM of CFTR and the cellular levels of GM1 gets to speculate on the ganglioside as possible actor.

To investigate this aspect, I took advantage of an experimental procedure developed in the laboratory where I performed my PhD project. In particular, by the use of a radioactive and photoactivable GM1 derivative, I demonstrated for the first time that in bronchial epithelial cells,

CFTR and GM1 reside in the same PM microenvironment, and this correlation is missed in case of F508del-CFTR.

Since the ganglioside GM1 is an important bioactive lipid involved in the control and stabilization of several proteins, this result opens a new scenario in the study of the CFTR and includes the ganglioside in the cluster of molecules belonging to CFTR interactome that changes in presence of the mutation F508del.

It is now clear that in a such complicated scenario which comprises several actors beside to CFTR, the therapies based on the rescue of mutated channel need to take in account that together with the recovery of CFTR, it is important to restore also its interactome both in terms of proteins and lipids composition.

A clear example is represented by the failure in the chronic use of Orkambi® for restoring the function of F508del-CFTR in CF cells. Orkambi® is a combination of corrector VX-809 and potentiator VX-770 (lumacaftor-Ivacaftor), approved for patients homozygous for the F508del mutation. Despite initial beneficial effects, the chronic treatment doesn't results efficacious. A recent study also shows that there is a potential non-specific effect of VX-770 on the lipid bilayer and suggests that this effect may account for its destabilizing effect on VX-809-rescued F508del-CFTR, underlining an important role of lipids of the PM in stabilizing CFTR [171]. Interestingly, we observed in F508del-CFTR bronchial epithelial cells that Orkambi® treatment induces a decrease in GM1 content further supporting a possible role of the ganglioside in the control of CFTR turnover.

To investigate this aspect, I evaluated the effect of the exogenous administration of GM1 on CFTR maturation in bronchial epithelial cells overexpressing the F508del-CFTR. Firstly I found that the cell take up the ganglioside without significant variation in the content of the other cell lipids but without an improvement in the maturation of F508del-CFTR. This result was quite expected because the mutation F508del impairs the folding of the protein in the ER where GM1 is not present, even when it is exogenously administered to the cells. For this reason I repeated the experiments in cells treated or not with GM1 and with the corrector VX-809. Interestingly, I found that the combined treatment results in an increase of the cellular levels of the mature form of F508del-CFTR and of its scaffolding proteins NHERF-1 and p-ezrin. In addition, by the use of F508del-CFBE-YFP cells, I evaluated the effect of GM1 together with VX-809 on CFTR activity. The results obtained revealed that the treatment with GM1 induces a slight but significant increase of the channel activity of the rescued protein, suggesting that the exogenous administration of GM1 restores the PM properties allowing the establishment of the proper physiological work condition

for the VX-809-rescued F508del-CFTR. To further improve the activity of VX-809-rescued F508del-CFTR, the cells were treated also with the potentiator VX-770. In the absence of GM1, we found that the treatment with VX-770 abolishes the maturation of F508del-CFTR promoted by VX-809 with the consequent decrease in the cellular levels of the scaffolding proteins NHERF-1 and p-ezrin. Whereas, the concomitant treatment of the cells with VX-809, VX-770 and GM1 antagonizes the negative effect of the potentiator in terms of F508del-CFTR maturation and cellular levels of the CFTR scaffolding proteins. Also in this case, by the use of F508del-CFBE-YFP I found that the treatment with corrector, potentiator and GM1 induces an important recovery of the channel activity.

All together, the results obtained point out that the exogenous administered GM1 becomes component of the PM of bronchial epithelial cells where it is able to re-organize a specific cell surface microenvironment that by the recruitment of scaffolding proteins stabilizing the F508del-CFTR matured by VX-809 and potentiated with VX-770 (Figure 37).

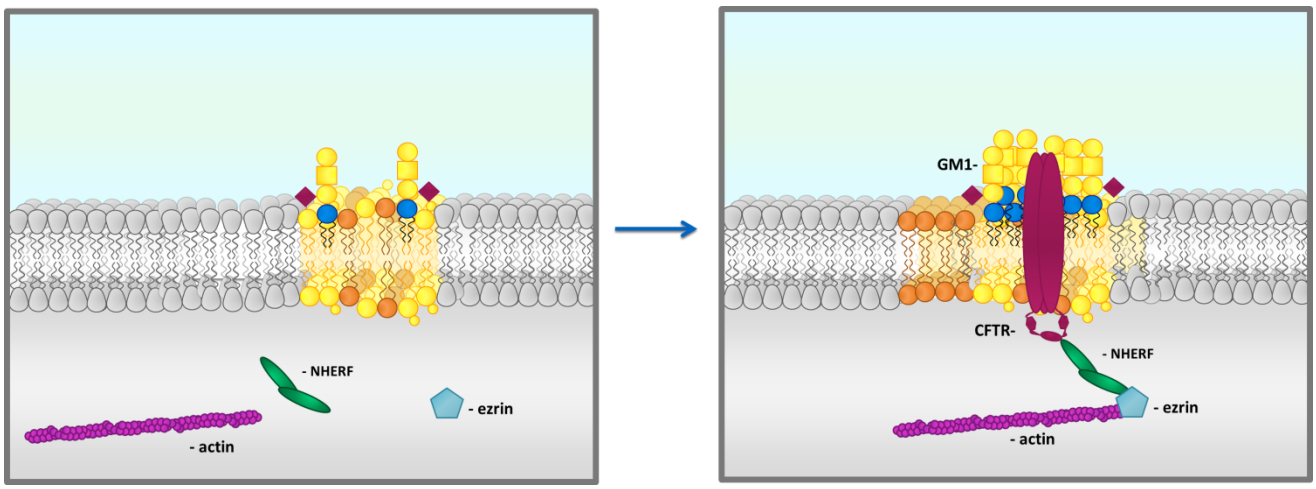

Figure 37: The exogenous administration of GM1 organizes plasma membrane CFTR microenvironment

In addition, since GM1 does not show any toxic effect on the CF bronchial epithelial cells it is reasonable to speculate on its use as adjuvant for the Orkambi® therapy.

References

[1] O'Sullivan BP, Freedman SD. Cystic fibrosis. Lancet 2009;373:1891-904.
[2] Elborn JS, Prescott RJ, Stack BH, Goodchild MC, Bates J, Pantin C, et al. Elective versus symptomatic antibiotic treatment in cystic fibrosis patients with chronic Pseudomonas infection of the lungs. Thorax 2000;55:355-8.
[3] Tsui LC, Dorfman R. The cystic fibrosis gene: a molecular genetic perspective. Cold Spring Harbor perspectives in medicine 2013;3:a009472.
[4] Ellsworth RE, Jamison DC, Touchman JW, Chissoe SL, Braden Maduro VV, Bouffard GG, et al. Comparative genomic sequence analysis of the human and mouse cystic fibrosis transmembrane conductance regulator genes. Proceedings of the National Academy of Sciences of the United States of America 2000;97:1172-7.
[5] Trezise AE, Chambers JA, Wardle CJ, Gould S, Harris A. Expression of the cystic fibrosis gene in human foetal tissues. Human molecular genetics 1993;2:213-8.
[6] Stoltz DA, Meyerholz DK, Welsh MJ. Origins of cystic fibrosis lung disease. The New England journal of medicine 2015;372:351-62.
[7] McCarthy VA, Harris A. The CFTR gene and regulation of its expression. Pediatric pulmonology 2005;40:1-8.
[8] Tizzano EF, Buchwald M. CFTR expression and organ damage in cystic fibrosis. Annals of internal medicine 1995;123:305-8.
[9] Gillen AE, Harris A. Transcriptional regulation of CFTR gene expression. Front Biosci (Elite Ed) 2012;4:587-92.
[10] Yoshimura K, Nakamura H, Trapnell BC, Dalemans W, Pavirani A, Lecocq JP, et al. The cystic fibrosis gene has a "housekeeping"-type promoter and is expressed at low levels in cells of epithelial origin. The Journal of biological chemistry 1991;266:9140-4.
[11] Dean M, Allikmets R. Complete characterization of the human ABC gene family. Journal of bioenergetics and biomembranes 2001;33:475-9.
[12] Higgins CF, Gottesman MM. Is the multidrug transporter a flippase? Trends Biochem Sci 1992;17:18-21.
[13] Hunt JF, Wang C, Ford RC. Cystic fibrosis transmembrane conductance regulator (ABCC7) structure. Cold Spring Harbor perspectives in medicine 2013;3:a009514.
[14] Moran O. On the structural organization of the intracellular domains of CFTR. The international journal of biochemistry & cell biology 2014;52:7-14.
[15] Anderson MP, Sheppard DN, Berger HA, Welsh MJ. Chloride channels in the apical membrane of normal and cystic fibrosis airway and intestinal epithelia. The American journal of physiology 1992;263:L1-14.
[16] Anderson MP, Welsh MJ. Regulation by ATP and ADP of CFTR chloride channels that contain mutant nucleotide-binding domains. Science 1992;257:1701-4.
[17] Frizzell RA. Ten years with CFTR. Physiological reviews 1999;79:S1-2.
[18] Quinton PM. Cystic fibrosis: impaired bicarbonate secretion and mucoviscidosis. Lancet 2008;372:415-7.
[19] Choi JY, Lee MG, Ko S, Muallem S. Cl(-)-dependent HCO3- transport by cystic fibrosis transmembrane conductance regulator. JOP : Journal of the pancreas 2001;2:243-6.
[20] Choi JY, Muallem D, Kiselyov K, Lee MG, Thomas PJ, Muallem S. Aberrant CFTR-dependent HCO3- transport in mutations associated with cystic fibrosis. Nature 2001;410:94-7.
[21] Cant N, Pollock N, Ford RC. CFTR structure and cystic fibrosis. The international journal of biochemistry & cell biology 2014;52:15-25.
[22] Bozoky Z, Ahmadi S, Milman T, Kim TH, Du K, Di Paola M, et al. Synergy of cAMP and calcium signaling pathways in CFTR regulation. Proceedings of the National Academy of Sciences of the United States of America 2017;114:E2086-E95.

[23] Callebaut I, Chong PA, Forman-Kay JD. CFTR structure. Journal of cystic fibrosis : official journal of the European Cystic Fibrosis Society 2018;17:S5-S8.
[24] Bozoky Z, Krzeminski M, Chong PA, Forman-Kay JD. Structural changes of CFTR R region upon phosphorylation: a plastic platform for intramolecular and intermolecular interactions. The FEBS journal 2013;280:4407-16.
[25] Bozoky Z, Krzeminski M, Muhandiram R, Birtley JR, Al-Zahrani A, Thomas PJ, et al. Regulatory R region of the CFTR chloride channel is a dynamic integrator of phospho-dependent intra- and intermolecular interactions. Proceedings of the National Academy of Sciences of the United States of America 2013;110:E4427-36.
[26] Milla CE, Moss RB. Recent advances in cystic fibrosis. Current opinion in pediatrics 2015;27:317-24.
[27] Pranke IM, Sermet-Gaudelus I. Biosynthesis of cystic fibrosis transmembrane conductance regulator. The international journal of biochemistry & cell biology 2014;52:26-38.
[28] Farinha CM, Matos P. Repairing the basic defect in cystic fibrosis - one approach is not enough. The FEBS journal 2016;283:246-64.
[29] Farinha CM, Matos P. Rab GTPases regulate the trafficking of channels and transporters - a focus on cystic fibrosis. Small GTPases 2018;9:136-44.
[30] Farinha CM, Miller E, McCarty N. Protein and lipid interactions - Modulating CFTR trafficking and rescue. Journal of cystic fibrosis : official journal of the European Cystic Fibrosis Society 2018;17:S9-S13.
[31] Ponsioen B, Gloerich M, Ritsma L, Rehmann H, Bos JL, Jalink K. Direct spatial control of Epac1 by cyclic AMP. Molecular and cellular biology 2009;29:2521-31.
[32] Ponsioen B, van Zeijl L, Langeslag M, Berryman M, Littler D, Jalink K, et al. Spatiotemporal regulation of chloride intracellular channel protein CLIC4 by RhoA. Molecular biology of the cell 2009;20:4664-72.
[33] Cholon DM, O'Neal WK, Randell SH, Riordan JR, Gentzsch M. Modulation of endocytic trafficking and apical stability of CFTR in primary human airway epithelial cultures. American journal of physiology Lung cellular and molecular physiology 2010;298:L304-14.
[34] Abu-Arish A, Pandzic E, Goepp J, Matthes E, Hanrahan JW, Wiseman PW. Cholesterol modulates CFTR confinement in the plasma membrane of primary epithelial cells. Biophys J 2015;109:85-94.
[35] Itokazu Y, Pagano RE, Schroeder AS, O'Grady SM, Limper AH, Marks DL. Reduced GM1 ganglioside in CFTR-deficient human airway cells results in decreased beta1-integrin signaling and delayed wound repair. American journal of physiology Cell physiology 2014;306:C819-30.
[36] Farinha CM, Canato S. From the endoplasmic reticulum to the plasma membrane: mechanisms of CFTR folding and trafficking. Cellular and molecular life sciences : CMLS 2017;74:39-55.
[37] De Boeck K, De Baets F, Malfroot A, Desager K, Mouchet F, Proesmans M. Do inhaled corticosteroids impair long-term growth in prepubertal cystic fibrosis patients? European journal of pediatrics 2007;166:23-8.
[38] De Boeck K, Wilschanski M, Castellani C, Taylor C, Cuppens H, Dodge J, et al. Cystic fibrosis: terminology and diagnostic algorithms. Thorax 2006;61:627-35.
[39] Fanen P, Wohlhuter-Haddad A, Hinzpeter A. Genetics of cystic fibrosis: CFTR mutation classifications toward genotype-based CF therapies. The international journal of biochemistry & cell biology 2014;52:94-102.

[40] Wilschanski M, Zielenski J, Markiewicz D, Tsui LC, Corey M, Levison H, et al. Correlation of sweat chloride concentration with classes of the cystic fibrosis transmembrane conductance regulator gene mutations. The Journal of pediatrics 1995;127:705-10.
[41] Veit G, Avramescu RG, Chiang AN, Houck SA, Cai Z, Peters KW, et al. From CFTR biology toward combinatorial pharmacotherapy: expanded classification of cystic fibrosis mutations. Molecular biology of the cell 2016;27:424-33.
[42] Malik NJ, Hergersberg M. [Molecular diagnosis of cystic fibrosis]. Therapeutische Umschau Revue therapeutique 1995;52:801-4.
[43] Haardt M, Benharouga M, Lechardeur D, Kartner N, Lukacs GL. C-terminal truncations destabilize the cystic fibrosis transmembrane conductance regulator without impairing its biogenesis. A novel class of mutation. The Journal of biological chemistry 1999;274:21873-7.
[44] Silvis MR, Picciano JA, Bertrand C, Weixel K, Bridges RJ, Bradbury NA. A mutation in the cystic fibrosis transmembrane conductance regulator generates a novel internalization sequence and enhances endocytic rates. The Journal of biological chemistry 2003;278:11554-60.
[45] Boat TF. The future of pediatric research. The Journal of pediatrics 2007;151:S21-7.
[46] Cantin AM, Hartl D, Konstan MW, Chmiel JF. Inflammation in cystic fibrosis lung disease: Pathogenesis and therapy. Journal of cystic fibrosis : official journal of the European Cystic Fibrosis Society 2015;14:419-30.
[47] Chmiel JF, Berger M, Konstan MW. The role of inflammation in the pathophysiology of CF lung disease. Clin Rev Allergy Immunol 2002;23:5-27.
[48] Chmiel JF, Konstan MW. Anti-inflammatory medications for cystic fibrosis lung disease: selecting the most appropriate agent. Treat Respir Med 2005;4:255-73.
[49] Becker KA, Riethmuller J, Luth A, Doring G, Kleuser B, Gulbins E. Acid sphingomyelinase inhibitors normalize pulmonary ceramide and inflammation in cystic fibrosis. Am J Respir Cell Mol Biol 2010;42:716-24.
[50] Boucher RC. Cystic fibrosis: a disease of vulnerability to airway surface dehydration. Trends in molecular medicine 2007;13:231-40.
[51] Boucher RC. Evidence for airway surface dehydration as the initiating event in CF airway disease. Journal of internal medicine 2007;261:5-16.
[52] Perez-Vilar J, Boucher RC. Reevaluating gel-forming mucins' roles in cystic fibrosis lung disease. Free radical biology & medicine 2004;37:1564-77.
[53] Perez-Vilar J, Randell SH, Boucher RC. C-Mannosylation of MUC5AC and MUC5B Cys subdomains. Glycobiology 2004;14:325-37.
[54] Nichols DP, Chmiel JF. Inflammation and its genesis in cystic fibrosis. Pediatric pulmonology 2015;50 Suppl 40:S39-56.
[55] Nichols JM, Maiellaro I, Abi-Jaoude J, Curci S, Hofer AM. "Store-operated" cAMP signaling contributes to Ca2+-activated Cl- secretion in T84 colonic cells. American journal of physiology Gastrointestinal and liver physiology 2015;309:G670-9.
[56] Hoegger MJ, Fischer AJ, McMenimen JD, Ostedgaard LS, Tucker AJ, Awadalla MA, et al. Impaired mucus detachment disrupts mucociliary transport in a piglet model of cystic fibrosis. Science 2014;345:818-22.
[57] Coakley RD, Grubb BR, Paradiso AM, Gatzy JT, Johnson LG, Kreda SM, et al. Abnormal surface liquid pH regulation by cultured cystic fibrosis bronchial epithelium. Proceedings of the National Academy of Sciences of the United States of America 2003;100:16083-8.
[58] Welsh MJ, Smith JJ. cAMP stimulation of HCO3- secretion across airway epithelia. JOP : Journal of the pancreas 2001;2:291-3.
[59] Poulsen SB, Praetorius J, Damkier HH, Miller L, Nelson RD, Hummler E, et al. Reducing alphaENaC expression in the kidney connecting tubule induces pseudohypoaldosteronism

type 1 symptoms during K+ loading. American journal of physiology Renal physiology 2016;310:F300-10.
[60] Poulsen JH, Fischer H, Illek B, Machen TE. Bicarbonate conductance and pH regulatory capability of cystic fibrosis transmembrane conductance regulator. Proceedings of the National Academy of Sciences of the United States of America 1994;91:5340-4.
[61] Pezzulo AA, Kelly PH, Nassar BS, Rutland CJ, Gansemer ND, Dohrn CL, et al. Abundant DNase I-sensitive bacterial DNA in healthy porcine lungs and its implications for the lung microbiome. Applied and environmental microbiology 2013;79:5936-41.
[62] De Lisle RC. Pass the bicarb: the importance of HCO3- for mucin release. The Journal of clinical investigation 2009;119:2535-7.
[63] Boucher RC. An overview of the pathogenesis of cystic fibrosis lung disease. Advanced drug delivery reviews 2002;54:1359-71.
[64] Pezzulo AA, Tang XX, Hoegger MJ, Abou Alaiwa MH, Ramachandran S, Moninger TO, et al. Reduced airway surface pH impairs bacterial killing in the porcine cystic fibrosis lung. Nature 2012;487:109-13.
[65] Kumar S, Tana A, Shankar A. Cystic fibrosis--what are the prospects for a cure? European journal of internal medicine 2014;25:803-7.
[66] Mogayzel PJ, Jr., Flume PA. Update in cystic fibrosis 2009. Am J Respir Crit Care Med 2010;181:539-44.
[67] Mogayzel PJ, Naureckas ET, Robinson KA, Mueller G, Hadjiliadis D, Hoag JB, et al. Cystic Fibrosis Pulmonary Guidelines Chronic Medications for Maintenance of Lung Health. Am J Resp Crit Care 2013;187:680-9.
[68] Doring G. Eradication of Pseudomonas aeruginosa by early antibiotic treatment has been one of the major advances in the last decade for subjects with CF. Introduction. Journal of cystic fibrosis : official journal of the European Cystic Fibrosis Society 2012;11:1.
[69] Lands LC, Stanojevic S. Oral non-steroidal anti-inflammatory drug therapy for lung disease in cystic fibrosis. The Cochrane database of systematic reviews 2016;4:CD001505.
[70] Balfour-Lynn IM. At last, Burkholderia spp. is one of the inclusion criteria--a negative (but published) randomised controlled trial. Journal of cystic fibrosis : official journal of the European Cystic Fibrosis Society 2014;13:241-2.
[71] Balfour-Lynn IM, Welch K. Inhaled corticosteroids for cystic fibrosis. The Cochrane database of systematic reviews 2014:CD001915.
[72] Gravelle A, Davidson G, Chilvers M. Cystic fibrosis adolescent transition care in Canada: A snapshot of current practice. Paediatrics & child health 2012;17:553-6.
[73] Haller W, Ledder O, Lewindon PJ, Couper R, Gaskin KJ, Oliver M. Cystic fibrosis: An update for clinicians. Part 1: Nutrition and gastrointestinal complications. Journal of gastroenterology and hepatology 2014;29:1344-55.
[74] Ledder O, Haller W, Couper RT, Lewindon P, Oliver M. Cystic fibrosis: an update for clinicians. Part 2: hepatobiliary and pancreatic manifestations. Journal of gastroenterology and hepatology 2014;29:1954-62.
[75] Alton E, Armstrong DK, Ashby D, Bayfield KJ, Bilton D, Bloomfield EV, et al. Repeated nebulisation of non-viral CFTR gene therapy in patients with cystic fibrosis: a randomised, double-blind, placebo-controlled, phase 2b trial. The Lancet Respiratory medicine 2015;3:684-91.
[76] Alton EW, Boyd AC, Porteous DJ, Davies G, Davies JC, Griesenbach U, et al. A Phase I/IIa Safety and Efficacy Study of Nebulized Liposome-mediated Gene Therapy for Cystic Fibrosis Supports a Multidose Trial. Am J Respir Crit Care Med 2015;192:1389-92.

[77] Yu H, Burton B, Huang CJ, Worley J, Cao D, Johnson JP, Jr., et al. Ivacaftor potentiation of multiple CFTR channels with gating mutations. Journal of cystic fibrosis : official journal of the European Cystic Fibrosis Society 2012;11:237-45.
[78] Van Goor F, Hadida S, Grootenhuis PD, Burton B, Cao D, Neuberger T, et al. Rescue of CF airway epithelial cell function in vitro by a CFTR potentiator, VX-770. Proceedings of the National Academy of Sciences of the United States of America 2009;106:18825-30.
[79] Van Goor F, Hadida S, Grootenhuis PD, Burton B, Stack JH, Straley KS, et al. Correction of the F508del-CFTR protein processing defect in vitro by the investigational drug VX-809. Proceedings of the National Academy of Sciences of the United States of America 2011;108:18843-8.
[80] Van Goor F, Yu H, Burton B, Hoffman BJ. Effect of ivacaftor on CFTR forms with missense mutations associated with defects in protein processing or function. Journal of cystic fibrosis : official journal of the European Cystic Fibrosis Society 2014;13:29-36.
[81] Ramsey BW, Davies J, McElvaney NG, Tullis E, Bell SC, Drevinek P, et al. A CFTR potentiator in patients with cystic fibrosis and the G551D mutation. The New England journal of medicine 2011;365:1663-72.
[82] Hadida S, Van Goor F, Zhou J, Arumugam V, McCartney J, Hazlewood A, et al. Discovery of N-(2,4-di-tert-butyl-5-hydroxyphenyl)-4-oxo-1,4-dihydroquinoline-3-carboxamide (VX-770, ivacaftor), a potent and orally bioavailable CFTR potentiator. Journal of medicinal chemistry 2014;57:9776-95.
[83] Du K, Sharma M, Lukacs GL. The DeltaF508 cystic fibrosis mutation impairs domain-domain interactions and arrests post-translational folding of CFTR. Nature structural & molecular biology 2005;12:17-25.
[84] Thibodeau PH, Brautigam CA, Machius M, Thomas PJ. Side chain and backbone contributions of Phe508 to CFTR folding. Nature structural & molecular biology 2005;12:10-6.
[85] Chin S, Hung M, Won A, Wu YS, Ahmadi S, Yang D, et al. Lipophilicity of the Cystic Fibrosis drug, Ivacaftor, and its destabilizing effect on the major CF-causing mutation: F508del. Molecular pharmacology 2018.
[86] van Meer G, Vaz WL. Membrane curvature sorts lipids. Stabilized lipid rafts in membrane transport. EMBO Rep 2005;6:418-9.
[87] Degroote S, Wolthoorn J, van Meer G. The cell biology of glycosphingolipids. Seminars in cell & developmental biology 2004;15:375-87.
[88] Futerman AH, Hannun YA. The complex life of simple sphingolipids. EMBO Rep 2004;5:777-82.
[89] Merrill AH, Jr. Sphingolipid and glycosphingolipid metabolic pathways in the era of sphingolipidomics. Chem Rev 2011;111:6387-422.
[90] Carter HE, Glick FJ, Norris WP, Phillips GE. Biochemisrty of sphingolipides. III. Structure of sphingosine. J Biol Chem 1947;170: 285-94.
[91] Hakomori S. Bifunctional role of glycosphingolipids. Modulators for transmembrane signaling and mediators for cellular interactions. The Journal of biological chemistry 1990;265:18713-6.
[92] Huwiler A, Kolter T, Pfeilschifter J, Sandhoff K. Physiology and pathophysiology of sphingolipid metabolism and signaling. Biochimica et biophysica acta 2000;1485:63-99.
[93] Merrill AH, Jr. De novo sphingolipid biosynthesis: a necessary, but dangerous, pathway. The Journal of biological chemistry 2002;277:25843-6.
[94] Kolter T, Proia RL, Sandhoff K. Combinatorial ganglioside biosynthesis. The Journal of biological chemistry 2002;277:25859-62.
[95] van Meer G, Lisman Q. Sphingolipid transport: rafts and translocators. The Journal of biological chemistry 2002;277:25855-8.

[96] Mandon EC, van Echten G, Birk R, Schmidt RR, Sandhoff K. Sphingolipid biosynthesis in cultured neurons. Down-regulation of serine palmitoyltransferase by sphingoid bases. Eur J Biochem 1991;198:667-74.

[97] Nagiec MM, Baltisberger JA, Wells GB, Lester RL, Dickson RC. The LCB2 gene of Saccharomyces and the related LCB1 gene encode subunits of serine palmitoyltransferase, the initial enzyme in sphingolipid synthesis. Proceedings of the National Academy of Sciences of the United States of America 1994;91:7899-902.

[98] Weiss B, Stoffel W. Human and murine serine-palmitoyl-CoA transferase--cloning, expression and characterization of the key enzyme in sphingolipid synthesis. Eur J Biochem 1997;249:239-47.

[99] Stoffel W, LeKim D, Sticht G. Metabolism of sphingosine bases. 8. Distribution, isolation and properties of D-3-oxosphinganine reductase. Stereospecificity of the NADPH-dependent reaction of 3-oxodihydrospingosine (2-amino-1-hydroxyoctadecane-3-one). Hoppe Seylers Z Physiol Chem 1968;349:1637-44.

[100] Rother J, van Echten G, Schwarzmann G, Sandhoff K. Biosynthesis of sphingolipids: dihydroceramide and not sphinganine is desaturated by cultured cells. Biochem Biophys Res Commun 1992;189:14-20.

[101] Merrill AH, Jr., Wang E. Biosynthesis of long-chain (sphingoid) bases from serine by LM cells. Evidence for introduction of the 4-trans-double bond after de novo biosynthesis of N-acylsphinganine(s). The Journal of biological chemistry 1986;261:3764-9.

[102] Geeraert L, Mannaerts GP, van Veldhoven PP. Conversion of dihydroceramide into ceramide: involvement of a desaturase. Biochem J 1997;327 (Pt 1):125-32.

[103] Merrill AH, Jr., van Echten G, Wang E, Sandhoff K. Fumonisin B1 inhibits sphingosine (sphinganine) N-acyltransferase and de novo sphingolipid biosynthesis in cultured neurons in situ. The Journal of biological chemistry 1993;268:27299-306.

[104] Futerman AH, Stieger B, Hubbard AL, Pagano RE. Sphingomyelin synthesis in rat liver occurs predominantly at the cis and medial cisternae of the Golgi apparatus. The Journal of biological chemistry 1990;265:8650-7.

[105] Aureli M, Schiumarini D, Loberto N, Bassi R, Tamanini A, Mancini G, et al. Unravelling the role of sphingolipids in cystic fibrosis lung disease. Chem Phys Lipids 2016;200:94-103.

[106] Prinetti A, Loberto N, Chigorno V, Sonnino S. Glycosphingolipid behaviour in complex membranes. Biochimica et biophysica acta 2009;1788:184-93.

[107] Ichikawa S, Hirabayashi Y. Glucosylceramide synthase and glycosphingolipid synthesis. Trends Cell Biol 1998;8:198-202.

[108] Jeckel D, Karrenbauer A, Burger KN, van Meer G, Wieland F. Glucosylceramide is synthesized at the cytosolic surface of various Golgi subfractions. J Cell Biol 1992;117:259-67.

[109] Merrill AH, Jr., Jones DD. An update of the enzymology and regulation of sphingomyelin metabolism. Biochimica et biophysica acta 1990;1044:1-12.

[110] Gault CR, Obeid LM, Hannun YA. An overview of sphingolipid metabolism: from synthesis to breakdown. Advances in experimental medicine and biology 2010;688:1-23.

[111] Bartke N, Hannun YA. Bioactive sphingolipids: metabolism and function. J Lipid Res 2009;50 Suppl:S91-6.

[112] Carter HE, Rothfus,J. A., Gigg, R. Biochemistry of the sphingolipids: XII. conversion of cerebrosides to ceramides and sphingosine; structure of Gaucher cerebroside. J Lipid Res 1961;2:228-34.

[113] Kytzia HJ, Sandhoff K. Evidence for two different active sites on human beta-hexosaminidase A. Interaction of GM2 activator protein with beta-hexosaminidase A. The Journal of biological chemistry 1985;260:7568-72.

[114] Fingerhut R, van der Horst GT, Verheijen FW, Conzelmann E. Degradation of gangliosides by the lysosomal sialidase requires an activator protein. Eur J Biochem 1992;208:623-9.
[115] Zschoche A, Furst W, Schwarzmann G, Sanhoff K. Hydrolysis of lactosylceramide by human galactosylceramidase and GM1-beta-galactosidase in a detergent-free system and its stimulation by sphingolipid activator proteins, sap-B and sap-C. Activator proteins stimulate lactosylceramide hydrolysis. Eur J Biochem 1994;222:83-90.
[116] Spence MW. Sphingomyelinases. Adv Lipid Res 1993;26:3-23.
[117] van Meer G, Voelker DR, Feigenson GW. Membrane lipids: where they are and how they behave. Nat Rev Mol Cell Biol 2008;9:112-24.
[118] Boot RG, Verhoek M, Donker-Koopman W, Strijland A, van Marle J, Overkleeft HS, et al. Identification of the non-lysosomal glucosylceramidase as beta-glucosidase 2. The Journal of biological chemistry 2007;282:1305-12.
[119] Aureli M, Bassi R, Loberto N, Regis S, Prinetti A, Chigorno V, et al. Cell surface associated glycohydrolases in normal and Gaucher disease fibroblasts. J Inherit Metab Dis 2012;35:1081-91.
[120] Aureli M, Gritti A, Bassi R, Loberto N, Ricca A, Chigorno V, et al. Plasma membrane-associated glycohydrolases along differentiation of murine neural stem cells. Neurochem Res 2011;37:1344-54.
[121] Aureli M, Loberto N, Bassi R, Ferraretto A, Perego S, Lanteri P, et al. Plasma membrane-associated glycohydrolases activation by extracellular acidification due to proton exchangers. Neurochem Res 2011;37:1296-307.
[122] Aureli M, Samarani M, Loberto N, Mancini G, Murdica V, Chiricozzi E, et al. Erratum to: Current and Novel Aspects on the Non-lysosomal beta-Glucosylceramidase GBA2. Neurochem Res 2016;41:221.
[123] Hannun YA, Obeid LM. Principles of bioactive lipid signalling: lessons from sphingolipids. Nat Rev Mol Cell Biol 2008;9:139-50.
[124] Ohanian J, Ohanian V. Sphingolipids in mammalian cell signalling. Cellular and molecular life sciences : CMLS 2001;58:2053-68.
[125] Ohanian J, Ohanian V. Lipid second messenger regulation: the role of diacylglycerol kinases and their relevance to hypertension. Journal of human hypertension 2001;15:93-8.
[126] Giussani P, Tringali C, Riboni L, Viani P, Venerando B. Sphingolipids: key regulators of apoptosis and pivotal players in cancer drug resistance. International journal of molecular sciences 2014;15:4356-92.
[127] Lahiri S, Futerman AH. The metabolism and function of sphingolipids and glycosphingolipids. Cellular and molecular life sciences : CMLS 2007;64:2270-84.
[128] Lahiri S, Lee H, Mesicek J, Fuks Z, Haimovitz-Friedman A, Kolesnick RN, et al. Kinetic characterization of mammalian ceramide synthases: determination of K(m) values towards sphinganine. FEBS Lett 2007;581:5289-94.
[129] Sonnino S, Aureli M, Grassi S, Mauri L, Prioni S, Prinetti A. Lipid Rafts in Neurodegeneration and Neuroprotection. Molecular neurobiology 2013.
[130] Simons K, Sampaio JL. Membrane organization and lipid rafts. Cold Spring Harb Perspect Biol 2011;3:a004697.
[131] Mansson JE, Fredman P, Bigner DD, Molin K, Rosengren B, Friedman HS, et al. Characterization of new gangliosides of the lactotetraose series in murine xenografts of a human glioma cell line. FEBS Lett 1986;201:109-13.
[132] Mansson JE, Mo HQ, Egge H, Svennerholm L. Trisialosyllactosylceramide (GT3) is a ganglioside of human lung. FEBS Lett 1986;196:259-62.

[133] Seitz AP, Grassme H, Edwards MJ, Pewzner-Jung Y, Gulbins E. Ceramide and sphingosine in pulmonary infections. Biol Chem 2015;396:611-20.
[134] Teichgraber V, Ulrich M, Endlich N, Riethmuller J, Wilker B, De Oliveira-Munding CC, et al. Ceramide accumulation mediates inflammation, cell death and infection susceptibility in cystic fibrosis. Nat Med 2008;14:382-91.
[135] Guilbault C, Wojewodka G, Saeed Z, Hajduch M, Matouk E, De Sanctis JB, et al. Cystic fibrosis fatty acid imbalance is linked to ceramide deficiency and corrected by fenretinide. Am J Respir Cell Mol Biol 2009;41:100-6.
[136] Guilbault C, De Sanctis JB, Wojewodka G, Saeed Z, Lachance C, Skinner TA, et al. Fenretinide corrects newly found ceramide deficiency in cystic fibrosis. Am J Respir Cell Mol Biol 2008;38:47-56.
[137] Vilela RM, Lands LC, Chan HM, Azadi B, Kubow S. High hydrostatic pressure enhances whey protein digestibility to generate whey peptides that improve glutathione status in CFTR-deficient lung epithelial cells. Mol Nutr Food Res 2006;50:1013-29.
[138] Vilela RM, Lands LC, Meehan B, Kubow S. Inhibition of IL-8 release from CFTR-deficient lung epithelial cells following pre-treatment with fenretinide. Int Immunopharmacol 2006;6:1651-64.
[139] Simons K, Ehehalt R. Cholesterol, lipid rafts, and disease. The Journal of clinical investigation 2002;110:597-603.
[140] Duncan MJ, Shin JS, Abraham SN. Microbial entry through caveolae: variations on a theme. Cellular microbiology 2002;4:783-91.
[141] Manes G, Bello P, Roche S. Slap Negatively Regulates Src Mitogenic Function but Does Not Revert Src-Induced Cell Morphology Changes

10.1128/MCB.20.10.3396-3406.2000. Mol Cell Biol 2000;20:3396-406.
[142] Manes S, Ana Lacalle R, Gomez-Mouton C, Martinez AC. From rafts to crafts: membrane asymmetry in moving cells. Trends in immunology 2003;24:320-6.
[143] Scheiffele P, Roth MG, Simons K. Interaction of influenza virus haemagglutinin with sphingolipid-cholesterol membrane domains via its transmembrane domain. The EMBO journal 1997;16:5501-8.
[144] Naslavsky N, Stein R, Yanai A, Friedlander G, Taraboulos A. Characterization of detergent-insoluble complexes containing the cellular prion protein and its scrapie isoform. The Journal of biological chemistry 1997;272:6324-31.
[145] Prior IA, Hancock JF. Compartmentalization of Ras proteins. Journal of cell science 2001;114:1603-8.
[146] Prior IA, Harding A, Yan J, Sluimer J, Parton RG, Hancock JF. GTP-dependent segregation of H-ras from lipid rafts is required for biological activity. Nature cell biology 2001;3:368-75.
[147] Kowalski MP, Pier GB. Localization of cystic fibrosis transmembrane conductance regulator to lipid rafts of epithelial cells is required for Pseudomonas aeruginosa-induced cellular activation. J Immunol 2004;172:418-25.
[148] Hamai H, Keyserman F, Quittell LM, Worgall TS. Defective CFTR increases synthesis and mass of sphingolipids that modulate membrane composition and lipid signaling. J Lipid Res 2009;50:1101-8.
[149] Ramu Y, Xu Y, Lu Z. Inhibition of CFTR Cl- channel function caused by enzymatic hydrolysis of sphingomyelin. Proceedings of the National Academy of Sciences of the United States of America 2007;104:6448-53.
[150] Stonehouse MJ, Cota-Gomez A, Parker SK, Martin WE, Hankin JA, Murphy RC, et al. A novel class of microbial phosphocholine-specific phospholipases C. Mol Microbiol 2002;46:661-76.

[151] Cholon DM, Quinney NL, Fulcher ML, Esther CR, Jr., Das J, Dokholyan NV, et al. Potentiator ivacaftor abrogates pharmacological correction of DeltaF508 CFTR in cystic fibrosis. Sci Transl Med 2014;6:246ra96.
[152] Veit G, Avramescu RG, Perdomo D, Phuan PW, Bagdany M, Apaja PM, et al. Some gating potentiators, including VX-770, diminish DeltaF508-CFTR functional expression. Sci Transl Med 2014;6:246ra97.
[153] Matthes E, Goepp J, Carlile GW, Luo Y, Dejgaard K, Billet A, et al. Low free drug concentration prevents inhibition of F508del CFTR functional expression by the potentiator VX-770 (ivacaftor). British journal of pharmacology 2015.
[154] Monterisi S, Favia M, Guerra L, Cardone RA, Marzulli D, Reshkin SJ, et al. CFTR regulation in human airway epithelial cells requires integrity of the actin cytoskeleton and compartmentalized cAMP and PKA activity. Journal of cell science 2012;125:1106-17.
[155] Sondo E, Tomati V, Caci E, Esposito AI, Pfeffer U, Pedemonte N, et al. Rescue of the mutant CFTR chloride channel by pharmacological correctors and low temperature analyzed by gene expression profiling. American journal of physiology Cell physiology 2011;301:C872-85.
[156] Scandroglio F, Venkata JK, Loberto N, Prioni S, Schuchman EH, Chigorno V, et al. Lipid content of brain, brain membrane lipid domains, and neurons from acid sphingomyelinase deficient mice. Journal of neurochemistry 2008;107:329-38.
[157] Scandroglio F, Loberto N, Valsecchi M, Chigorno V, Prinetti A, Sonnino S. Thin layer chromatography of gangliosides. Glycoconj J 2008.
[158] Ishizuka I. Chemistry and functional distribution of sulfoglycolipids. Progress in lipid research 1997;36:245-319.
[159] Aureli M, Gritti A, Bassi R, Loberto N, Ricca A, Chigorno V, et al. Plasma membrane-associated glycohydrolases along differentiation of murine neural stem cells. Neurochem Res 2012;37:1344-54.
[160] Gatti R, Lombardo C, Filocamo M, Borrone C, Porro E. Comparative study of 15 lysosomal enzymes in chorionic villi and cultured amniotic fluid cells. Early prenatal diagnosis in seven pregnancies at risk for lysosomal storage diseases. Prenat Diagn 1985;5:329-36.
[161] Aureli M, Loberto N, Lanteri P, Chigorno V, Prinetti A, Sonnino S. Cell surface sphingolipid glycohydrolases in neuronal differentiation and aging in culture. J Neurochem 2011;116:891-9.
[162] Aureli M, Masilamani AP, Illuzzi G, Loberto N, Scandroglio F, Prinetti A, et al. Activity of plasma membrane beta-galactosidase and beta-glucosidase. FEBS letters 2009;583:2469-73.
[163] Overkleeft HS, Renkema GH, Neele J, Vianello P, Hung IO, Strijland A, et al. Generation of specific deoxynojirimycin-type inhibitors of the non-lysosomal glucosylceramidase. The Journal of biological chemistry 1998;273:26522-7.
[164] Whiting P, Al M, Burgers L, Westwood M, Ryder S, Hoogendoorn M, et al. Ivacaftor for the treatment of patients with cystic fibrosis and the G551D mutation: a systematic review and cost-effectiveness analysis. Health Technol Assess 2014;18:1-106.
[165] Pedemonte N, Lukacs GL, Du K, Caci E, Zegarra-Moran O, Galietta LJ, et al. Small-molecule correctors of defective DeltaF508-CFTR cellular processing identified by high-throughput screening. The Journal of clinical investigation 2005;115:2564-71.
[166] Pedemonte N, Sonawane ND, Taddei A, Hu J, Zegarra-Moran O, Suen YF, et al. Phenylglycine and sulfonamide correctors of defective delta F508 and G551D cystic fibrosis transmembrane conductance regulator chloride-channel gating. Molecular pharmacology 2005;67:1797-807.

[167] Yang H, Shelat AA, Guy RK, Gopinath VS, Ma T, Du K, et al. Nanomolar affinity small molecule correctors of defective Delta F508-CFTR chloride channel gating. The Journal of biological chemistry 2003;278:35079-85.
[168] Brodlie M, McKean MC, Johnson GE, Gray J, Fisher AJ, Corris PA, et al. Ceramide is increased in the lower airway epithelium of people with advanced cystic fibrosis lung disease. Am J Respir Crit Care Med 2010;182:369-75.
[169] Pankow S, Bamberger C, Calzolari D, Bamberger A, Yates JR, 3rd. Deep interactome profiling of membrane proteins by co-interacting protein identification technology. Nat Protoc 2016;11:2515-28.
[170] Pankow S, Bamberger C, Calzolari D, Martinez-Bartolome S, Lavallee-Adam M, Balch WE, et al. F508 CFTR interactome remodelling promotes rescue of cystic fibrosis. Nature 2015;528:510-6.
[171] Chin S, Hung M, Won A, Wu YS, Ahmadi S, Yang D, et al. Lipophilicity of the Cystic Fibrosis Drug, Ivacaftor (VX-770), and Its Destabilizing Effect on the Major CF-causing Mutation: F508del. Molecular pharmacology 2018;94:917-25.